

VISCOELASTIC CHARACTERIZATION
OF ANGLE PLY ADVANCED COMPOSITES,

by


Ashok B. Thakker

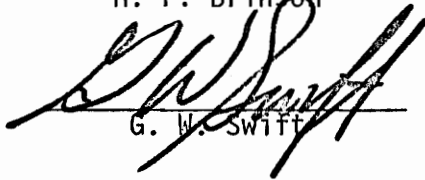
Dissertation submitted to the Graduate Faculty of the
Virginia Polytechnic Institute and State University
in partial fulfillment of the requirements for the degree of
DOCTOR OF PHILOSOPHY
in
Engineering Mechanics

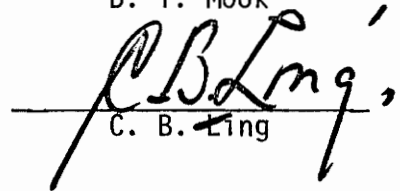
APPROVED:


R. A. Heller, Chairman


H. F. Brinson


D. T. Mook


G. W. Swift


C. B. Ling

October, 1974
Blacksburg, Virginia

LD
5655
V856
1974
T45
c. 2

ACKNOWLEDGMENTS

The author wishes to express:

his gratitude to his advisor, Dr. R. A. Heller, for his suggestions and guidance during the course of this investigation.

his thanks to Dr. H. F. Brinson and other committee members for their valuable comments and criticisms;

his appreciation to Dr. W. W. Stinchcomb, Ms. A. S. Heller, Mr. C. A. Arthur, Mr. C. T. Liu, Mr. G. K. McCauley, and the department's research staff for their help during the experimental work;

his gratefulness to the Air Force Materials Laboratory, Wright-Patterson Air Force Base, Ohio for their financial assistance under Air Force Contract F33615-72-C-2111;

his thanks to Mrs. Peggy Epperly for typing the manuscript;

and his regards to his parents for encouraging advanced studies.

TABLE OF CONTENTS

<u>Chapter</u>	<u>Page</u>
ACKNOWLEDGEMENTS	ii
LIST OF FIGURES	iv
LIST OF TABLES	ix
NOMENCLATURE	x
I. INTRODUCTION	1
II. LITERATURE REVIEW	3
III. EXPERIMENTAL INVESTIGATION AND DATA REDUCTION	13
Materials and Specimens	14
Vibration Tests	15
Constant Rate Tests	24
Tensile Creep Tests	43
Data Reduction and Statistical Conditioning	47
IV. VISCOELASTIC CHARACTERIZATION	64
Time-Temperature Superposition	64
Predicting Strain Rate and Creep Properties	86
A. Mechanical Model Representation	86
B. Interconversion by Integral Equation	99
C. Numerical Integration Method	109
V. DISCUSSION OF RESULTS AND CONCLUSIONS	128
VI. REFERENCES	138
APPENDICES	
A. SPECIMEN PREPARATION AND PROCUREMENT	147
B. DETERMINATION OF STORAGE MODULUS AND LOSS RATIO	153
C. TABULATION OF STRAIN RATE DATA	155
VITA	179

LIST OF FIGURES

<u>Figure</u>		<u>Page</u>
1.	Specimen Configurations	16
2.	Details of Forced Vibration Test Setup	17
3.	Forced Vibration Test Setup	18
4.	Schematic Diagram of Vibration Testing System	19
5.	Typical Impedence vs. Frequency Curves for Boron/Epoxy	21
6.	Effects of Mass Cancellation on Resonance and Antiresonance Peaks	22
7.	Vibration Tests on 2024-T3 Aluminum, Under Axial and Bending Loads	23
8.	Vibration Test Results on Boron/Epoxy Specimens at 300°F	25
9.	Vibration Test Results on Graphite/Epoxy Specimens at 200°F	26
10.	Variation of Modulus with Moisture Content	27
11.	Constant-Rate Test Setup	29
12.	Load-Time Trace for Constant Head Rate Test on Instron Machine; Graphite/Epoxy Specimen at .002 In/Min	32
13.	Strain-Time Trace for Constant Head Rate Test on Instron Machine; Graphite/Epoxy Specimen at .002 In/Min	33
14.	Stress-Strain Curve for Graphite/Epoxy Specimen Derived from Figures 12 and 13; Average Strain Rate = 2.3 μ In/In/Sec	34
15.	Load-Time and Strain-Time Traces for Constant Load Rate Tests on MTS Machine. Boron/Epoxy Specimen; 100 Hz, 50 KIP Range at 200°F	35

<u>Figure</u>	<u>Page</u>
16. Stress-Strain Curve for Boron/Epoxy Specimen Derived from Figure 15; Average Strain Rate 305,800 μ In/In/Sec. at 200°F	36
17. Initial Modulus-Strain Rate Test Results for Boron/Epoxy Specimens at -50°F	37
18. Fracture Strength-Strain Rate Test Results for Boron/Epoxy Specimens at 200°F	38
19. Fracture Strain-Strain Rate Test Results for Boron/Epoxy Specimens at -50°F	39
20. Initial Modulus-Strain Rate Test Results for Graphite/Epoxy Specimens at 300°F	40
21. Fracture Strength-Strain Rate Test Results for Graphite/Epoxy Specimens at -50°F	41
22. Fracture Strain-Strain Rate Test Results for Graphite/Epoxy Specimens at 80°F	42
23. Typical Tension Failures of Boron/Epoxy and Graphite/Epoxy Specimens	44
24. Tensile Creep Test Setup	45
25. Details of Creep Test Setup	46
26. Creep Curve for Boron/Epoxy at 300°F	48
27. Creep Curves for Boron/Epoxy at 200°F	49
28. Contours for the Initial Modulus of Boron/Epoxy	51
29. Contours for the Initial Modulus of Graphite/Epoxy	52
30. Probability Curves for the Initial Modulus of Boron/Epoxy at 80°F as a Function of Strain Rate	55
31. Probability Curves for the Initial Modulus of Boron/Epoxy at -50°F as a Function of Strain Rate	56
32. Probability Curves for the Initial Modulus of Graphite/Epoxy at 80°F as a Function of Strain Rate	57

<u>Figure</u>		<u>Page</u>
33.	Probability Curves for the Initial Modulus of Graphite/Epoxy at -50°F as a Function of Strain Rate	58
34.	Constant-Temperature Initial Modulus Curves for Boron/Epoxy as a Function of Strain Rate	59
35.	Constant-Temperature Initial Modulus Curves for Graphite/Epoxy as a Function of Strain Rate	60
36.	Fracture Strength as a Function of Temperature for Boron/Epoxy	62
37.	Fracture Strength as a Function of Temperature for Graphite/Epoxy	63
38.	Determination of Softening Temperature for Boron/Epoxy Composite	68
39.	Horizontal and Vertical Shift	70
40.	Master Curve for the Initial Modulus of Boron/Epoxy for a Reference Temperature of 80°F (300°K)	72
41.	Master Curve for the Initial Modulus of Graphite/Epoxy for a Reference Temperature of 80°F (300°K)	73
42.	Master Curve for the Damping Ratio of Boron/Epoxy for a Reference Temperature of 80°F (300°K)	74
43.	Master Curve for the Damping Ratio of Graphite/Epoxy for a Reference Temperature of 80°F (300°K)	75
44.	Temperature Shift Factor, a_T , for the Storage Modulus of Boron/Epoxy vs. Inverse Temperature	79
45.	Temperature Shift Factor, a_T , for the Loss Modulus of Boron/Epoxy vs. Inverse Temperature	80
46.	Temperature Shift Factor, a_T , for the Storage Modulus of Graphite/Epoxy vs. Inverse Temperature	81

<u>Figure</u>	<u>Page</u>
47. Temperature Shift Factor, a_T , for the Loss Modulus of Graphite/Epoxy vs. Inverse Temperature	82
48. Temperature Shift Factor, a_T , for the Initial Modulus of Boron/Epoxy vs. Inverse Temperature . .	83
49. Temperature Shift Factor, a_T , for the Initial Modulus of Graphite/Epoxy vs. Inverse Temperature	84
50. Temperature Shift Factor, a_T , vs. Inverse Temperature for Comparison of Graphite/Epoxy Systems	87
51. Maxwell Model Representation of Vibration Test Results on Boron/Epoxy Specimens at 80°F	89
52. Prediction of Stress Strain Curves at Various Strain Rates from Dynamic Test for Boron/Epoxy at 80°F Using Maxwell Model	92
53. Mechanical Model Representation	93
54. Least Square Fit to Determine Constants of Triparameter Viscoelastic Model from Vibration Test Results on Boron/Epoxy Specimens at 80°F	98
55. Prediction of Stress Strain Curves at Various Strain Rates from Dynamic Test for Boron/Epoxy at 80°F Using Triparameter Model	100
56. Viscoelastic Interconversion Relations	106
57. Variation of Constants a and b with Time, for Boron/Epoxy at 300°F as Obtained from Dynamic Tests	108
58. Prediction of Stress-Strain Curve at a Constant Strain Rate from Dynamic Tests by Sims and Halpin Equation [69] for Boron/Epoxy	110
59. Prediction of Stress-Strain Curve at a Constant Strain Rate from Dynamic Tests by Sims and Halpin Equation [69] for Boron/Epoxy	111

<u>Figure</u>		<u>Page</u>
60.	Prediction of Stress-Strain Curve at a Constant Strain Rate from Dynamic Tests by Sims and Halpin Equation [69] for Graphite/Epoxy	112
61.	Prediction of Stress-Strain Curve at a Constant Strain Rate from Dynamic Tests by Sims and Halpin Equation [69] for Graphite/Epoxy	113
62.	Comparison of Storage and Relaxation Moduli for Boron/Epoxy	121
63.	Comparison of Storage and Relaxation Moduli for Graphite/Epoxy	122
64.	Prediction of Stress-Strain Curve at a Constant Strain Rate from Dynamic Tests by Numerical Integration Method for Boron/Epoxy	124
65.	Prediction of Stress-Strain Curve at a Constant Strain Rate from Dynamic Tests by Numerical Integration Method for Boron/Epoxy	125
66.	Prediction of Stress-Strain Curve at a Constant Strain Rate Tests by Numerical Integration Method for Graphite/Epoxy	126
67.	Prediction of Stress-Strain Curve at a Constant Strain Rate Tests by Numerical Integration Method for Graphite/Epoxy	127
68.	Relaxation Modulus for Boron/Epoxy Obtained from Dynamic, High Strain Rate and Creep Test	133
69.	Creep Compliance for Boron/Epoxy Obtained from Dynamic, High Strain Rate and Creep Test	134
70.	Relaxation Modulus for Graphite/Epoxy Obtained from Dynamic, High Strain Rate and Creep Test	135

LIST OF TABLES

<u>Table</u>		<u>Page</u>
1.	R^2 , σ and the Coefficients of Eq. (3.3) for $1/T$ in Degrees Kelvin and $\dot{\epsilon}$ in Inches/in/Sec	53
2.	Determination of Activation Energy from Regression Coefficients	85
3.	Coefficients of Eq. (4.71) for $1/T$ in Degrees Kelvin and Period in Secs	119
A-1.	Quality Control Data on the Boron/Epoxy Panels	149
A-2.	Quality Control Data on the Graphite/Epoxy Panels	151

NOMENCLATURE

E	Elastic Modulus
$E^*(\omega)$	Complex Modulus
$E'(\omega)$	Storage Modulus
$E''(\omega)$	Loss Modulus
ω	Circular Frequency
i	$\sqrt{-1}$
δ	Loss Ratio
C	Wave Speed
l	Length
f	Frequency, Hertz
ρ	Mass Density
h	Thickness of Beam
σ	Stress
ϵ	Strain
μ	Viscosity Coefficient for Dashpot
k	Spring Constant or Moduli
$\dot{\epsilon}$	Strain Rate
a_T	Time-Temperature Shift Factor
τ	Relaxation or Retardation Time; Argument of H or L
ζ	Viscosity
T_g	Glass-Transition Temperature
ΔH	Activation Energy
R	Universal Gas Constant

ΔH_a	Apparent Activation Energy
$E(t)$	Tensile-Relaxation Modulus
$D(t)$	Tensile Creep Compliance
$D^*(\omega)$	Tensile Complex Compliance
$D'(\omega)$	Tensile Storage Compliance
$D''(\omega)$	Tensile Loss Compliance
t	Time
K	Constant
σ_0	Stress Amplitude
a, b	Constants
E_e	Equilibrium Modulus
H	Relaxation Spectrum in Extension
L	Retardation Spectrum in Extension

I. INTRODUCTION

Advanced composites are gaining wide acceptance due to their high structural performance. They offer engineers the unique convenience to design totally new materials with the precise combination of properties needed for a specific purpose. A primary concern in the utilization of a composite system having a polymeric binder is the effect of the time dependent properties of the binder material. This behavior must be known to achieve an efficiently designed structure. Their potential role in high performance aircraft requires characterization of their time dependent mechanical response in a service environment.

It is desirable to develop reliable characterization procedures for these materials in order to utilize the properties established over shorter time periods to design structures with longer useful lives. An accelerated testing technique could be established for polymeric composites to predict intermediate and long-term behavior from short-term tests, using viscoelastic theory. Although, some effort in this direction has been made for filled elastomers and for unidirectional composites, structurally significant fiber controlled angle ply laminated composites have not been studied extensively.

The behavior below the glass transition temperature, or at short times is also of considerable interest because this is a useful range for many structural applications of polymers and their composites. It is, therefore, one of the objectives of this study to investigate

the behavior of advanced filamentary composites in their glassy state.

Because of the large number of possible combinations of variables, as well as the high statistical variability of test results, multiple regression techniques were used to condition the experimental data. This method allows efficient utilization of specimens. By generating response surfaces for significant variables time-temperature superposition has been established for various tests. This in turn makes it possible to minimize the amount of data required for reliable engineering design.

Dynamic tests and constant strain rate tests were used as a means of accelerated testing to predict long term creep test results based on viscoelastic characterization of the materials. Several different approaches were tried to achieve this aim. Mechanical model representation, integral equation formulation and numerical integration methods based on linear viscoelasticity were used to predict constant strain rate and long time creep behavior of composites from nondestructive short-time dynamic tests.

From a theoretical point of view, none of the predictions appear to be completely satisfactory. However, by studying various limitations and qualitative predictions, they do afford approximations useful to the designer.

II. LITERATURE REVIEW

That linear viscoelasticity was advanced mainly by the advent of polymers is extensively documented and experimentally varified for polymeric materials [1-10]*. Rigorous treatment of the representation of time dependent materials by mechanical models, time temperature superposition techniques and their dynamic mechanical testing is treated in the above references. McClintock [8] has given an elegant treatment on the subject from the micro and dislocation point of view. Exact and approximate interrelations among the linear viscoelastic functions and comparisons of viscoelastic behavior in seven typical polymer systems are discussed by Ferry [9]. A unified theoretical formulation from a continuum mechanics approach has been presented by Christensen [10].

Vincent [11], Halpin [12], and Leaderman [13] provide brief reviews of the subject and its limitations. An interesting concept, that absorption of relatively small amounts of a swelling agent affects the time-scale in the same way as an increase in temperature is also discussed by Halpin [12] and Leaderman [13].

Even though experiments may cover a wide range of times, no single experimental method can be used to cover the entire range. For a complete viscoelastic characterization of materials over a wide range of time, a large number of different experimental

*Numbers in brackets refer to References.

techniques have to be used. These are reviewed and discussed by Schmitz [14] and Kolsky [15].

Bland [16] has suggested empirical rules for fitting models to experimentally determined complex moduli or compliances for a particular frequency interval. A numerical method of calculating the spring and dashpot constants for generalized Maxwell or Kelvin models by fitting their response to experimental stress-strain data is given by Schapery [17]. Measurement of the complex modulus is the most convenient way of experimentally characterizing some mechanical properties. By direct conversion, the relaxation function may be obtained for times several orders of magnitude shorter than is possible by a relaxation experiment. Gottenberg and Christensen [18] carried out this conversion by numerical integration. Ninomiya and Ferry [19] have developed a very useful method of calculating the relaxation or retardation spectrum without differentiation, using two or more measured values equally spaced on the logarithmic frequency scale. They have also extended Catsiff's and Tobolsky's work [20] to develop an approximation for obtaining the relaxation modulus from the storage modulus. Schwarzl [21] has presented a system of numerical formulae for interconverting measurable functions for linear viscoelastic materials with bounds for the errors. He has also discussed the behavior of viscoelastic material functions in the transition region.

Schapery [22-23] showed that for quasi-static viscoelastic, stress analysis could be simplified by using approximate methods of

Laplace transform inversion and by using elastic solutions wherein elastic constants are replaced by the transforms of time-dependent creep or relaxation functions. Physical conditions which require a non-negative real part of the complex modulus are discussed by Christensen [24].

Brinson [25] used photoviscoelasticity to characterize an epoxy polymer by applying time-temperature superposition. Moehlenpah [26] applied the time-temperature superposition principle to yield stress, initial tangent modulus, and relaxation modulus data for tension, compression and flexural loading. He came up with an interesting conclusion that shift factors may be stress dependent.

Empirical constitutive equations to predict stress-strain behavior at various strain rates and temperatures for aluminum alloys and nonmetallic materials are suggested by McLellan [27].

The preceding discussion is a review of only a few of the works out of a vast literature according to which the theory of viscoelasticity has been extensively varified for polymers in their rubbery and leathery states.

There also has been considerable activity in the area of applying the time-temperature superposition principle in the glassy region of materials [28-34]. Lohr [28-29] has shown that a yield stress master curve similar in principle to the stress relaxation master curve could apply to essentially amorphous polymers tested in their glassy temperature range. Smith [30-31] has detailed properties of polymers and has attempted time temperature superposition. The

relative merits of time-temperature superposition normalization procedures (those of Leaderman, Tobolsky, Ferry, Kê, McCrum, and Morris) have been assessed for relaxation of an epoxy resin by McCrum [33].

Lazan [35] is an excellent reference on the study of damping micromechanisms for linear and nonlinear materials. He has proposed several mechanical models for different damping behaviors in materials.

Experimental verification of the applicability of viscoelastic theory to highly damped materials such as filled elastomers was shown by Heller [36-37]. He has also discussed the relative merits of forced and freely damped oscillations in measuring complex moduli [37]. Meinecke [38] has shown how polymeric foams could be treated as viscoelastic materials in a manner similar to that for solid polymers. He has described stress relaxation behavior of foams and mathematical tools to predict the response to other load or deformation histories such as constant rate of strain (stress-strain curve), creep, or sinusoidal strains.

Theoretical formulation of heterogeneous and anisotropic viscoelastic materials has been proposed by several authors [39-42]. Christensen [39] has established bounds upon the effective viscoelastic properties using viscoelastic minimum theorems. Hashin [40] has also used variational principles to obtain bounds for elastic moduli of multi-phase nonhomogeneous materials.

A symposium has been held and several papers have been written [43-48] to characterize solid rocket propellants as viscoelastic materials. Baltrukonis [44] has presented a survey of solid

propellant rocket motors considering infinitesimal deformations of propellant grains and thus restricting himself to linear elastic and viscoelastic development. Schapery [45-46] has done considerable work in this area. Schapery [45-46], Koh [47] and Lockett [48] have emphasized the nonlinear stress-strain behavior of propellants in their development of viscoelastic theories. Krokosky [49] has written a state-of-the-art review on time dependent behavior of composite materials which are mostly solid propellants. He has provided a comprehensive study by considering ways to determine linearity, interconvertibility of linear viscoelastic data, and time temperature superposition of filled systems. Terrel [50] studied the dynamic viscoelastic properties of asphalt treated materials. He has compared shift factors for various asphalt contents and grain sizes.

Viscoelastic properties of continuous filament glass reinforced plastics have been adequately studied [51-59]. Gauchel [51] has performed similar studies as proposed in this investigation for polymeric matrix materials, glass bead systems, glass fiber reinforced materials and glass reinforced quasi-isotropic laminates. Even though the systems he studied are basically different from advanced composites used in this investigation, consideration of applying viscoelastic theory to anisotropic materials in the glassy region makes his work very relevant. He has shown that given isothermal relaxation data for temperatures from below the secondary transition to the rubbery region, the master curves for the dynamic and creep properties at small strains can be constructed using linear viscoelastic relationships.

Cessna [52] demonstrated the validity of using a time-stress superposition procedure to generalize the creep behavior of a glass fiber-reinforced polypropylene material. The evidence of the existence of different controlling mechanisms (fiber and matrix) is shown by Pink [53-54] in his study of strain rate and temperature effects on the deformations of glass reinforced polymers. Schapery [56] studied the nonlinear viscoelastic behavior of a unidirectional glass fiber epoxy composite material. He performed isothermal uniaxial creep and recovery tests and proposed a constitutive equation based on thermodynamic theory. Zakhariyev [57] proposed a rheological model to represent the viscoelastic behavior of glass-reinforced plastics. Kokoshvili [58] has attempted to develop a procedure for calculating relaxation spectra from tensile tests conducted at constant strain rates for a fabric-reinforced glass laminate. Bodner [59] has reviewed various methods of dynamic viscoelastic characterization and strength determination. He performed experiments on samples of an unfilled and quartz particle filled epoxy resin.

Quite a number of articles have been published describing the mechanical properties of advanced composites. Until recently research effort has been directed towards the improvement of the constituents, or the geometric stacking sequence of plies and towards the study of the mechanics of different configurations.

A close examination reveals the lack of literature on viscoelastic studies of advanced composite systems. However, a beginning in this area has been made by several workers [60-75]. The main

effort has been directed towards either studying unidirectional composites using the micromechanics approach or studying viscoelastic properties as functions of orientation of fibers.

Hashin [60] has investigated time dependent properties of uniaxially fiber reinforced materials composed of a linear viscoelastic matrix and elastic fibers. He has also given simple calculations for the static and dynamic properties of this material and has put forth the concept of effective viscoelastic properties of composites [61]. Hashin has used the principle of minimum potential energy to predict the response of an elastic-elastic composite. He then applied the correspondence principle of linear viscoelasticity to obtain the solution for elastic-viscoelastic composites.

Calvit [62] has also developed an "effective modulus" theory for quasi-static analysis of fiber-reinforced materials. He uses the continuum theory of mixtures to predict the effective modulus. He has shown good agreement with Hashin's theory. Sutherland and Calvit [62] further proposed that by assuming geometric dispersion to be smaller than viscoelastic dispersion, the constitutive equation can be extended from a quasi-static regime to a dynamic regime for unidirectional composites.

Schultz and Tsai [64-65] measured storage and loss moduli for laminated glass fiber reinforced composites with different ply orientations. They proposed a micromechanics solution to predict laminate properties from ply properties. Tsai [66] also considered an analytical approach for predicting environmental effects based on

rate theory.

Schapery [67-68] has made a major contribution in the field by studying dynamic and creep behavior of advanced composites. He has proposed analyses of predicting effective viscoelastic properties and has used time-temperature superposition to generate master curves for relaxation moduli and creep compliances.

Sims and Halpin [69] have suggested an analysis by which creep behavior of any laminate can be predicted from laminated plate theory once the unidirectional material is characterized. They also derived viscoelastic interconversion formulae which relate the creep test, constant loading rate test, and dynamic test when the creep compliance can be approximated by a power law and if linear viscoelastic behavior is assumed.

Ericksen [70] has shown that at low stresses Borsic-Aluminum composites follow a logarithmic-time law in creep. Stinchcomb [71] has reported frequency dependent damage in angle ply Boron/Epoxy and Boron/Aluminum composites, suggesting time dependent behavior. Laird [72] and Jones [73] have performed experiments to measure complex moduli and damping coefficients. Meyn [74] and Chiao [75] reported large scatter in the data gathered from tensile tests, indicating the importance of statistical analysis in data reduction.

Introduction of an inert filler in certain linearly viscoelastic polymers results in nonlinear viscoelastic behavior, which is manifested in several ways. Numerous publications exist on the

treatment of nonlinear viscoelasticity [76-89]. Smart [76] has made comparisons of several single-integral non-linear viscoelastic theories. Brinson [77] studied polycarbonate and reported it to be a ductile material with elastic, viscoelastic and plastic behavior regimes. He also proposed a Bingham type model and discussed it with respect to the constitutive equation characterization of polycarbonate [78].

A constitutive equation for a particular form of the isothermal nonlinear stress for materials with fading memory was obtained by Christensen [79]. Davis [80] improved the single integral Voigt and the single Maxwell model to incorporate quadratic and cubic non-linearity. Distefano [81] has considered nonlinear integral equations to characterize a class of nonlinear viscoelastic materials subject to uniaxial effects. Gottenberg [82] formulated the multiple integral form of the constitutive relation for nonlinear viscoelasticity and correlated this with experimental results on a polymeric material in uniaxial tension. Mathematical treatment of nonlinear viscoelasticity is given by Lockett [89].

In order to remain within the scope of the present investigation nonlinear viscoelasticity is not discussed in detail, because the present goal is to examine available linear viscoelastic theories and employ them to predict the gross properties of the advanced composite systems under study.

Several reports [91-94] have been written during the progress of this investigation and they have been referred to for details.

It was not intended that this survey be a complete bibliographical study but rather a presentation of progress in the field investigated.

III. EXPERIMENTAL INVESTIGATION AND DATA REDUCTION

Because polymers have in the past been successfully characterized with the aid of the theory of viscoelasticity, polymeric based composite materials were tested to characterize them using analogous techniques. The significant variables for these advanced composite materials are load and load history, time (frequency, load rate), temperature, and chemical environment in addition to geometric and lamina/laminate properties.

While the theoretical analysis of a composite material can be based on all relevant variables, the influence of these variables on the experimental results will by no means be equally significant.

To determine the individual contributions of time, temperature, humidity, load rate, load sequence, specimen geometry, physical properties, and fiber-matrix composition to the long term behavior of composite materials would require an inordinately large number of specimens and tests. In order to isolate the variables with significant contributions and their ranges, experiments have been designed for maximum utilization of specimens.

First nondestructive, axial and transverse vibration tests were performed from which frequency dependent damping and relaxation moduli can be determined.

Based on these results, destructive experiments such as constant strain rate and creep tests involving various test temperatures, have been performed.

A statistical evaluation utilizing multiple regression techniques was performed to establish the relative significance of the variables.

MATERIALS AND SPECIMENS

Because the aim of the program was to establish accelerated testing techniques rather than to determine the mechanical properties of specific composite materials, the specimens chosen for the experiments were fiber controlled laminates with epoxy matrices. One metallic and one nonmetallic fiber was used. Specimens were fabricated by the Brunswick Corporation of Marion, Va.

The materials investigated were Graphite/Epoxy and Boron/Epoxy composites with a basic ply arrangement of 50% zero and 50% $\pm 45^\circ$ fiber orientation.

For Boron/Epoxy specimens, Avco 55-05 tape was used in a layup $(0/-45/+45/0)_S$. The specimens were 8 plies thick (0.045") with 55 to 60% fiber volume and 5% maximum void content. Hercules X3501A-S graphite tape was used for Graphite/Epoxy specimens with a layup similar to that described above. More detail regarding specimen preparation and procurement is given in Appendix A.

Specimen geometries and types are shown in Figure 1. Type I specimens were affixed with fiberglass end tabs. They were used for creep and constant-strain rate tests; Type III specimens were of various lengths and were used for complex modulus tests.

Specimens were stored in sealed polythelene bags in desiccators to protect them from the environment. Their end tabs were marked with identification numbers.

VIBRATION TESTS

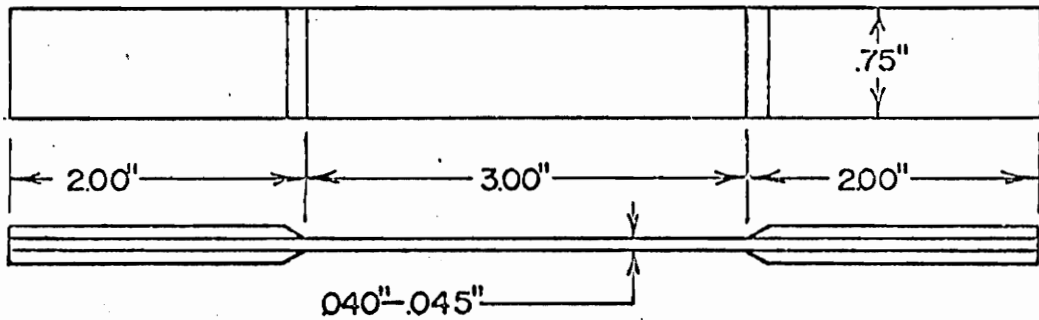
Forced vibration tests were performed using axial and transverse excitation on Type III specimens of different lengths as shown in Figure 1. At least five specimens of each length were used for each axial as well as transverse excitation to determine the Elastic (storage) Modulus and the Damping Ratio for both Graphite/Epoxy and Boron/Epoxy composites as functions of frequency. The tests were carried out in a temperature controlled cabinet at six different temperature levels ranging from -50°F to $+300^{\circ}\text{F}$, in the frequency range of 20 to 17,000 Hz.

For Bending Vibration tests double cantilever beams were clamped across their width at midspan. The clamps were attached to an accelerometer which in turn was secured to the moving element of an electrodynamic shaker (Figure 2). For Axial Vibration tests one end of the specimen was clamped to an adapter which was secured to the accelerometer by a screw.

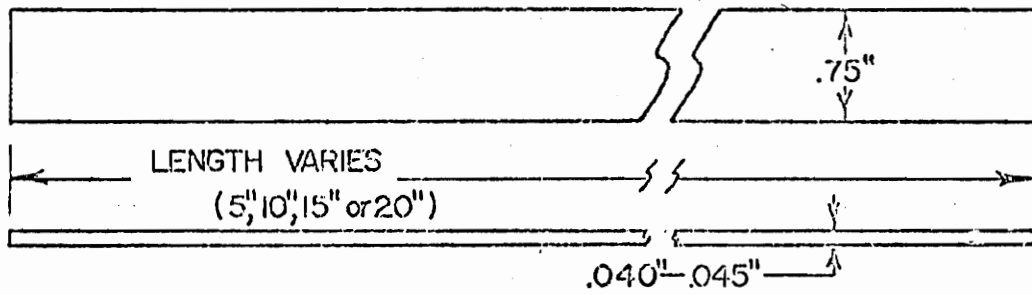
The beams were vibrated vertically by sinusoidal excitation with constant amplitude acceleration, while the frequency was swept over the range of interest.

A test setup view and a schematic line diagram of various units employed in the system are shown in Figures 3 and 4. Frequency was monitored by an electronic counter.

TYPE I SPECIMENS



TYPE III SPECIMENS



CREEP, CONSTANT STRAIN RATE SPECIMENS (TYPE I)
AND COMPLEX MODULUS SPECIMENS (TYPE III)

Figure 1. Specimen Configurations.

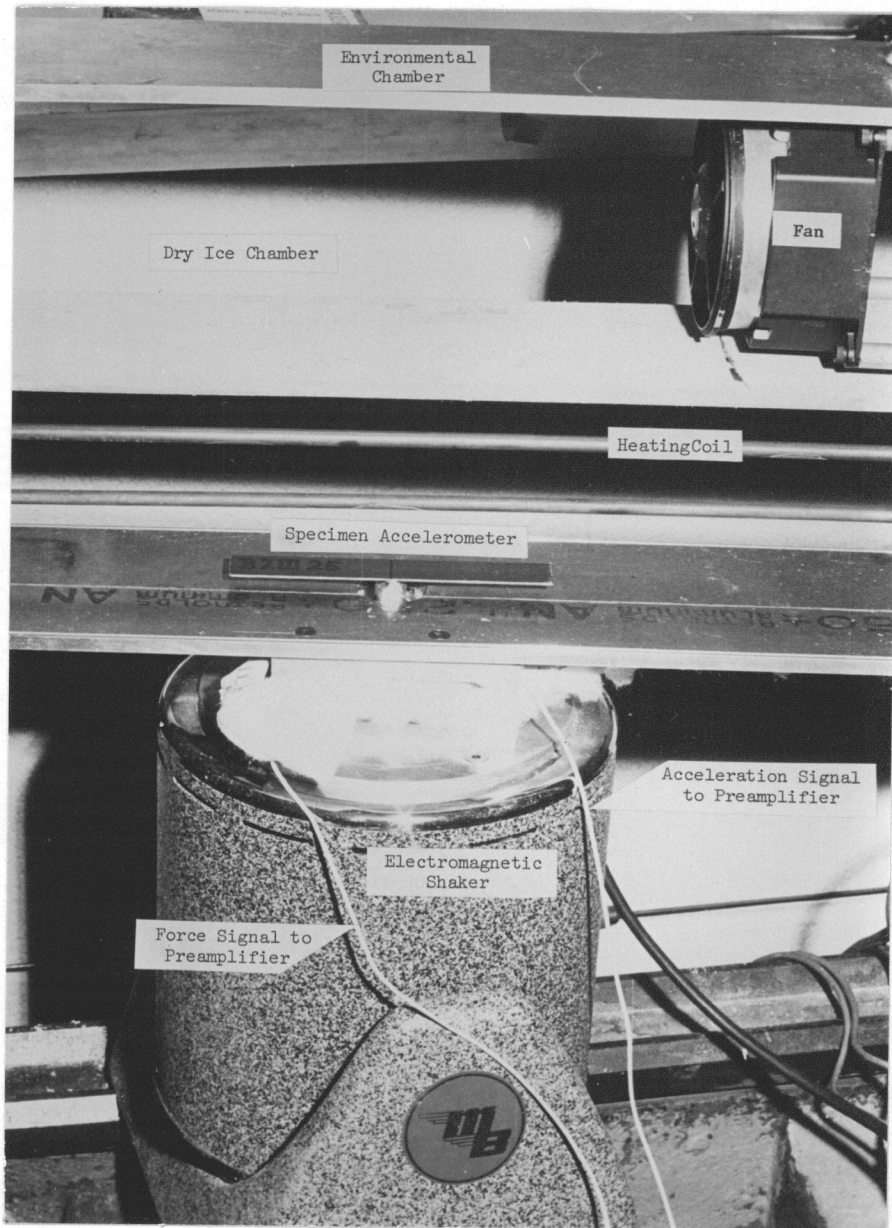


Figure 2. Details of Forced Vibration Test Setup.

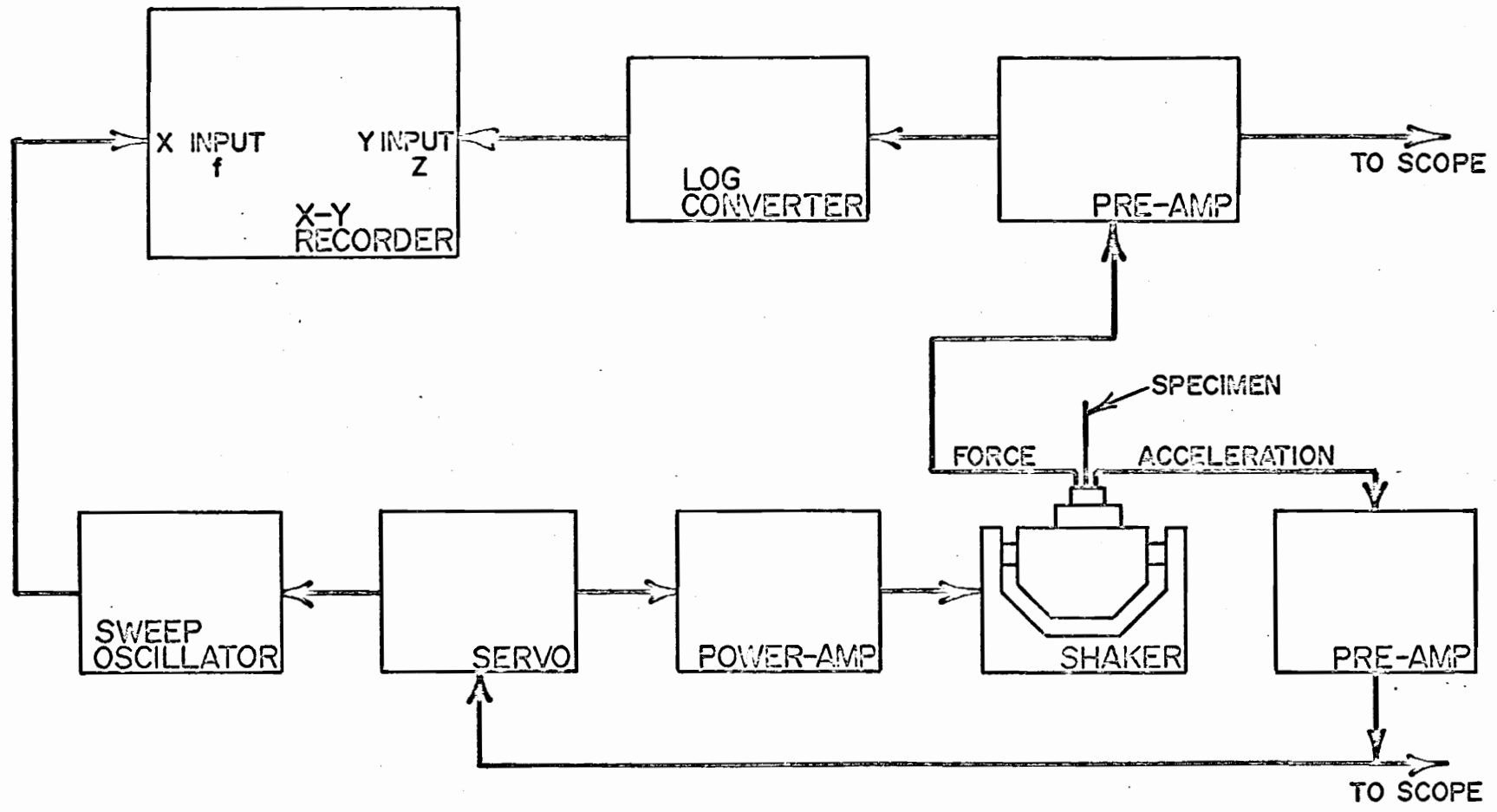


Figure 4. Schematic Diagram of Vibration Testing System.

A frequency versus acceleration/force, diagram was automatically recorded on an x-y plotter. Such curves reach a minimum value at a resonant frequency (when the amplitude of motion is the largest) and a maximum at the anti-resonant frequency (when the amplitude of motion is a minimum). Typical acceleration/force vs. frequency curves from the x-y plotter at different temperatures are shown in Figure 5.

The dynamic mass contribution of the accelerometer and adapter can be eliminated from the measurement by the technique of mass cancellation. While this is often a useful method, it needs more instrumentation. This problem can be easily dealt with by computing storage modulus and damping ratio from the anti-resonance peak instead of the resonance peak. Figure 6 shows that the resonance peak is shifted due to the apparent mass of the accelerometer and adapter while the anti-resonance peak is unaffected. The lowest three anti-resonant peaks were generated for each specimen in bending as well as in axial excitation. Initially specimens were attached to the accelerometer using an adhesive, but analysis of new and old data raised doubts about the validity of these axial test results. Control tests on 2024-T3 aluminum in both bending and axial excitation indicated that adhesive attachment of axially loaded specimens introduced additional damping (Figure 7). The fixture was therefore redesigned to a mechanical clamping arrangement and tests on Graphite/Epoxy specimens were repeated. Results compare favorably with those reported in Reference [65].

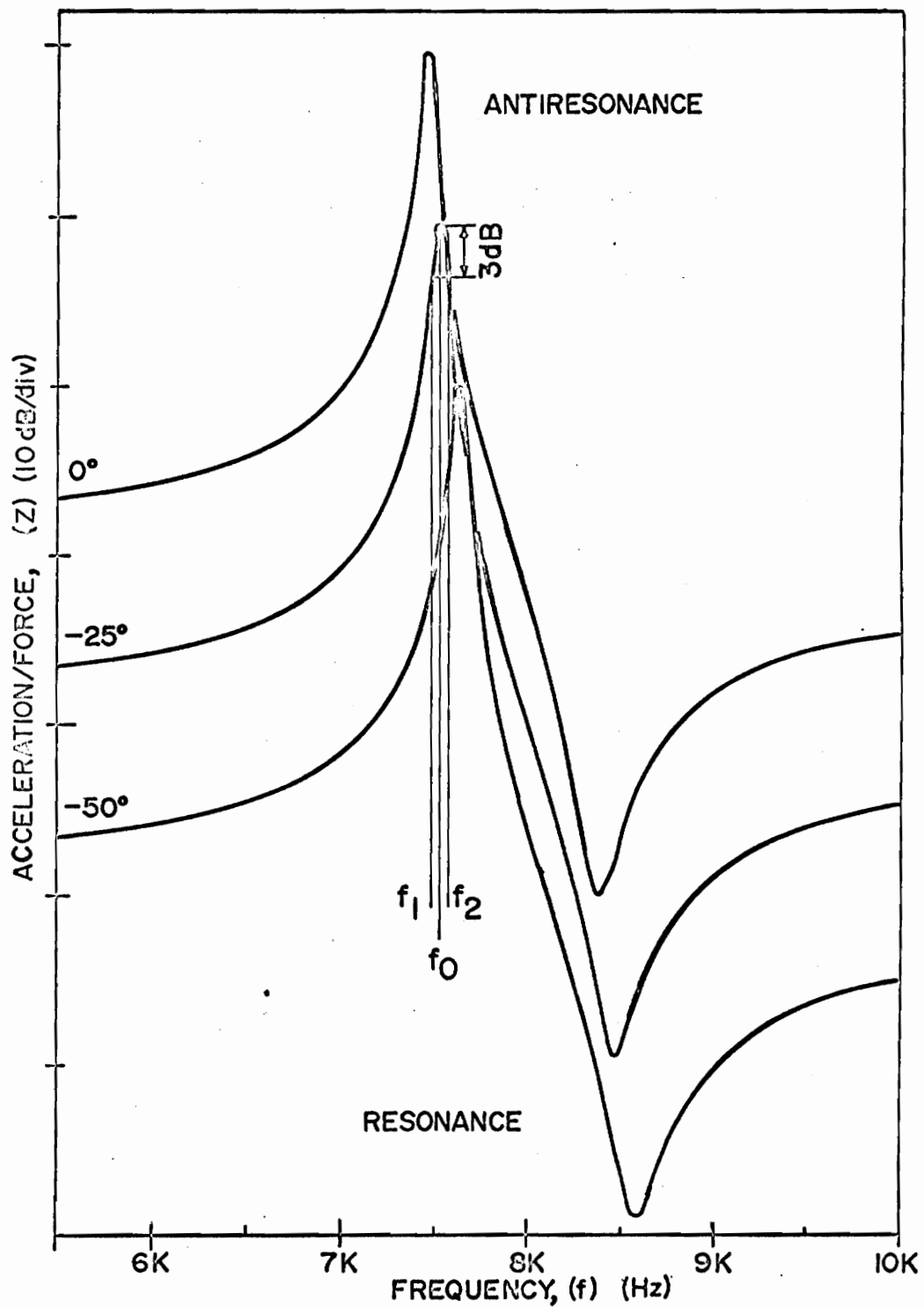


Figure 5. Typical Impedance vs. Frequency Curves for Boron/Epoxy.

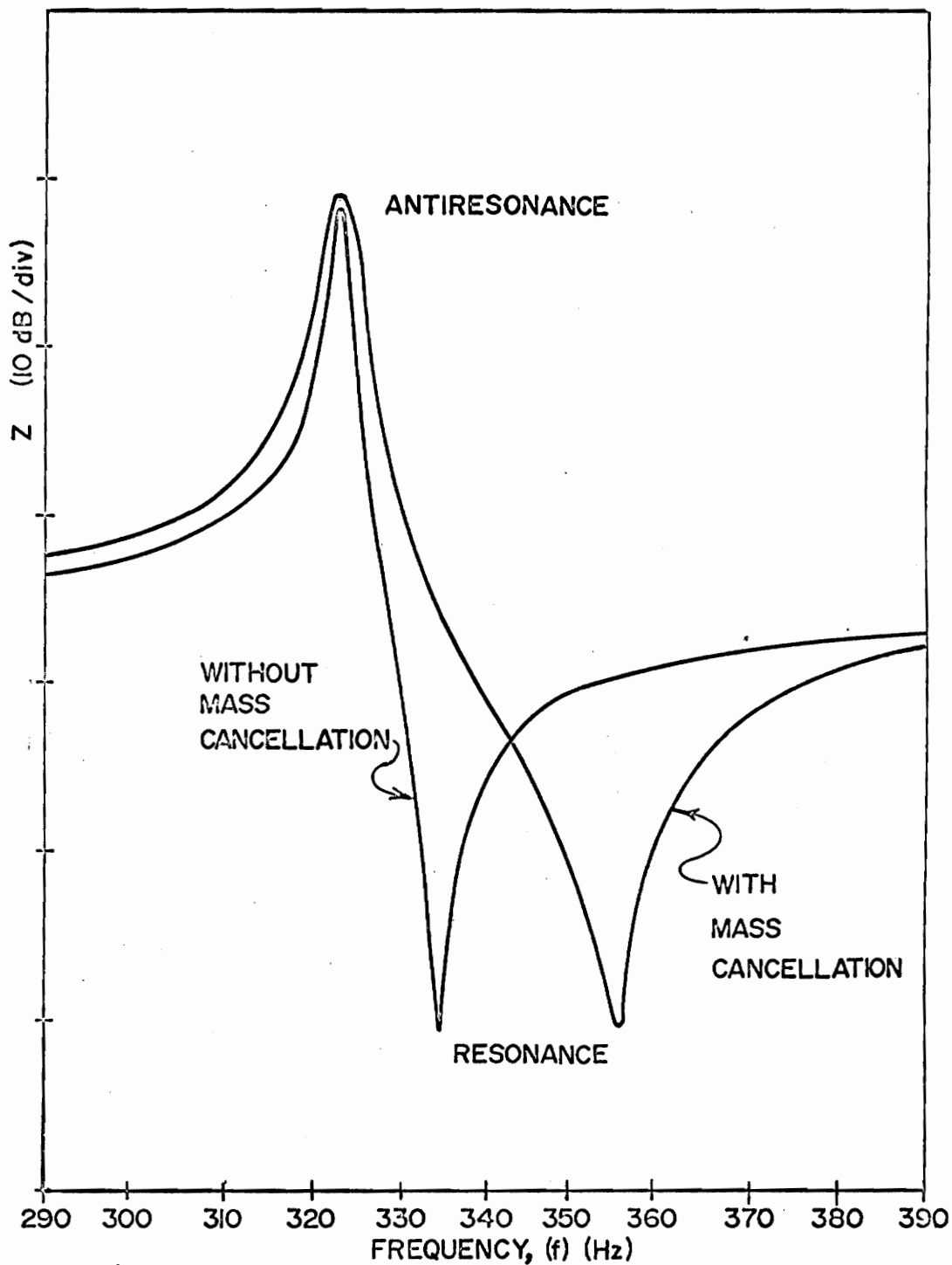


Figure 6. Effects of Mass Cancellation on Resonance and Antiresonance Peaks.

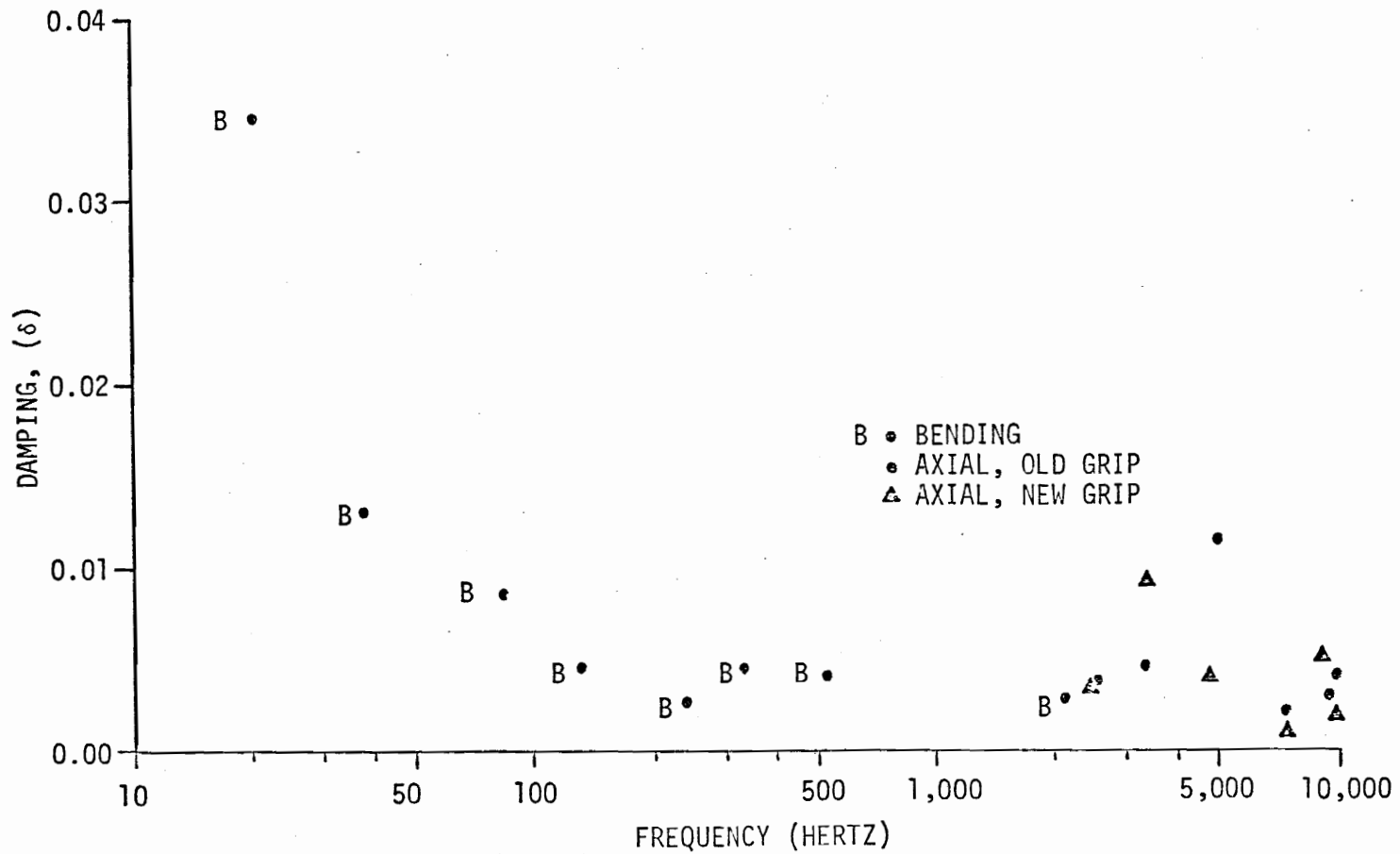


Figure 7. Vibration Tests on 2024-T3 Aluminum, Under Axial and Bending Loads.

The equations for computing storage modulus and damping ratio are given in Appendix B. Reference [94] provides more detail for these tests.

A typical plot of storage modulus and damping ratio vs. frequency is shown in Figures 8 and 9. Plots at different temperatures are reported in References [91] and [92].

Tests were also conducted on specimens in a humid environment. Specimens were conditioned in steam, their moisture content was measured by careful weighing, and storage modulus and damping ratios were determined as indicated in Figure 10.

Tests under various humidity and temperature combinations were also performed. Controlled conditions of relative humidity were achieved by continuous recirculation of the air from a Webber temperature humidity chamber across an insulated test cabinet. The operating range for the temperature-humidity chamber was from -100°F to $+350^{\circ}\text{F}$ for dry conditions. Zero to 100% relative humidity can be regulated for temperatures between the freezing and boiling points of water. The chamber is equipped with a two-pen, two cam programming and recording controller for controlling and recording both wet and dry bulb conditions. At the time of the writing of this report, the data obtained has not been analyzed.

CONSTANT RATE TESTS

Tensile tests to determine the effects of strain rate and temperature on the mechanical properties of Boron/Epoxy and Graphite/Epoxy specimens were conducted over a wide range of strain rates and

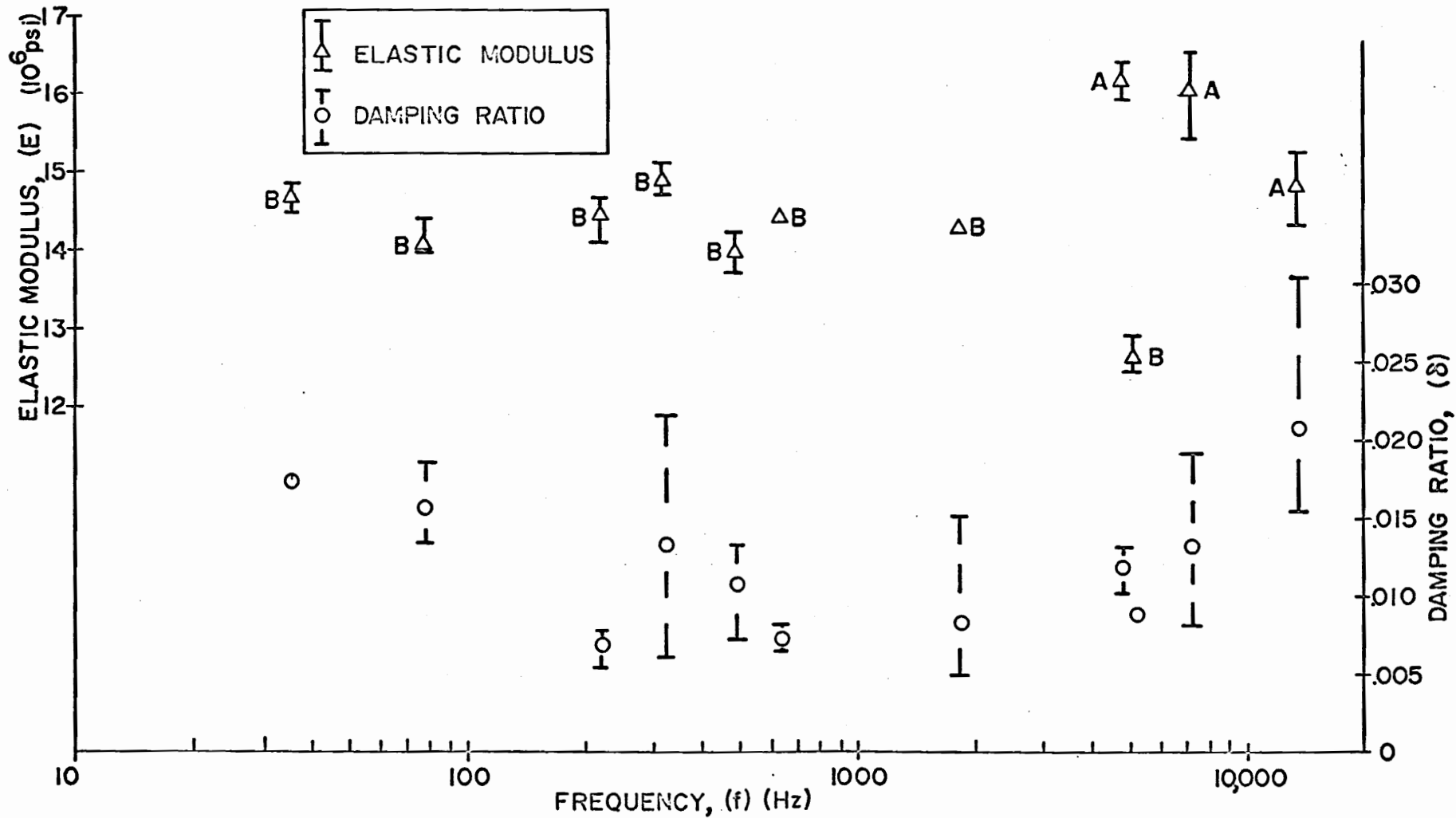


Figure 8. Vibration Test Results on Boron/Epoxy Specimens at 300°F.

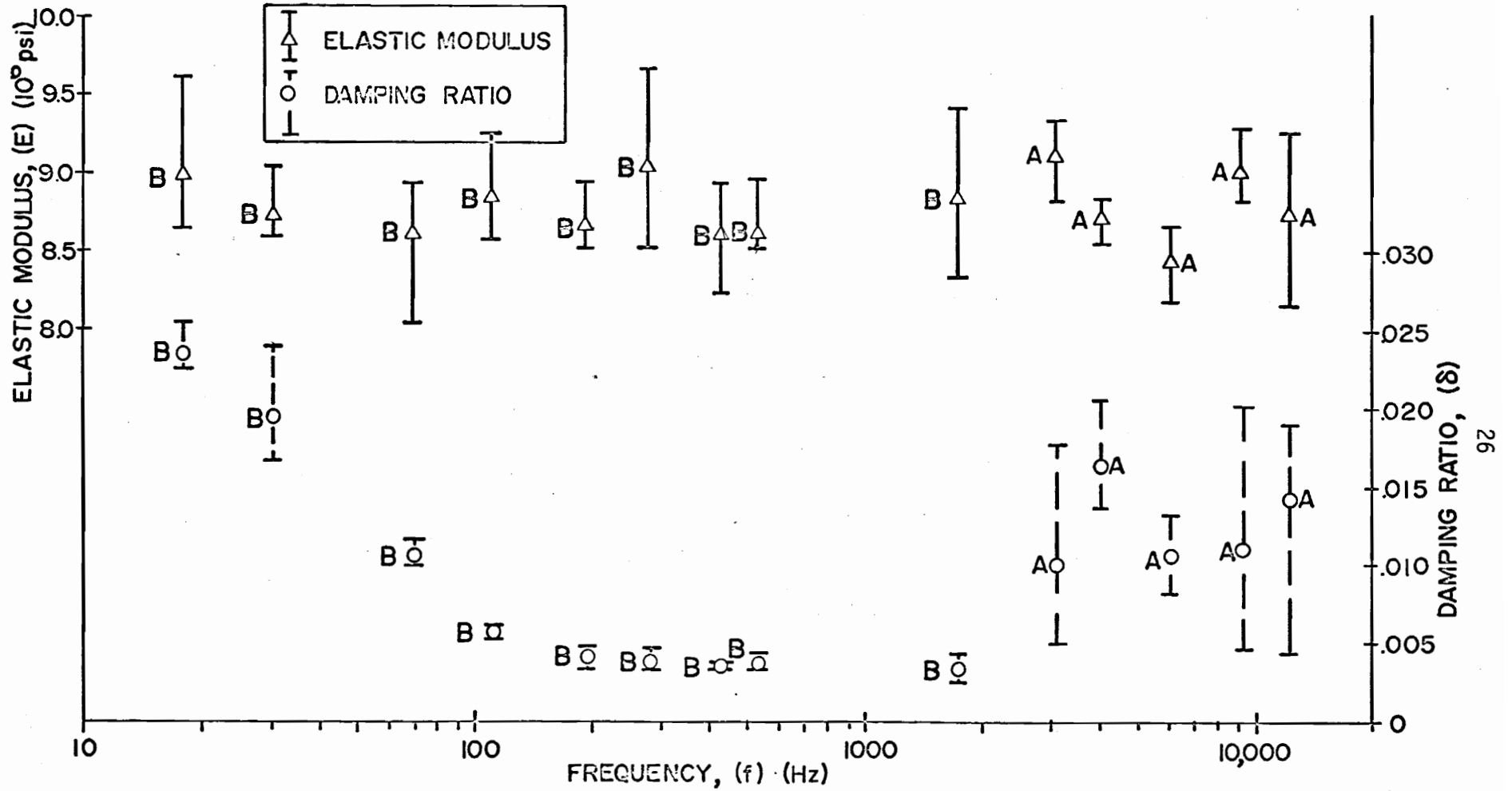


Figure 9. Vibration Test Results on Graphite/Epoxy Specimens at 200°F.

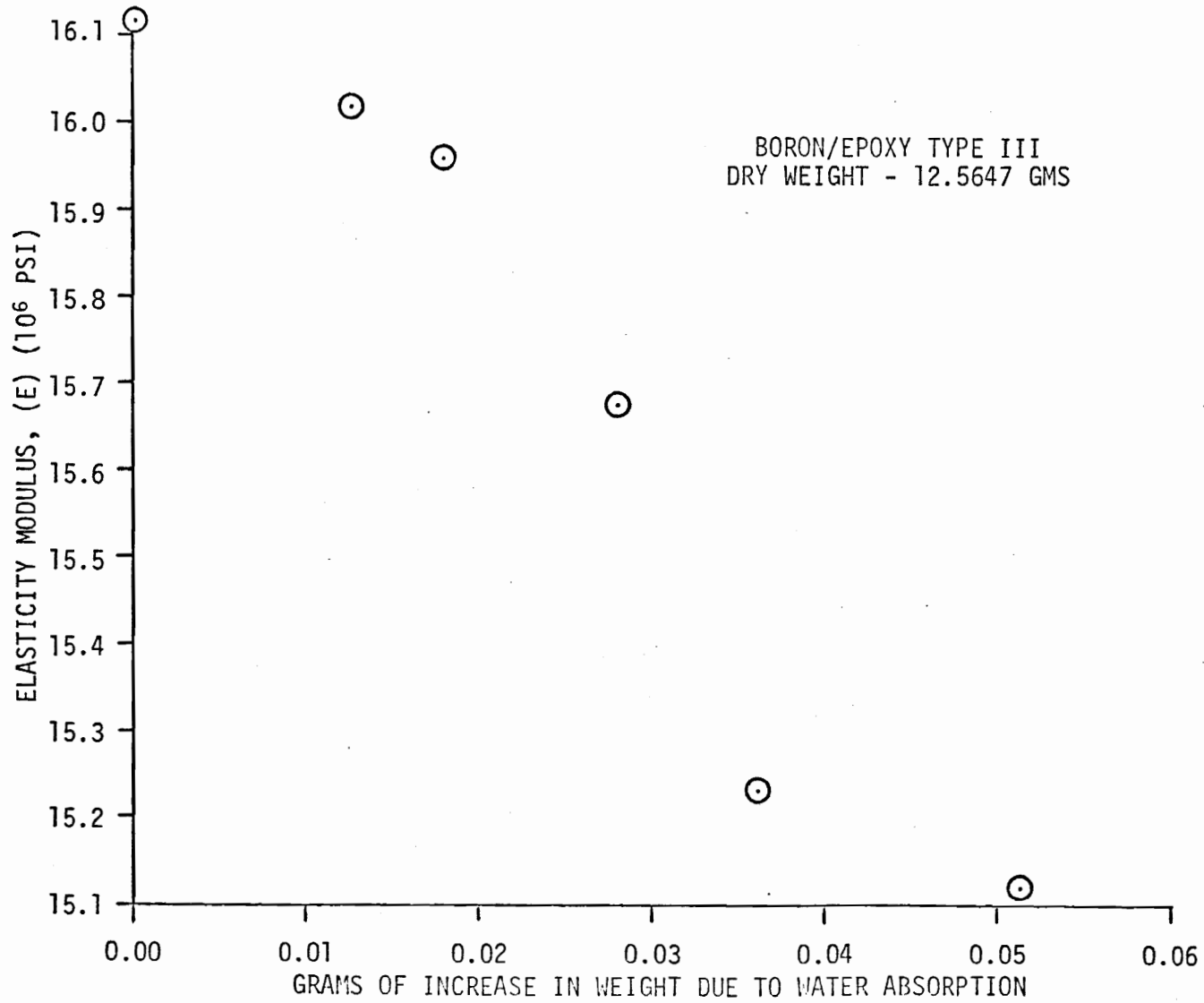


Figure 10. Variation of Modulus with Moisture Content.

temperatures. Several tests were performed at each temperature level of -50°F , 0°F , 80°F , 200°F and 300°F and at four strain rates ranging from 1.5μ in/in/sec to $5 \times 10^5\mu$ in/in/sec for Boron/Epoxy and from 2.1μ in/in/sec to $2.5 \times 10^4\mu$ in/in/sec for Graphite/Epoxy.

The lower strain rate on tests for each material were carried out on an Instron universal testing machine. Specimens were mounted in standard wedge grips with a universal joint positioned between the upper grip and the load cell to maintain alignment. The output of the load cell was continuously recorded in the form of load-time plots on a strip chart recorder. Strains were measured with strain gages attached to the specimens. Strains were also recorded as continuous functions of time on a strip chart recorder.

High temperatures were achieved by positioning a resistance coil heater around the specimen. For low temperatures a dry-ice chamber was added to the set up. This together with the coil heater was used to stabilize temperatures at the desired levels. Temperatures were measured using thermocouples attached to the specimen. The test specimen and compensating specimen were allowed to soak at the test temperature for 30 minutes before testing. The upper grip was not tightened until after the soak period to prevent any thermal stresses.

As a part of some peripheral studies, Acoustic Emission was also monitored during tensile strain rate tests. The constant-rate test setup showing details of equipment and accessories used is presented in Figure 11.

Tensile tests for the higher strain rates were performed on an MTS closed loop hydraulic testing machine operated in a manual

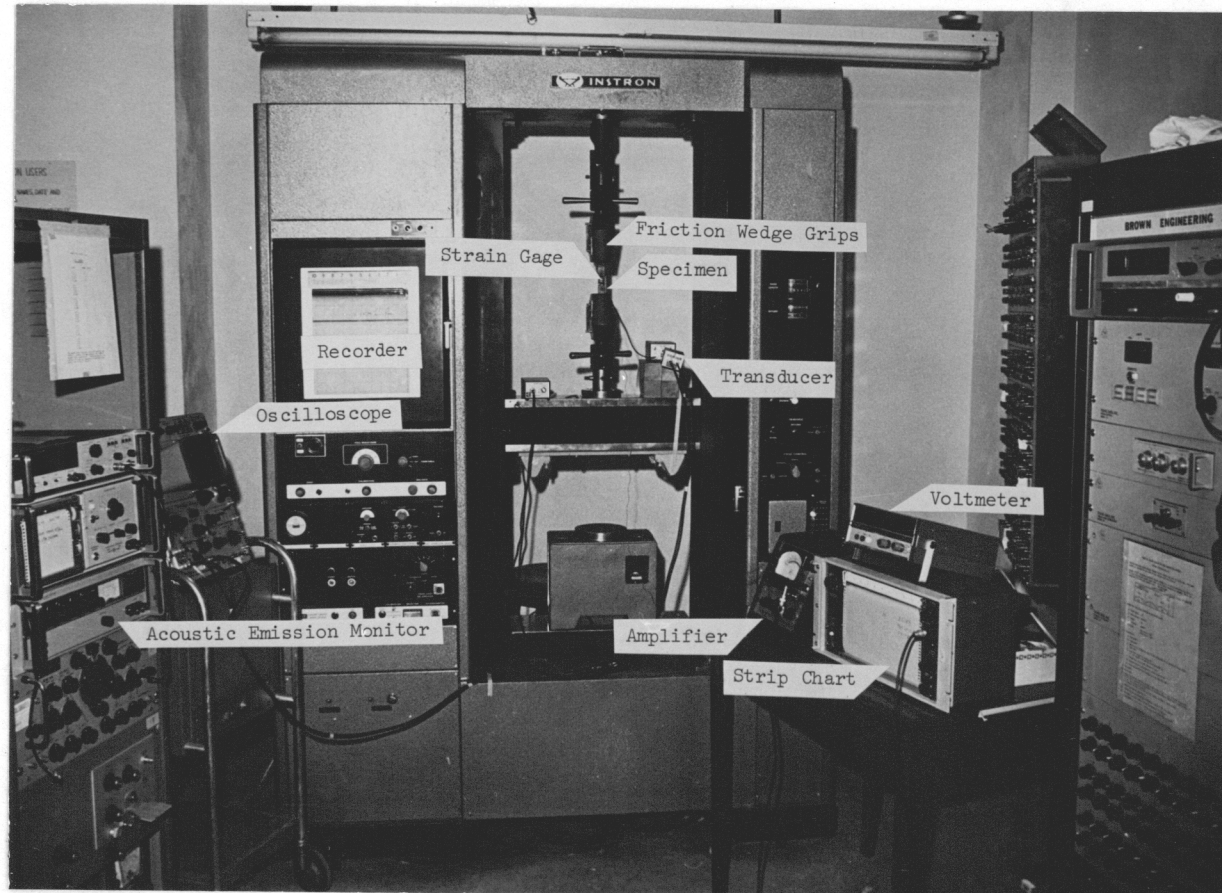


Figure 11. Constant-Rate Test Setup.

control mode. The specimens were mounted in Instron wedge grips similar to those used in the lower rate tests. Again, a universal joint was positioned between the upper grip and the load cell; however, because of the high strain rates imposed during these particular tests, it was necessary to bind the universal joint to prevent large rotations. Periodic alignment of the grip-universal system was checked with a steel specimen by monitoring load, torque, and angle of twist outputs of the MTS system and necessary adjustments were made.

The load and strain data were recorded as functions of time on a dual trace storage oscilloscope. The stored traces were then photographed for analysis. The trigger for the trace sweep was taken from the 0-10 volt square wave output of the MTS function generator.

High and low temperature tests were conducted in a manner similar to those described for the Instron tests. Since these tests (MTS) were load controlled, it was possible to tighten both grips before the specimen reached test temperature. Periodic checks made during the temperature stabilization time confirmed that the testing machine corrected for thermal expansion effects.

The data for both the lower and higher strain rate tests were recorded in load-time and strain-time form. Time was taken as a common parameter in reducing the data and plotting the stress-strain curves for each test. To reduce the error in this step, the time scales of the recorders were calibrated and appropriate time correction factors were determined. The calibration of all instrumentation was checked periodically.

Sample load-time and strain-time data from an Instron test are shown in Figures 12 and 13. The stress-strain curve for this test is shown in Figure 14 where stress is computed as the applied load divided by the original cross-sectional area of the specimen. Figure 15 represents typical oscilloscope traces for load-time and strain-time data. The resulting stress-strain curve is shown in Figure 16.

The linearity of the strain time traces (Figures 14 and 16) through most of the experiments shows that the strain rate is essentially constant.

The fracture strength of the specimens (ultimate load divided by the original cross-sectional area) was measured but strain measurements could not be made at fracture because in most experiments the bonding material of the strain gages failed before the specimens fractured. An estimate of the strain at failure may be made by dividing fracture stress with the modulus of elasticity. Because the material behavior is nearly linear almost to fracture, such an estimate is conservative.

An average strain rate was also computed based on the estimated strain at failure and the time to failure. Typical results for Fracture Strength and Elastic Modulus at different strain rates are shown in Figures 17 through 22. Plots of Fracture Strength, Elastic Modulus and Fracture Strain at various strain rates and temperatures are reported in Reference [91]. The strain rate data is listed in Appendix C of this report.

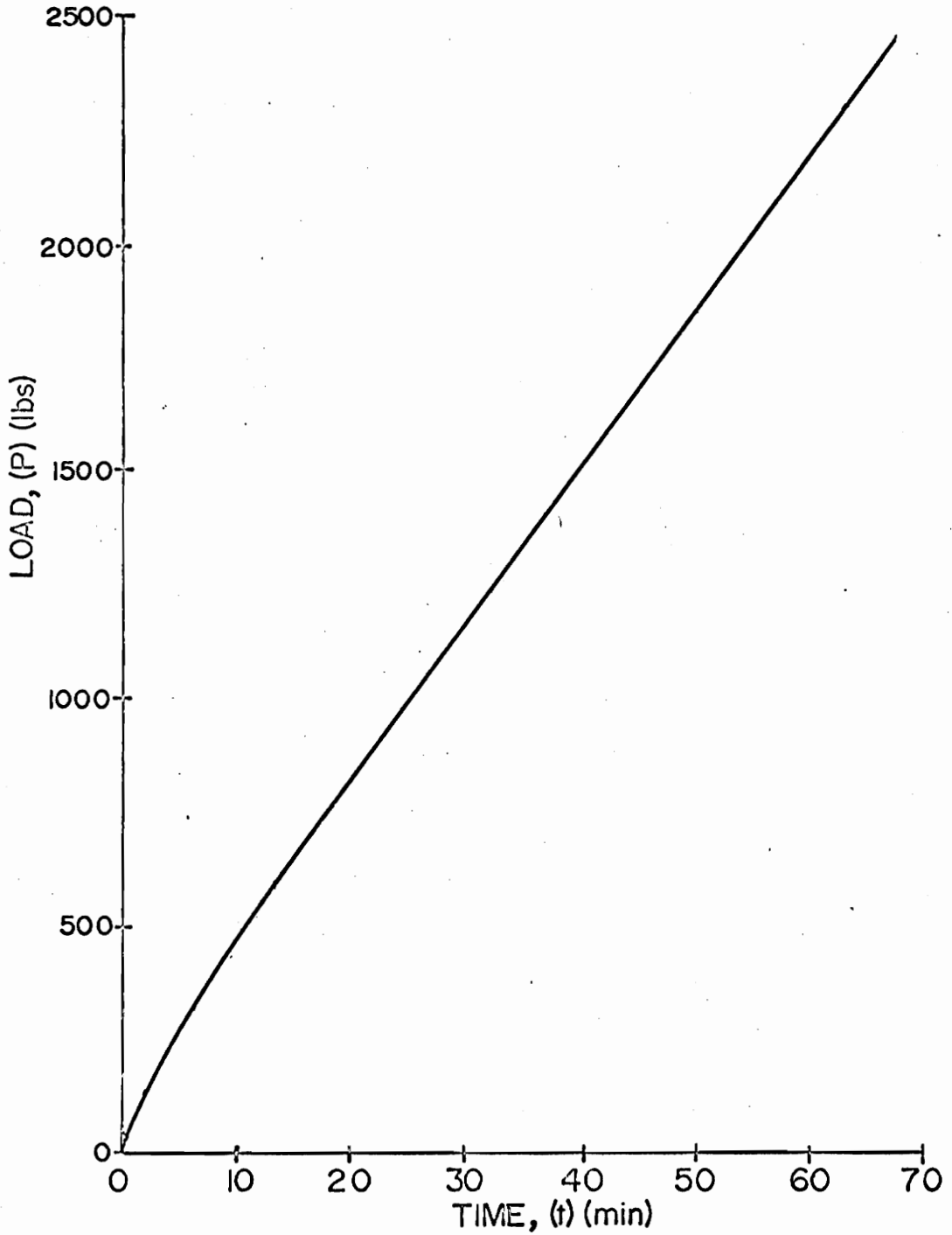


Figure 12. Load-Time Trace for Constant Head Rate Test on Instron Machine; Graphite/Epoxy Specimen at .002 In/Min.

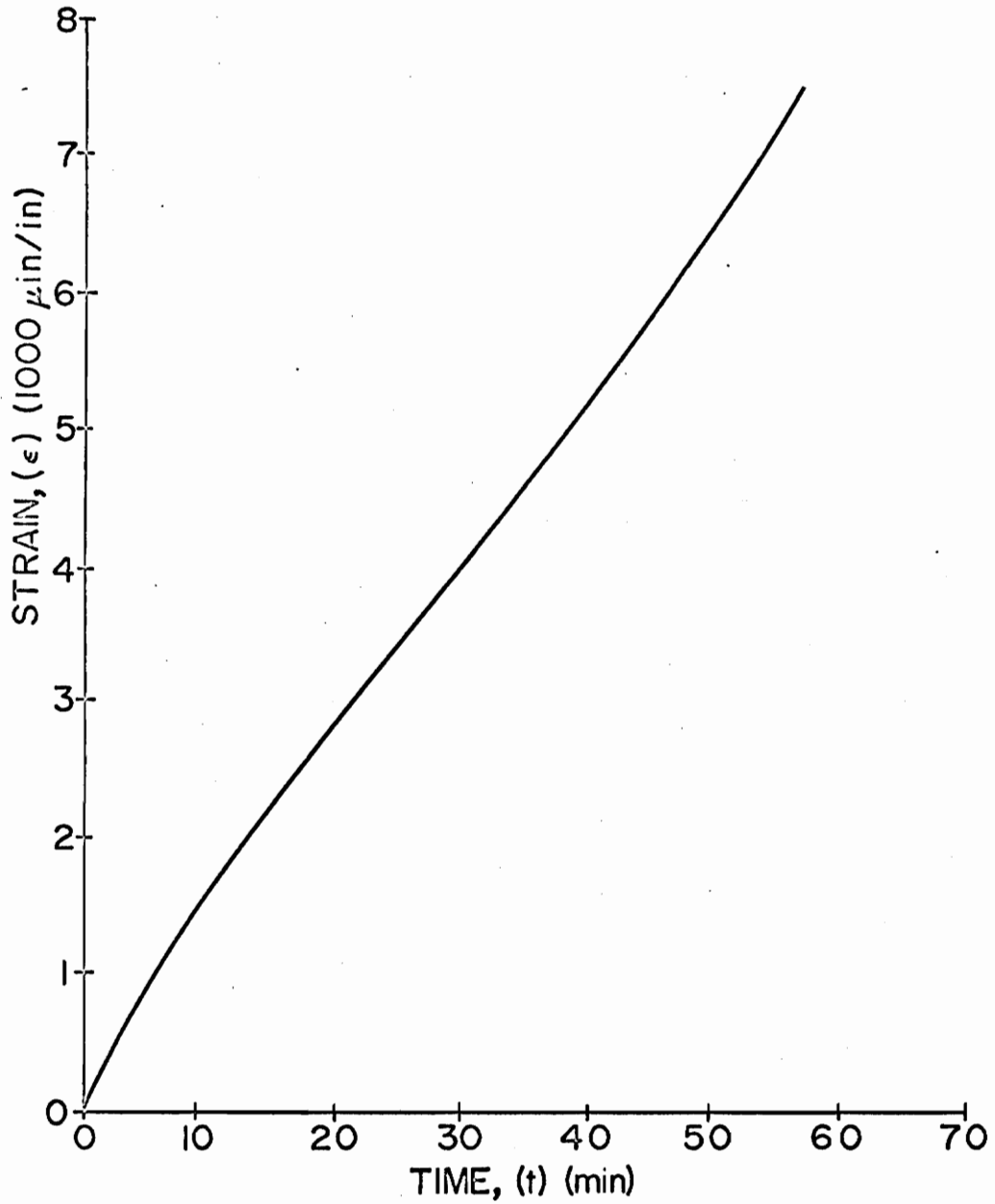


Figure 13. Strain-Time Trace for Constant Head Rate Test on Instron Machine; Graphite/Epoxy Specimen at .002 In/Min.

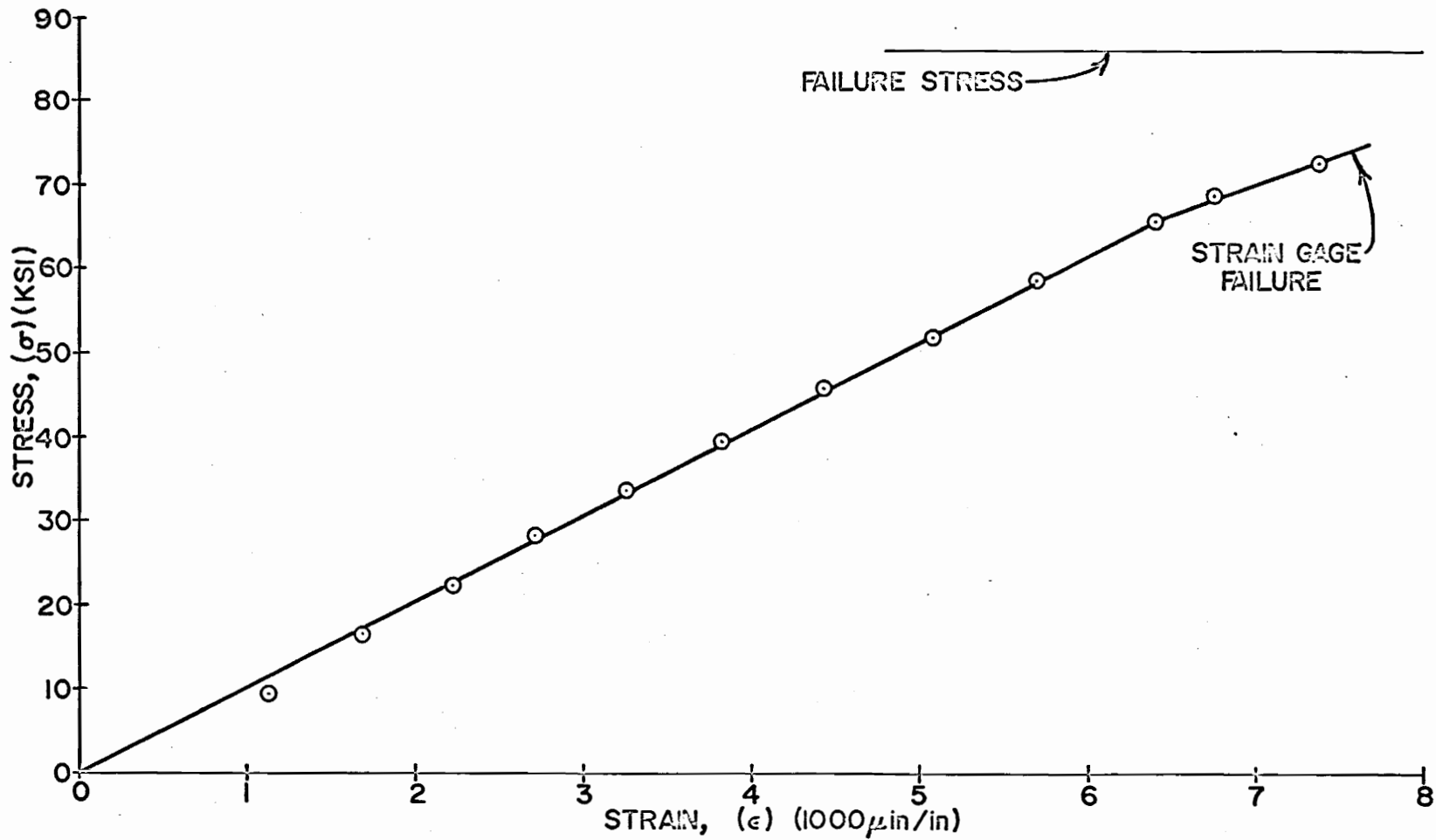


Figure 14. Stress-Strain Curve for Graphite/Epoxy Specimen Derived from Figures 12 and 13; Average Strain Rate = $2.3 \mu \text{ In/In/Sec.}$

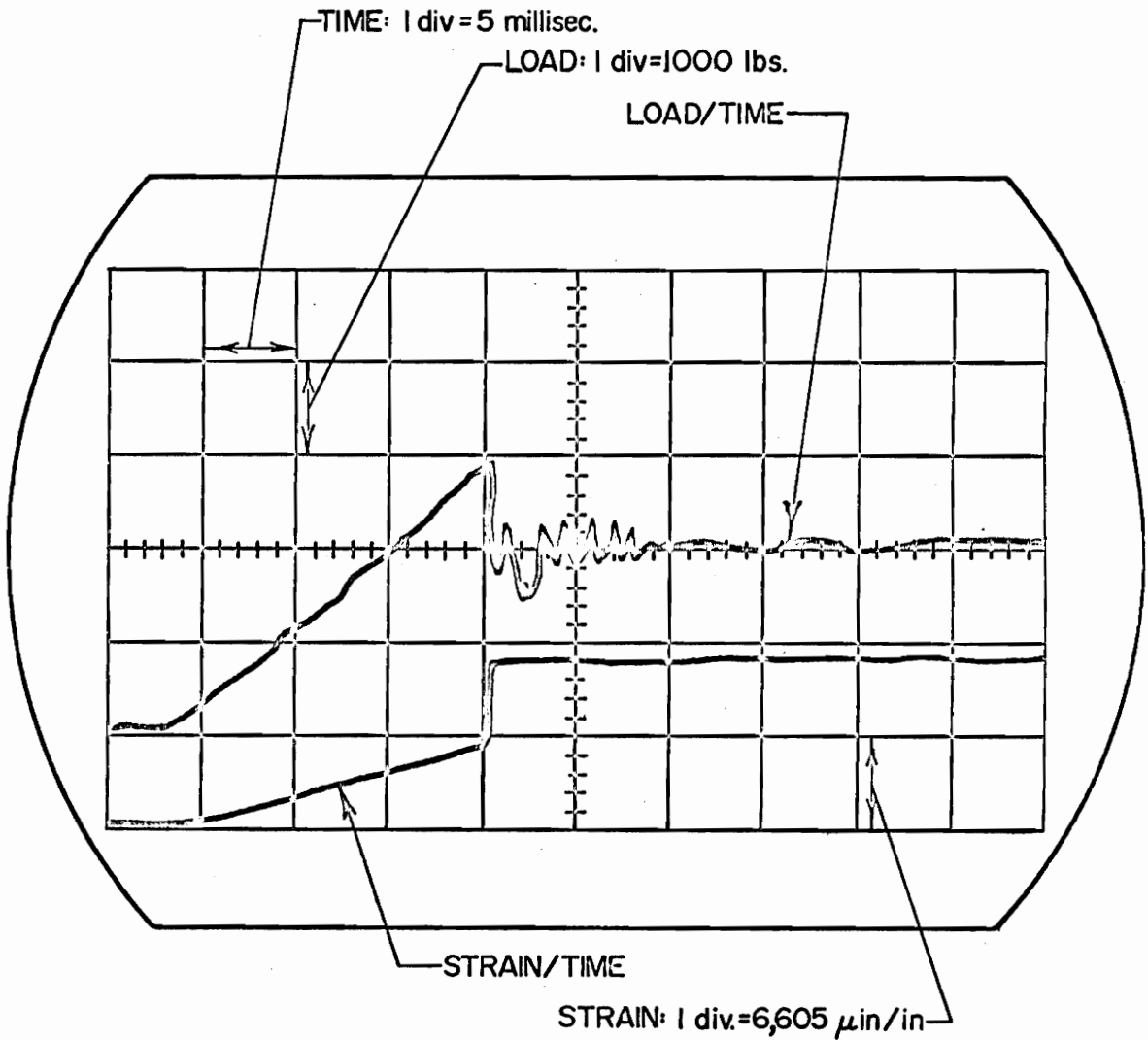


Figure 15. Load-Time and Strain-Time Traces for Constant Load Rate Tests on MTS Machine. Boron/Epoxy Specimen; 100 Hz, 50 KIP Range at 200°F.

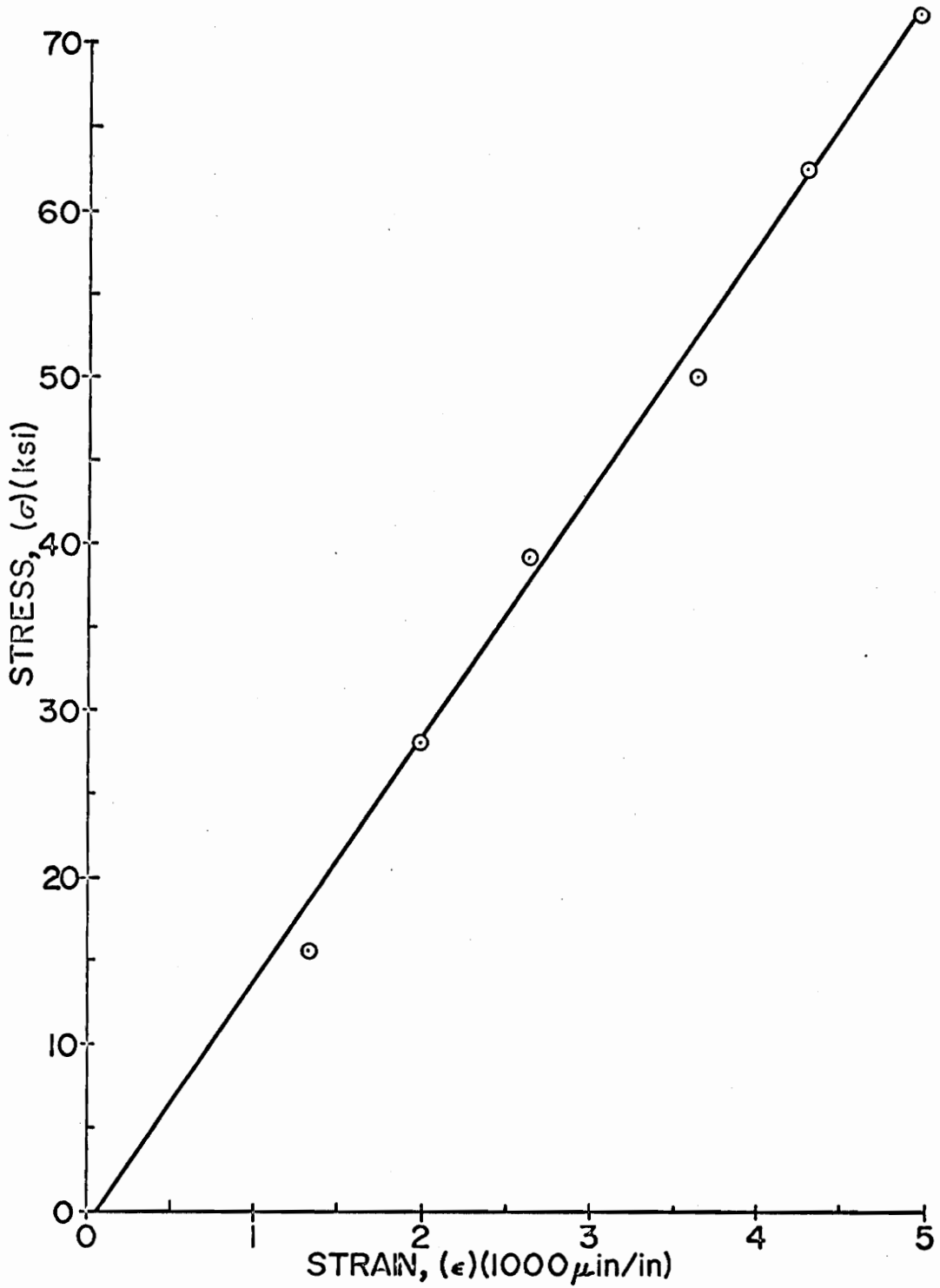


Figure 16. Stress-Strain Curve for Boron/Epoxy Specimen
Derived from Figure 15; Average Strain
Rate 305,800 μ In/In/Sec. at 200°F.

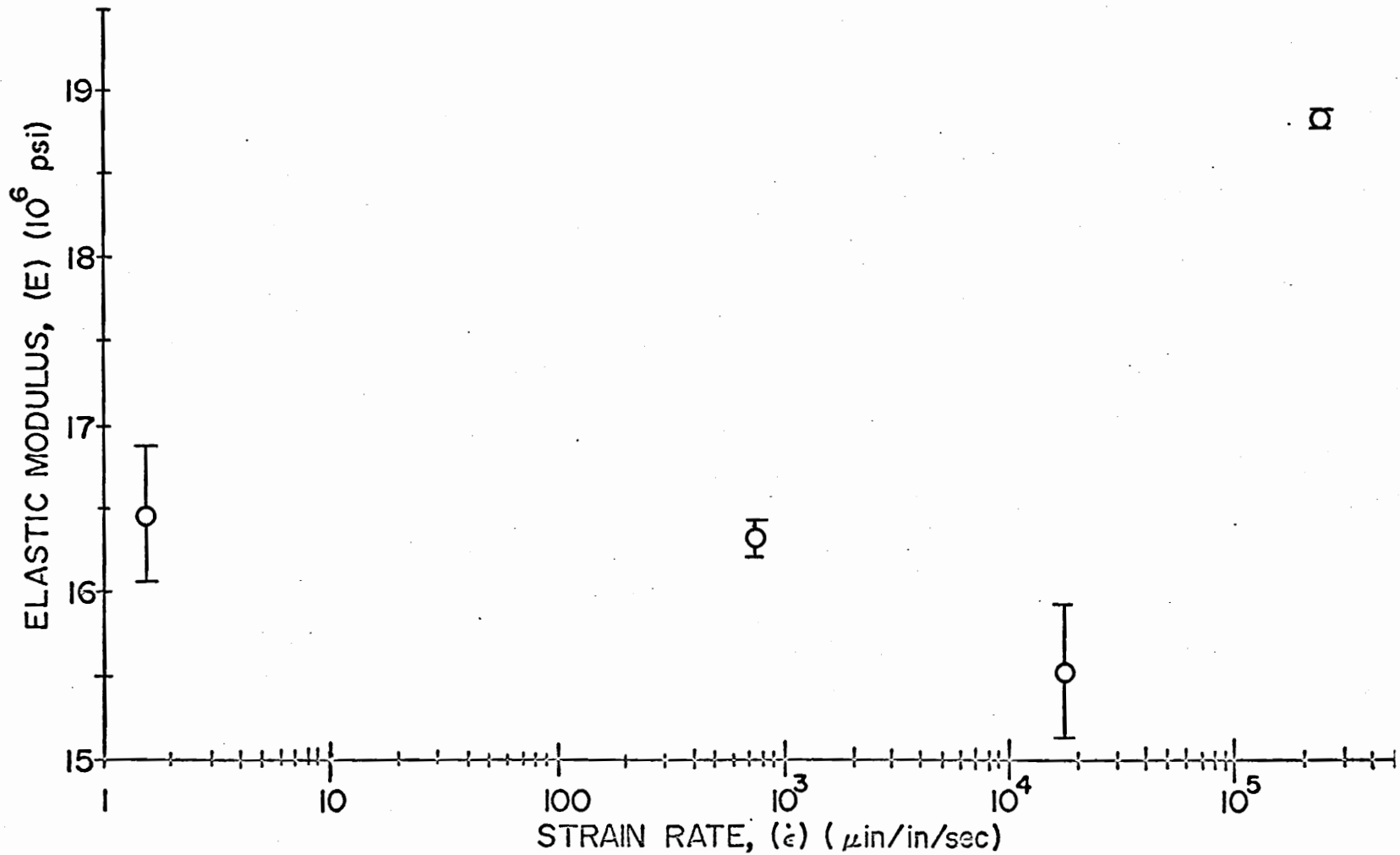


Figure 17. Initial Modulus-Strain Rate Test Results for Boron/Epoxy Specimens at -50°F .

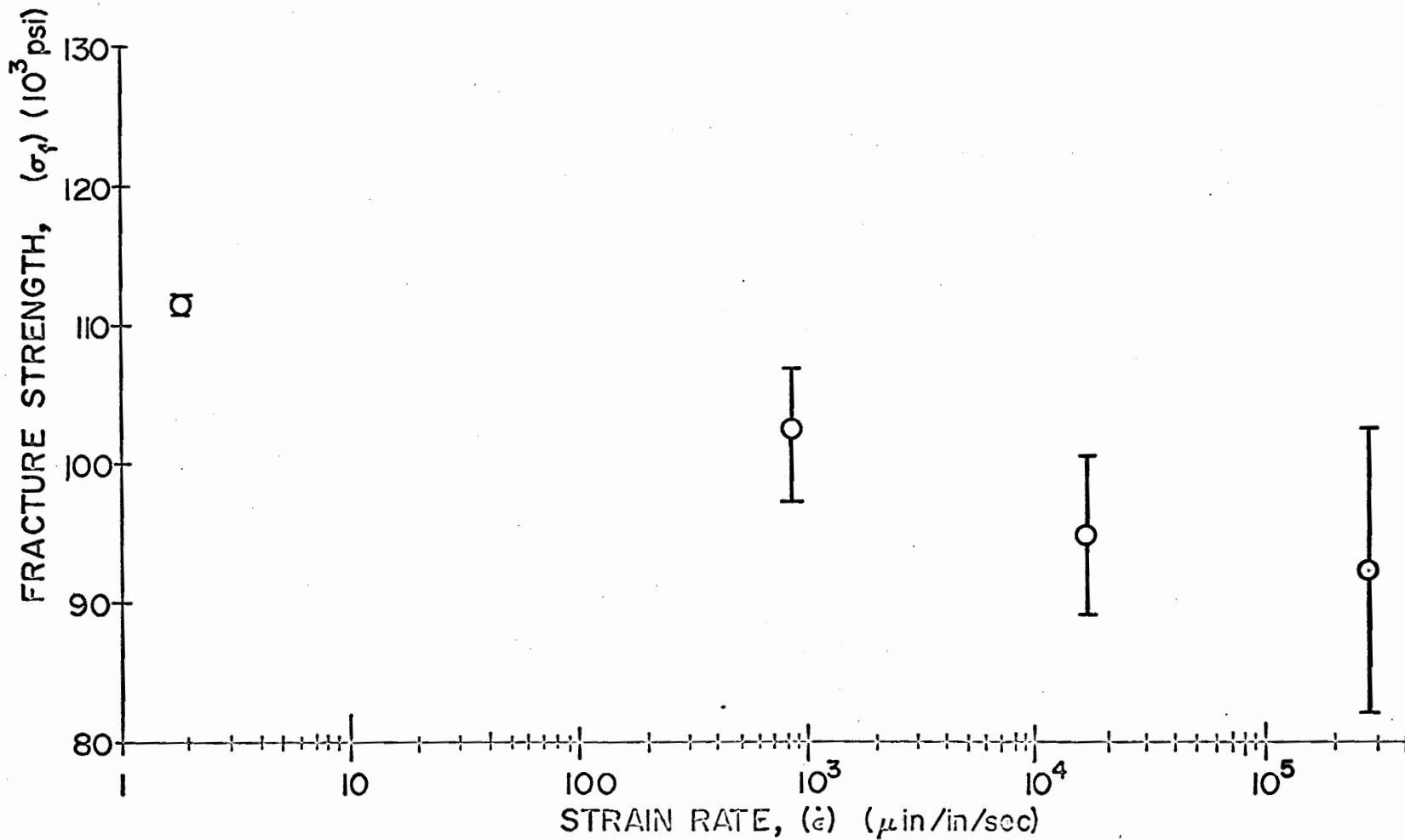


Figure 18. Fracture Strength-Strain Rate Test Results for Boron/Epoxy Specimens at 200°F.

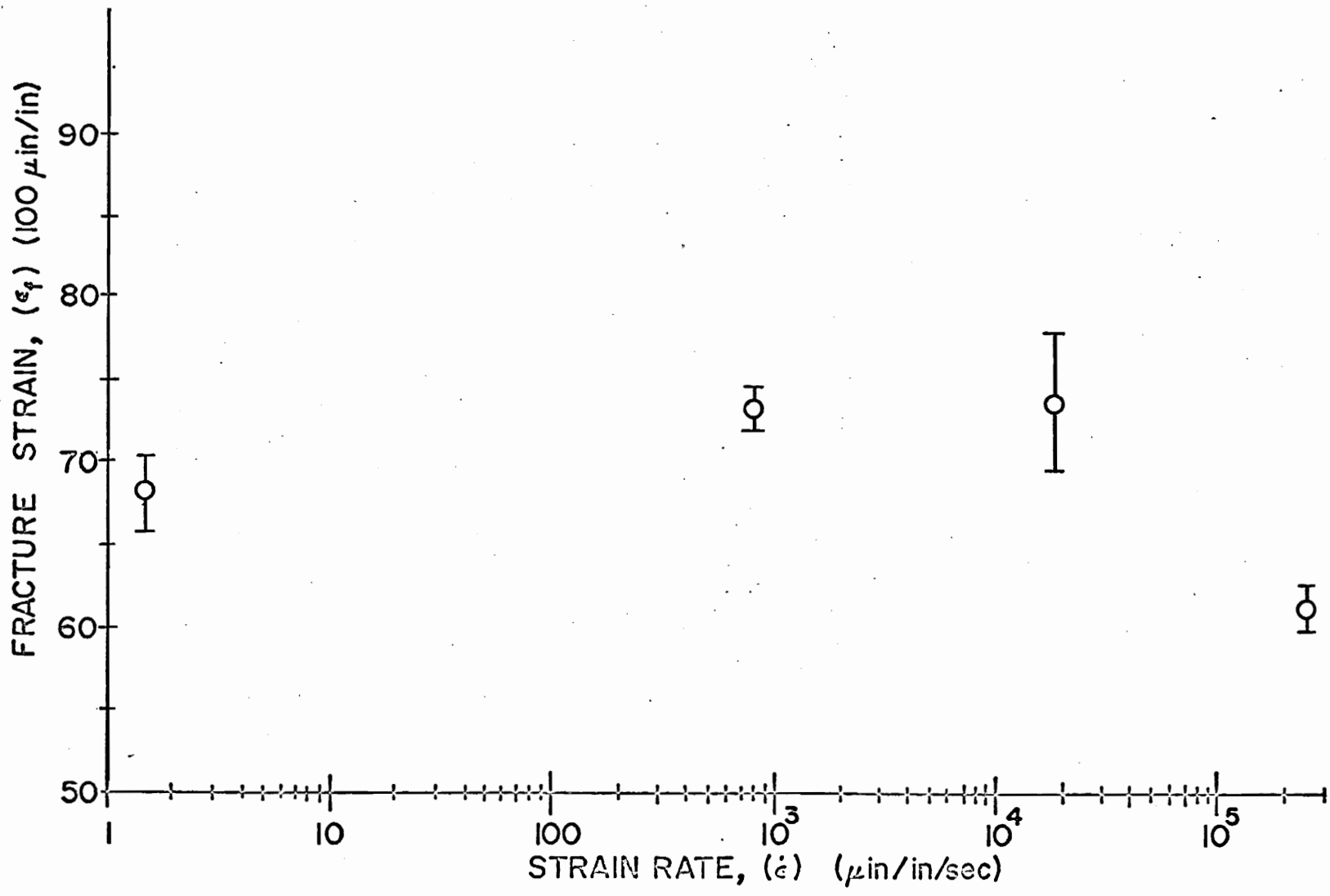


Figure 19. Fracture Strain-Strain Rate Test Results for Boron/Epoxy Specimens at -50°F .

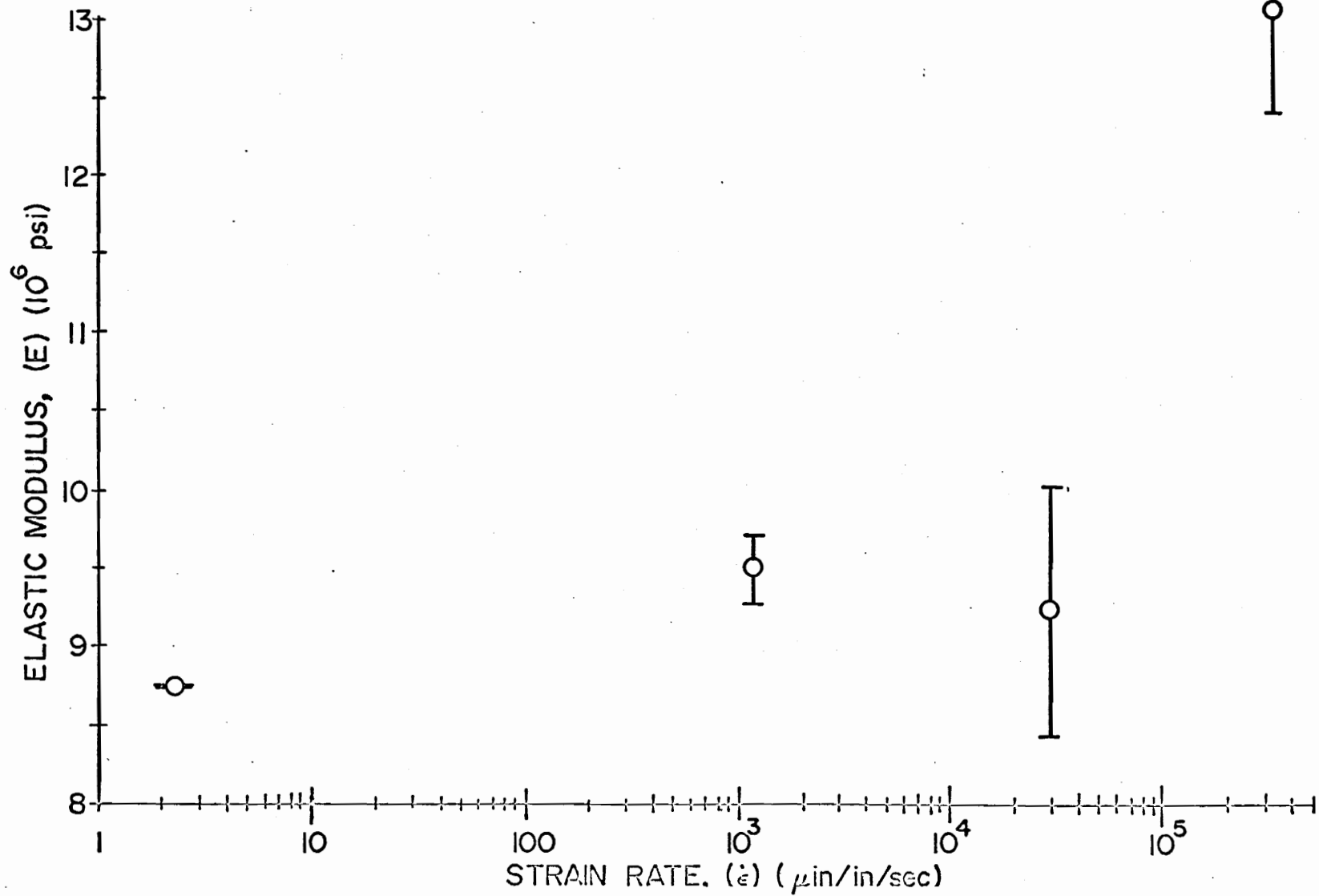


Figure 20. Initial Modulus-Strain Rate Test Results for Graphite/Epoxy Specimens at 300°F.

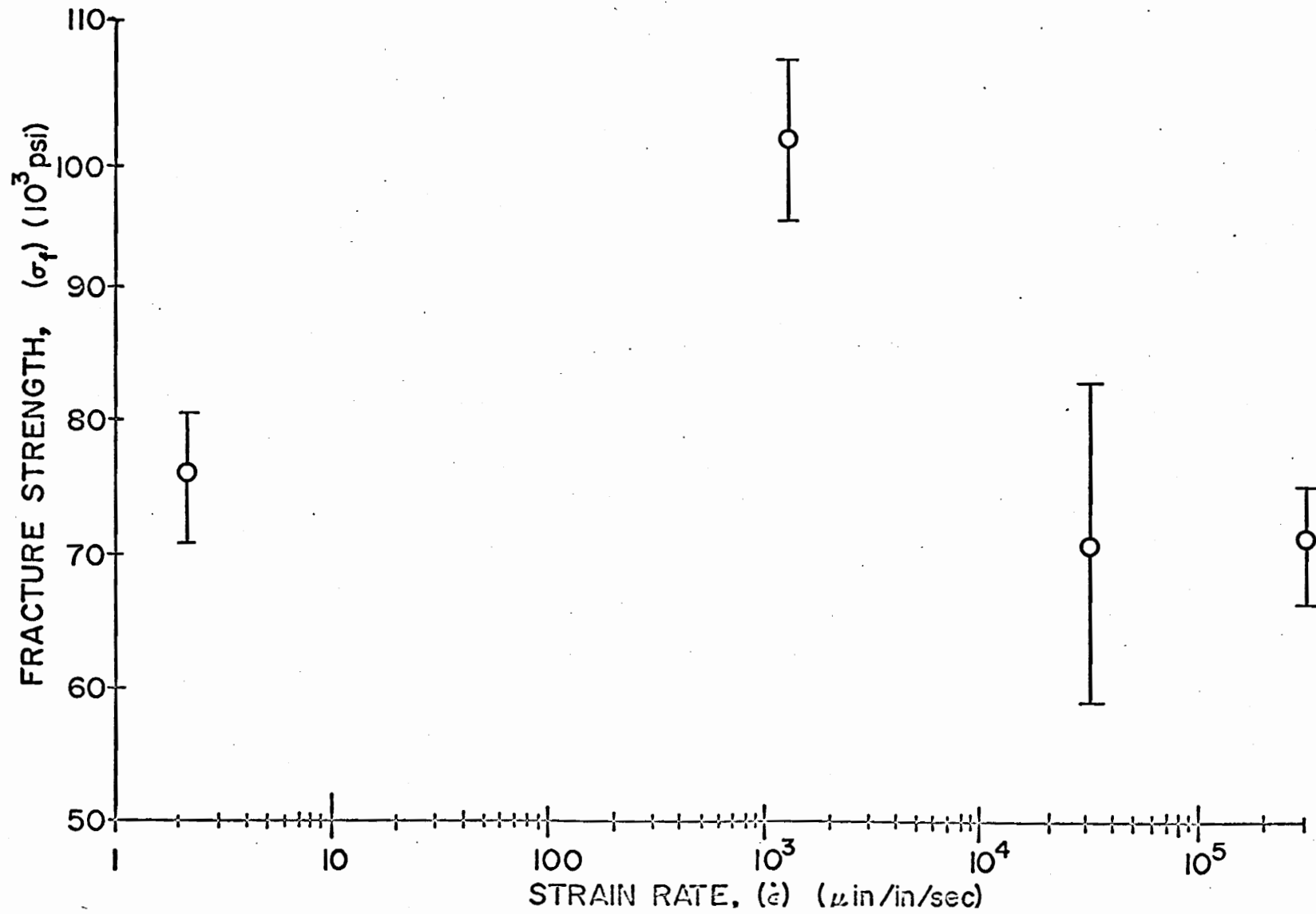


Figure 21. Fracture Strength-Strain Rate Test Results for Graphite/Epoxy Specimens at -50°F .

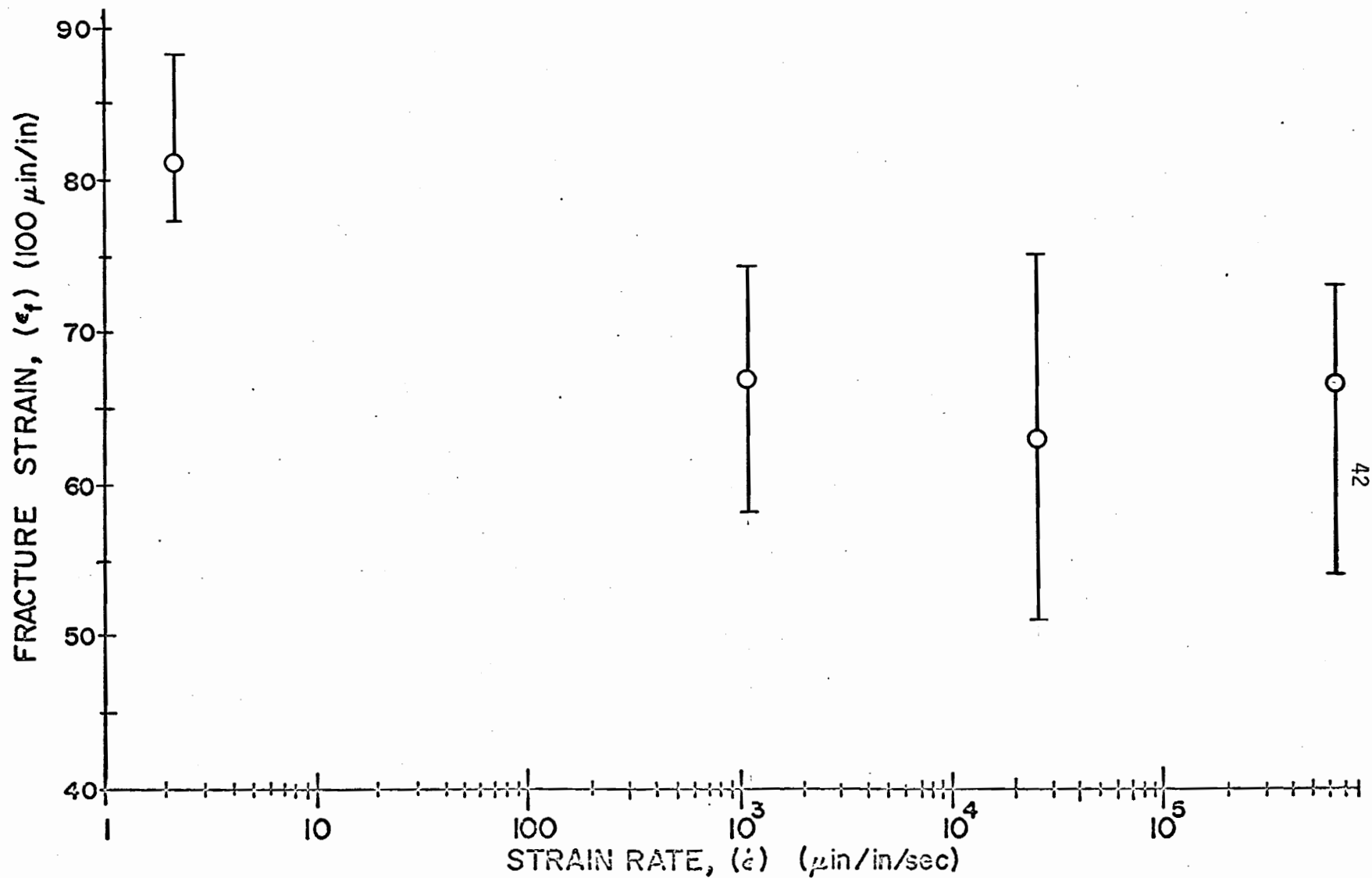


Figure 22. Fracture Strain-Strain Rate Test Results for Graphite/Epoxy Specimens at 80°F.

Typical tensile failures of Boron/Epoxy and Graphite/Epoxy specimens are shown in Figure 23. While Graphite/Epoxy shows a brittle fracture at 200°F, a weakened matrix is evidenced by Boron/Epoxy at 300°F.

TENSILE CREEP TESTS

High temperature creep tests were performed at different load levels. A Riehle creep machine was fitted with an environmental chamber. Constant temperature was maintained with the help of a thermocouple-temperature controller-and heating coil circuit. Two thermocouples at different locations were hooked up to a potentiometer to monitor temperature. They differed at the most by $\pm 3^\circ\text{F}$. A fan was mounted at the bottom of an oven to maintain uniform temperature.

The machine was equipped with grips to test specimens in chains of three or one at a time. Creep was measured by an optical extensometer which was aimed through a transparent window at a metal strip attached to the specimens. Strip gages were made of two platinum strips which could slide independently with respect to each other. Very fine markings were inscribed on it. The platinum strip assembly was attached to the test specimen with mounting clamps. The optical extensometer was calibrated for 20 microinches/division with a magnification of 50 times and an 8 inch relay lens to permit creep measurement without contacting specimen.

The creep test assembly and details of the loading system are shown in Figures 24 and 25.

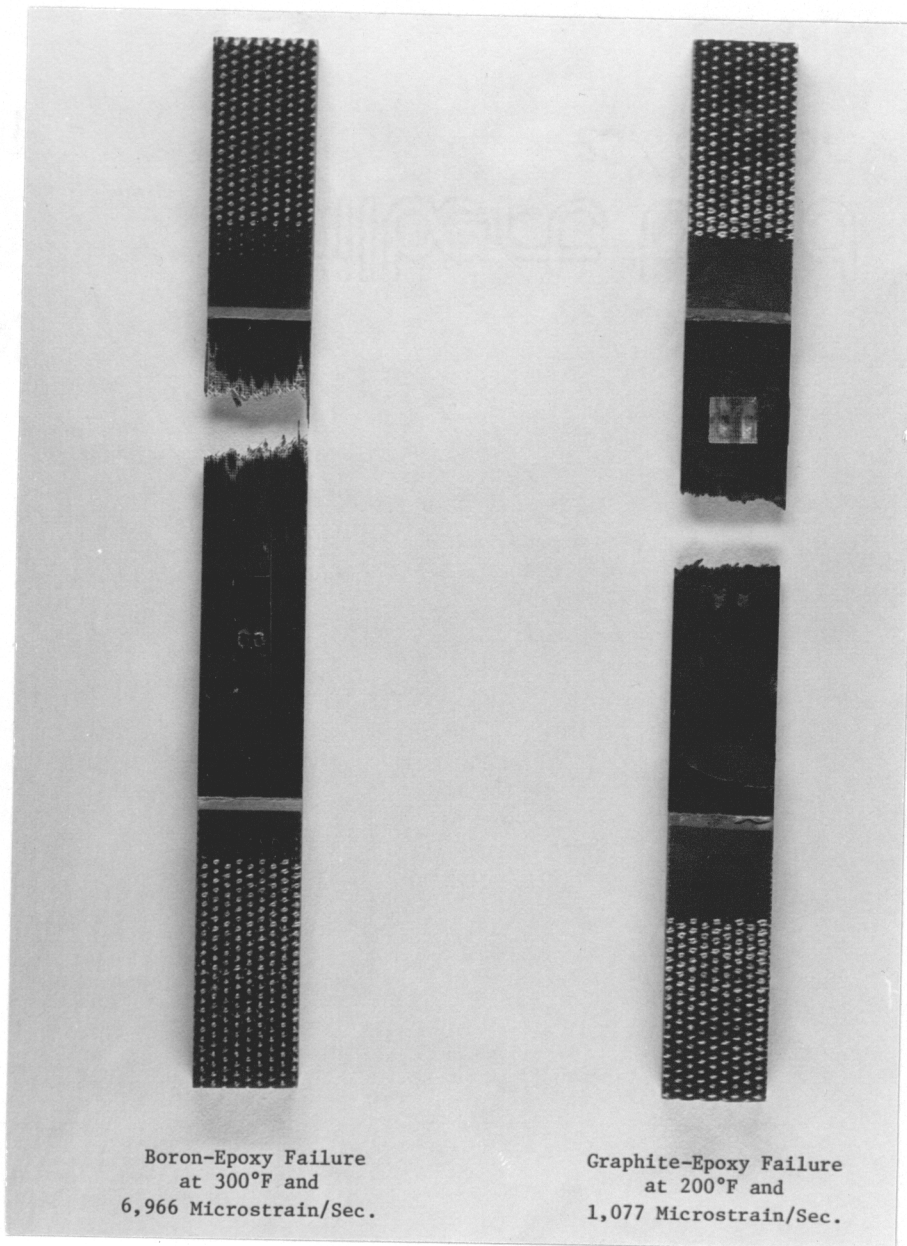


Figure 23. Typical Tension Failures of Boron/Epoxy and Graphite/Epoxy Specimens.



Figure 24. Tensile Creep Test Setup.

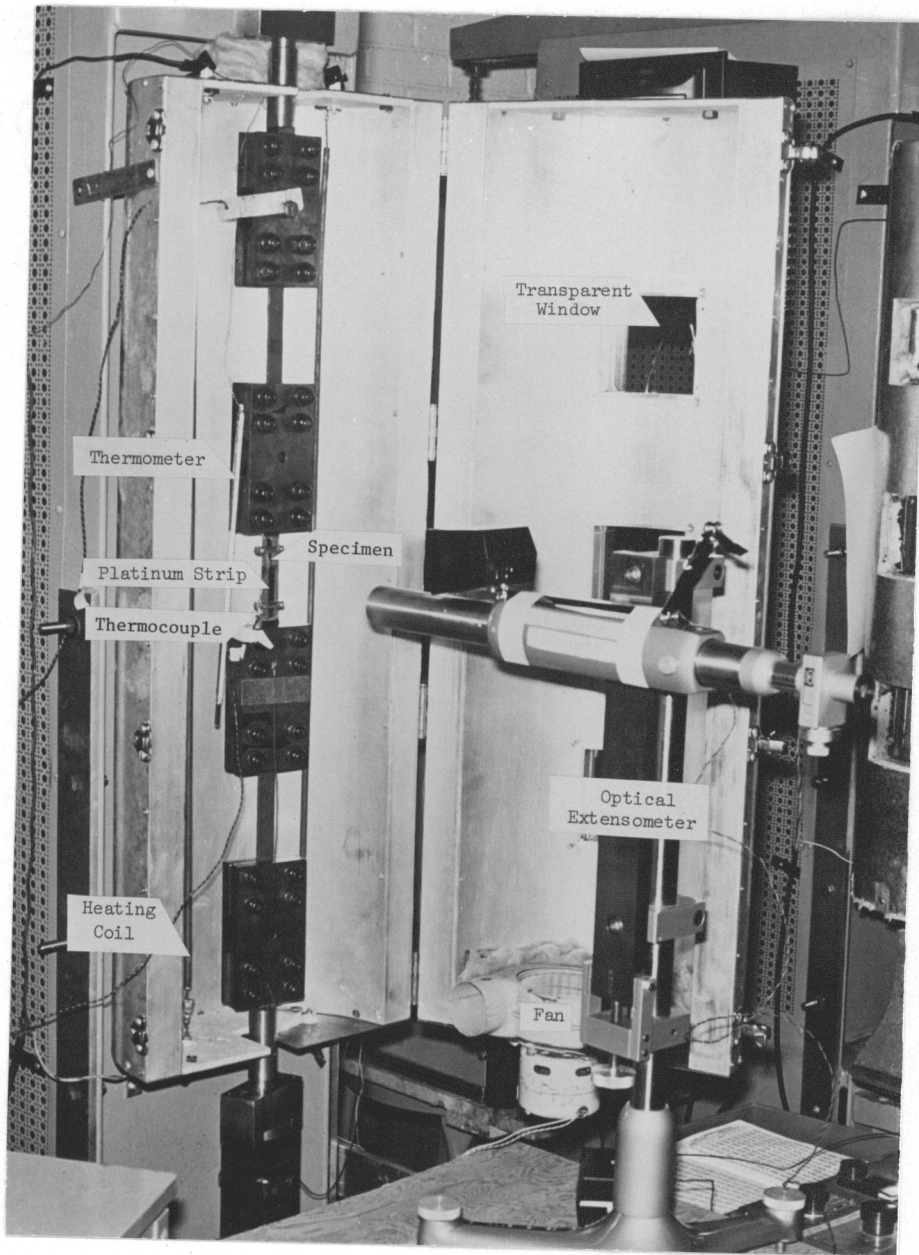


Figure 25. Details of Creep Test Setup.

The system was initially checked by measuring creep strain with high elongation strain gages. Polycarbonate specimens were also used to check the optical results with those given in Reference [78] obtained by using strain gages. They were in good agreement.

At the time of writing of this report not all tests were completed. Available creep curves at 300° and 200°F for Boron/Epoxy at various load levels are shown in Figures 26 and 27.

DATA REDUCTION AND STATISTICAL CONDITIONING

While measured mechanical properties are statistically variable, composites exhibit a comparatively higher scatter in such measurements than those found in other materials. To obtain a functional relationship between independent variables such as time, temperature, and humidity and dependent variables of modulus, damping, strength, fatigue life and reliability a multi-dimensional response surface can be generated. This "Response Surface Methodology" [97] utilizes a multi-variate least square technique to find the best fitting relationship for all data points. The surface can then be utilized for extrapolation or interpolation purposes.

It is possible to consider the modulus to be a function of strain rate and temperature and to fit a three dimensional response surface to the individual modulus values. The technique utilizes a set of multiple regression equations of the form [97].

$$y = \beta_0 + \beta_1 x_1 + \beta_2 x_2 + \beta_{11} x_1^2 + \beta_{22} x_2^2 + \beta_{12} x_1 x_2 + \dots + e \quad (3.1)$$

where the coefficients β_0, β_1, \dots , are estimated from values of the

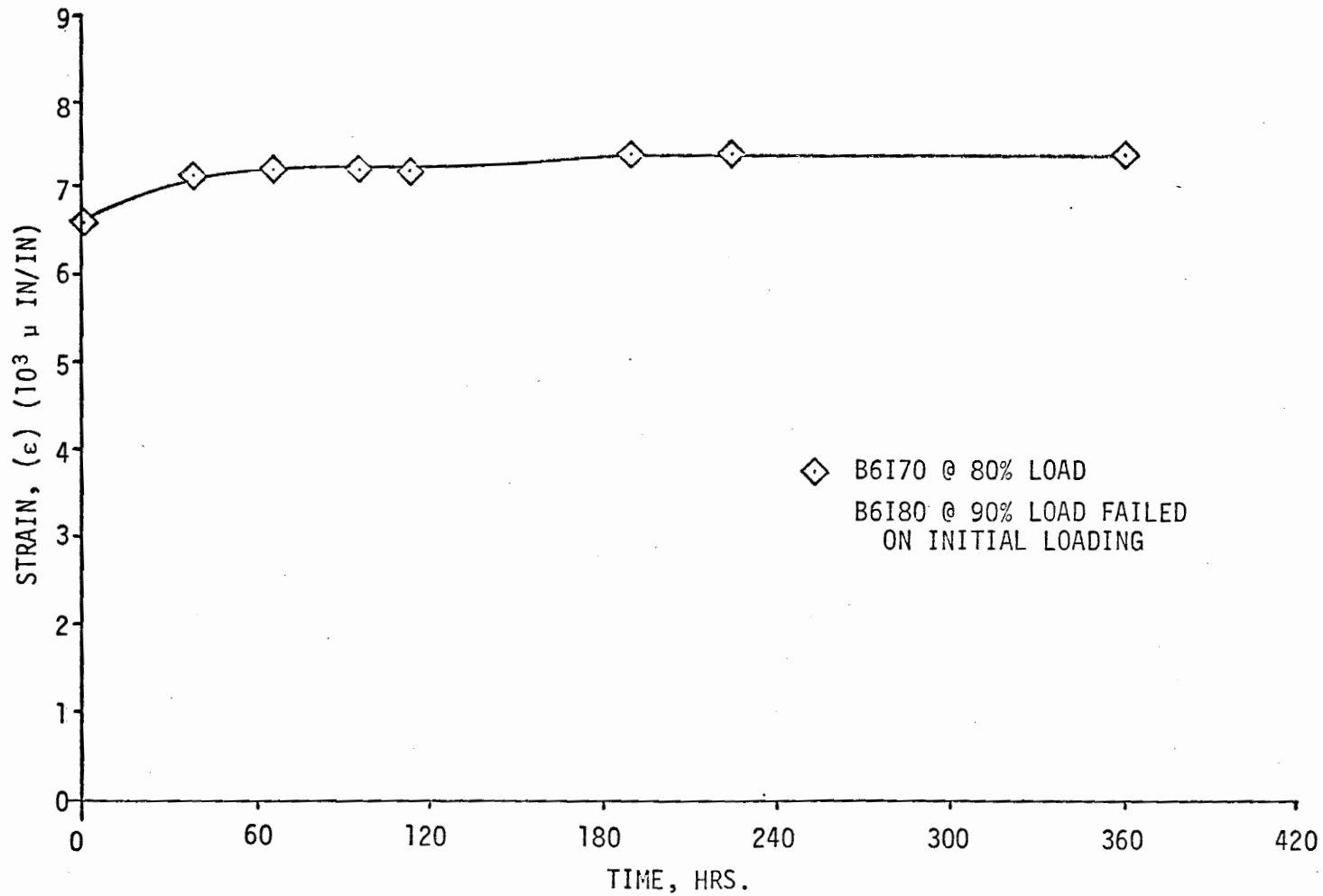


Figure 26. Creep Curve for Boron/Epoxy at 300°F.

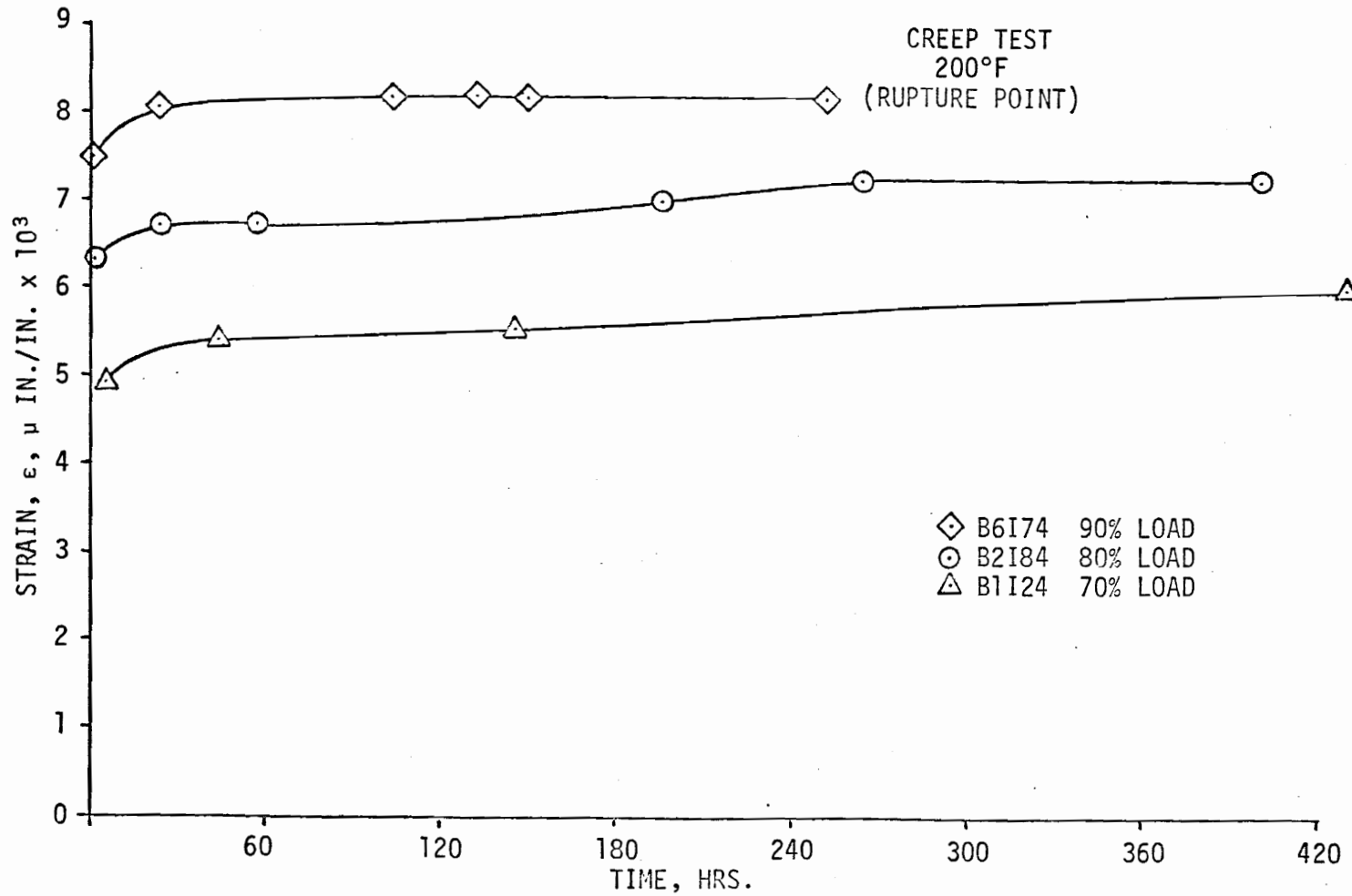


Figure 27. Creep Curves for Boron/Epoxy at 200°F.

measured response, y , which is a polynomial function of the independent variables x_1, x_2, \dots , and \underline{e} is a random error which is normally distributed. The above response surface, equation (3.1) can be written in matrix form as

$$\underline{y} = [\underline{x}]\underline{\beta} + \underline{e} \quad (3.2)$$

In the problem at hand y is the modulus of elasticity, E ; x_1 is the logarithm of the strain rate, $\dot{\epsilon}$; and x_2 is temperature, $1/T$.

A computer program [96] is used to estimate the coefficients of the response. The program minimizes the squared error between observation and estimate. Consequently an equation for a mean response surface is obtained. Figure 28 shows a three dimensional plot of modulus as a function of strain-rate and temperature in the form of contour bands for Boron/Epoxy. A similar response surface is presented for Graphite/Epoxy in Figure 29.

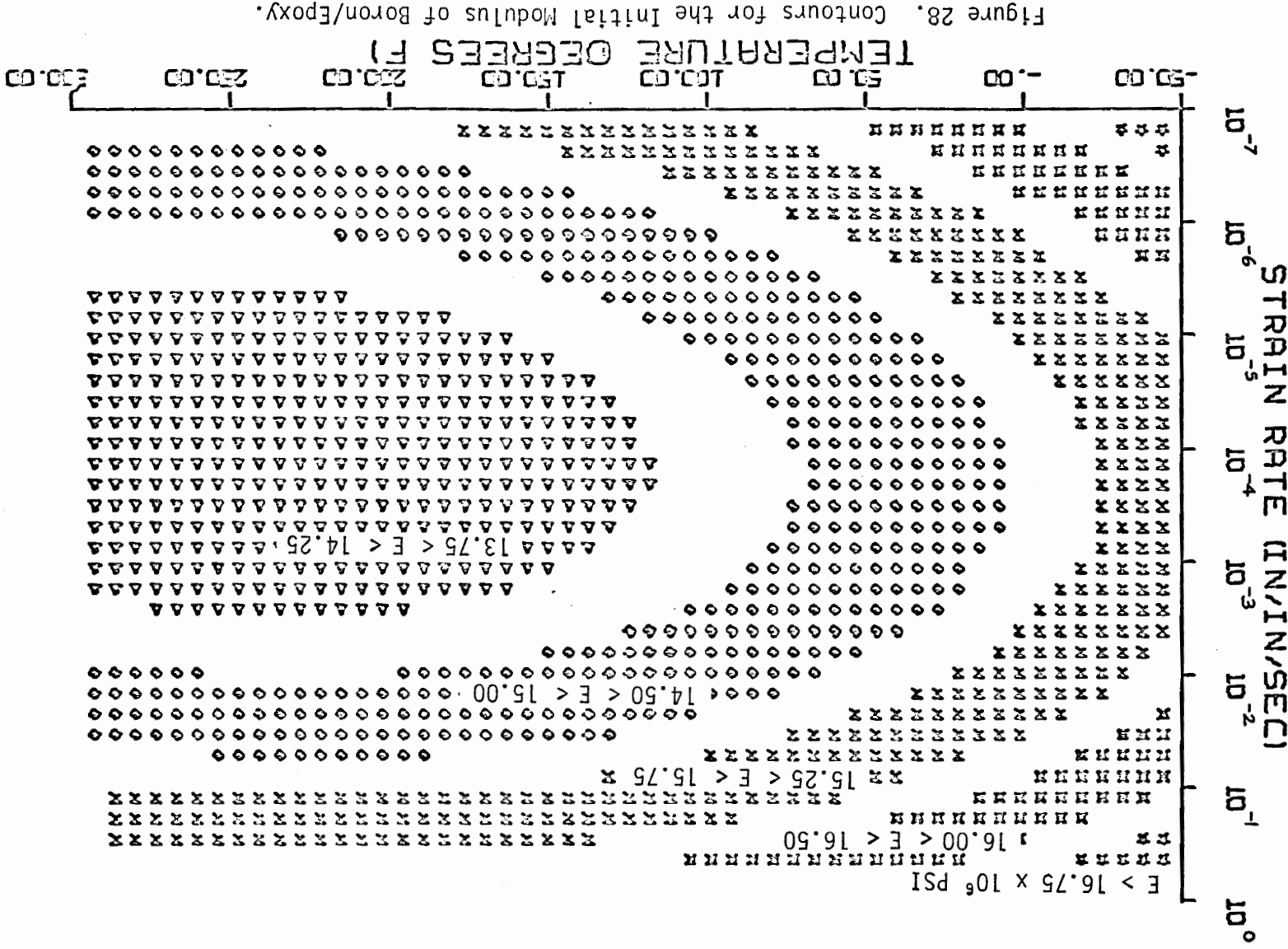
The equation of the surfaces may be written in the form:

$$E(\dot{\epsilon}, T) = A + B \ln \dot{\epsilon} + C/T + D(\ln \dot{\epsilon})^2 + E/T^2 + F(\ln \dot{\epsilon})/T \quad (3.3)$$

where the coefficients are listed in Table 1.

Both surfaces have dished shapes. The elliptic contours have axes rotated with respect to the coordinate system. This rotation is signified by the coefficient of the interaction term, $\ln \dot{\epsilon} T$.

The significance of this interaction term and its relation to the time-temperature shift parameter will be explained later.



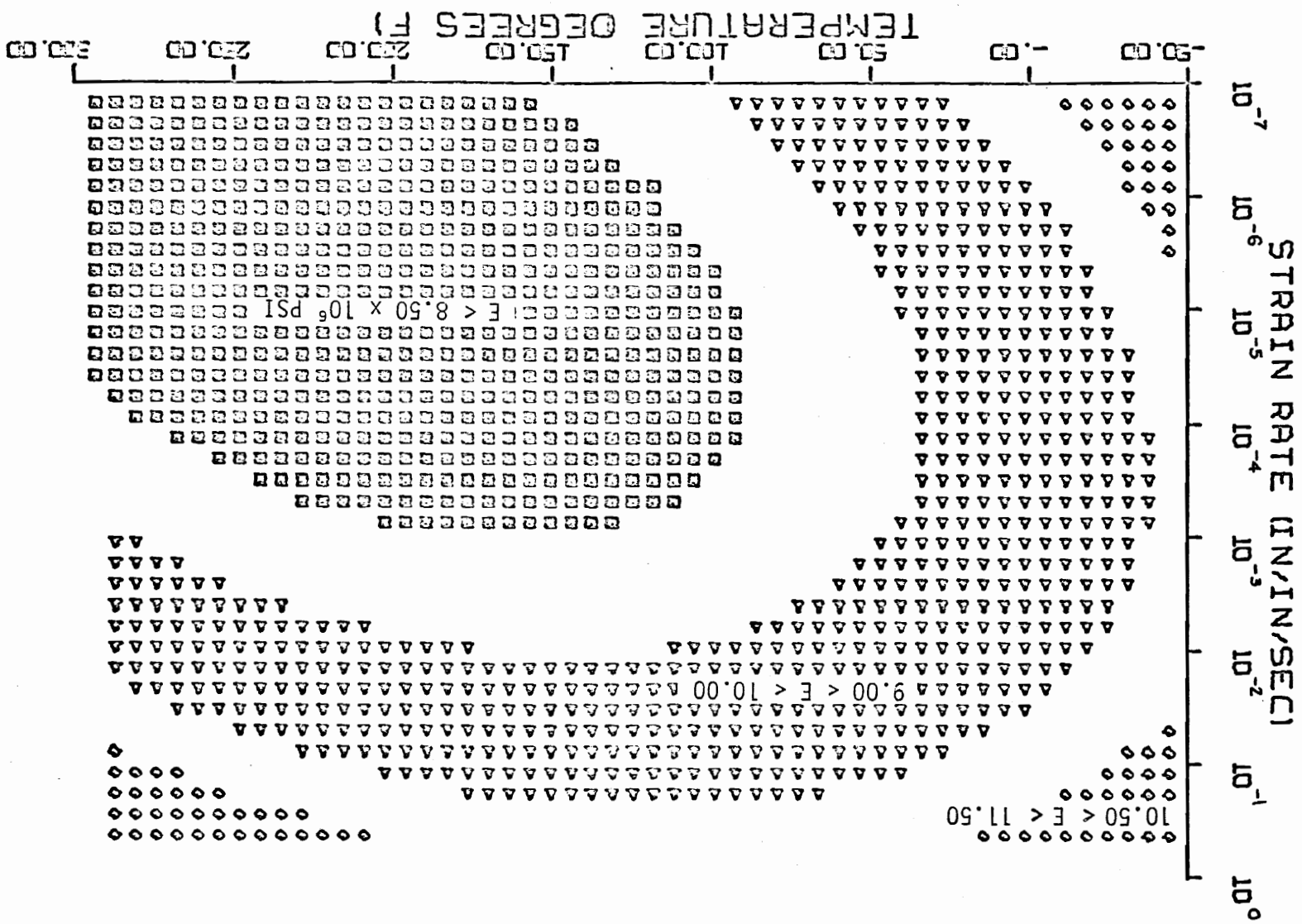


Figure 29. Contours for the Initial Modulus of Graphite/Epoxy.

Table 1

R^2 , σ AND THE COEFFICIENTS OF EQ. (3.3) FOR $1/T$ IN DEGREES KELVIN
AND $\dot{\epsilon}$ IN INCHES/IN/SEC.

	BORON/EPOXY	GRAPHITE/EPOXY
R^2	0.5618	0.5430
A	1.97×10^7	2.184×10^7
B	5.98×10^5	8.00×10^5
C	-2.44×10^9	-6.37×10^9
D	2.75×10^4	1.736×10^4
E	4.36×10^{11}	8.90×10^{11}
F	-3.53×10^7	-1.269×10^8

Confidence and tolerance bands may also be estimated for the modulus. Because it has been assumed that the error, e is normally distributed, the probability that a new observation will fall within the limits prescribed by y' is $\alpha/2\%$ where

$$y' \cong y \pm Z_{\alpha/2} \sigma \quad (3.4)$$

Here y is the mean response given by equation (3.1) or (3.3), $Z_{\alpha/2}$ is the normal statistic corresponding to the $\alpha/2$ probability of exceedence and σ is the standard deviation of the response listed in Table 2. Equation (3.4) is an approximation; the exact relations have been detailed in Reference [93]. For a 95% probability, $Z_{\alpha/2} = 1.96$ and hence there is a 95% chance that a new observation will fall within the bands prescribed by

$$y' \cong y \pm 1.96\sigma \quad (3.5)$$

If the response surfaces of Figures 28 and 29 are cut with constant temperature planes, curves of modulus versus strain rate result. The 95% probability bands together with the experimental observations superimposed on the mean line are shown for the two materials in Figures 30-33. Plots for the mean moduli versus strain rate at various temperatures are shown in Figures 34 and 35.

The detailed discussion regarding differences between stress-strain curves obtained from individual regression lines and through the response surface is reported in Reference [99].

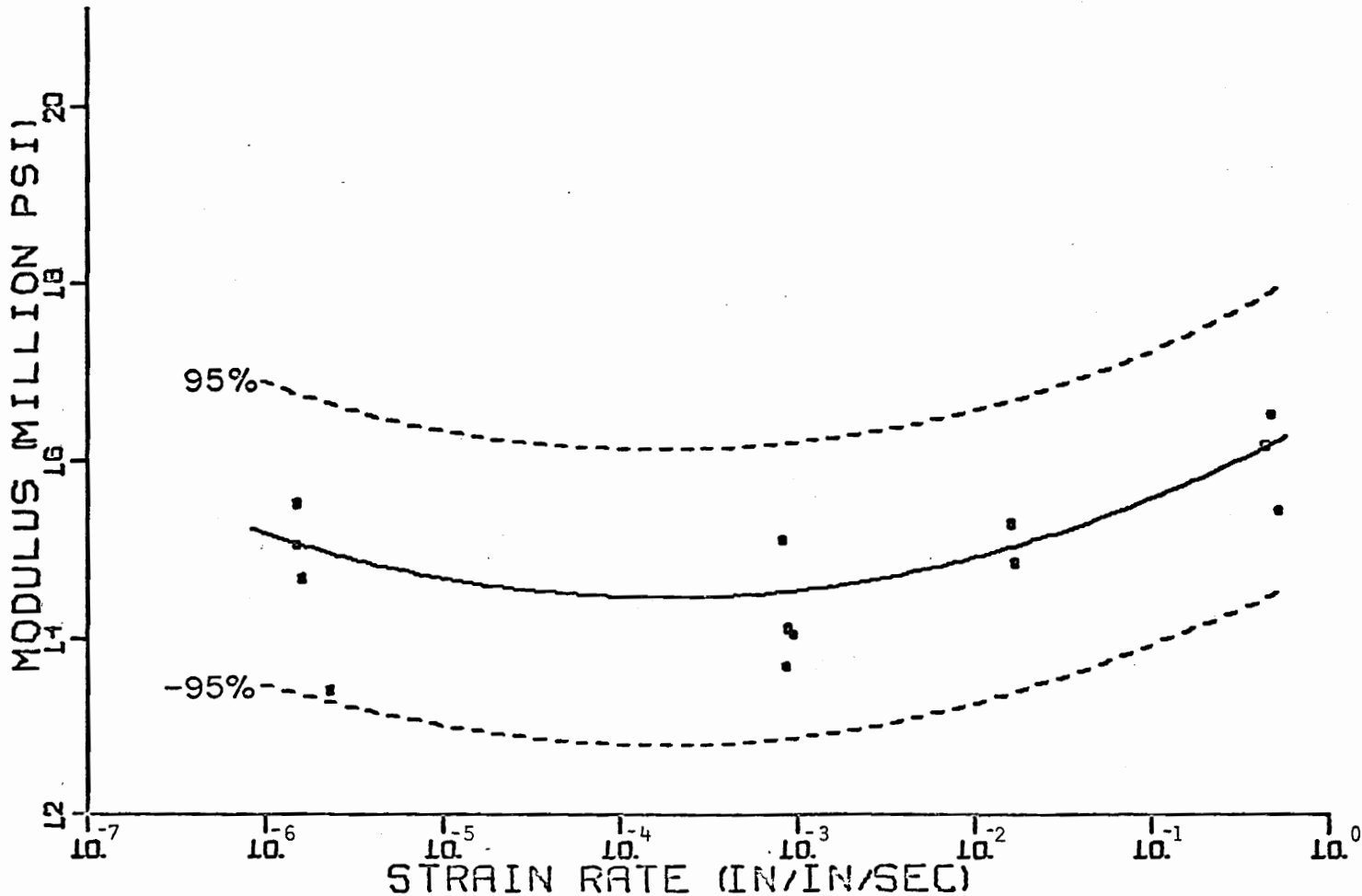


Figure 30. Probability Curves for the Initial Modulus of Boron/Epoxy at 80°F as a Function of Strain Rate.

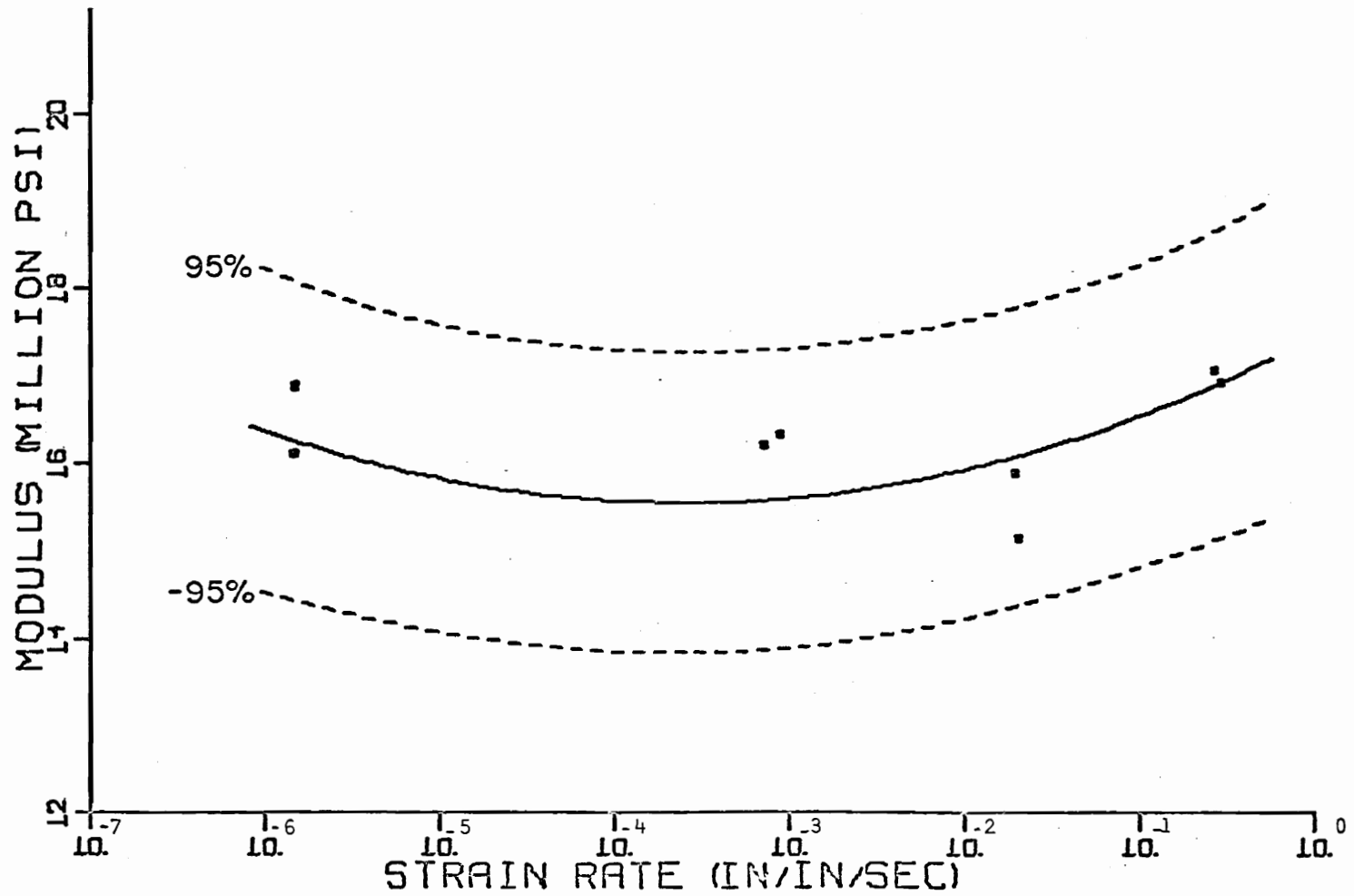


Figure 31. Probability Curves for the Initial Modulus of Boron/Epoxy at -50°F as a Function of Strain Rate.

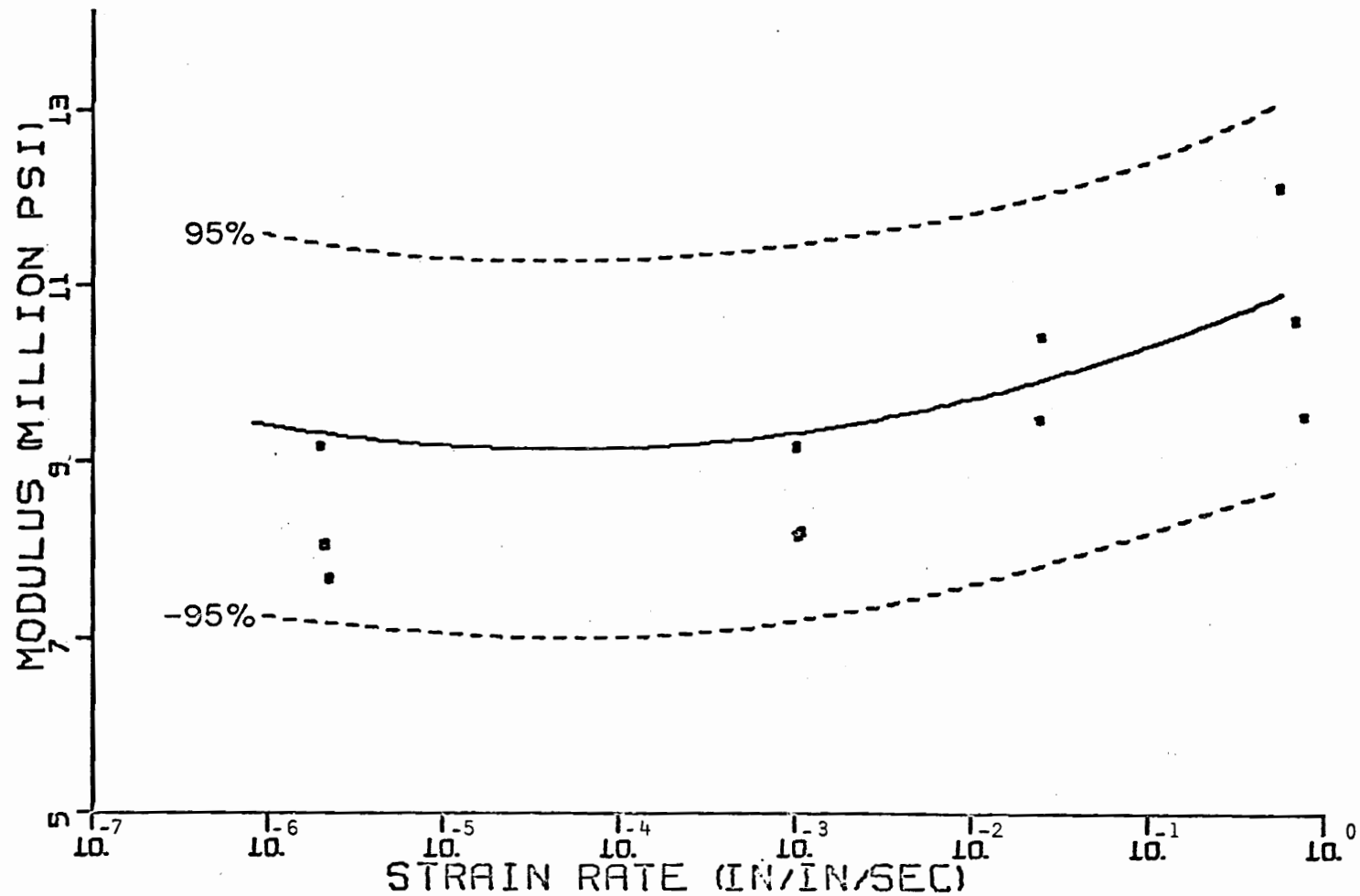


Figure 32. Probability Curves for the Initial Modulus of Graphite/Epoxy at 80°F as a Function of Strain Rate.

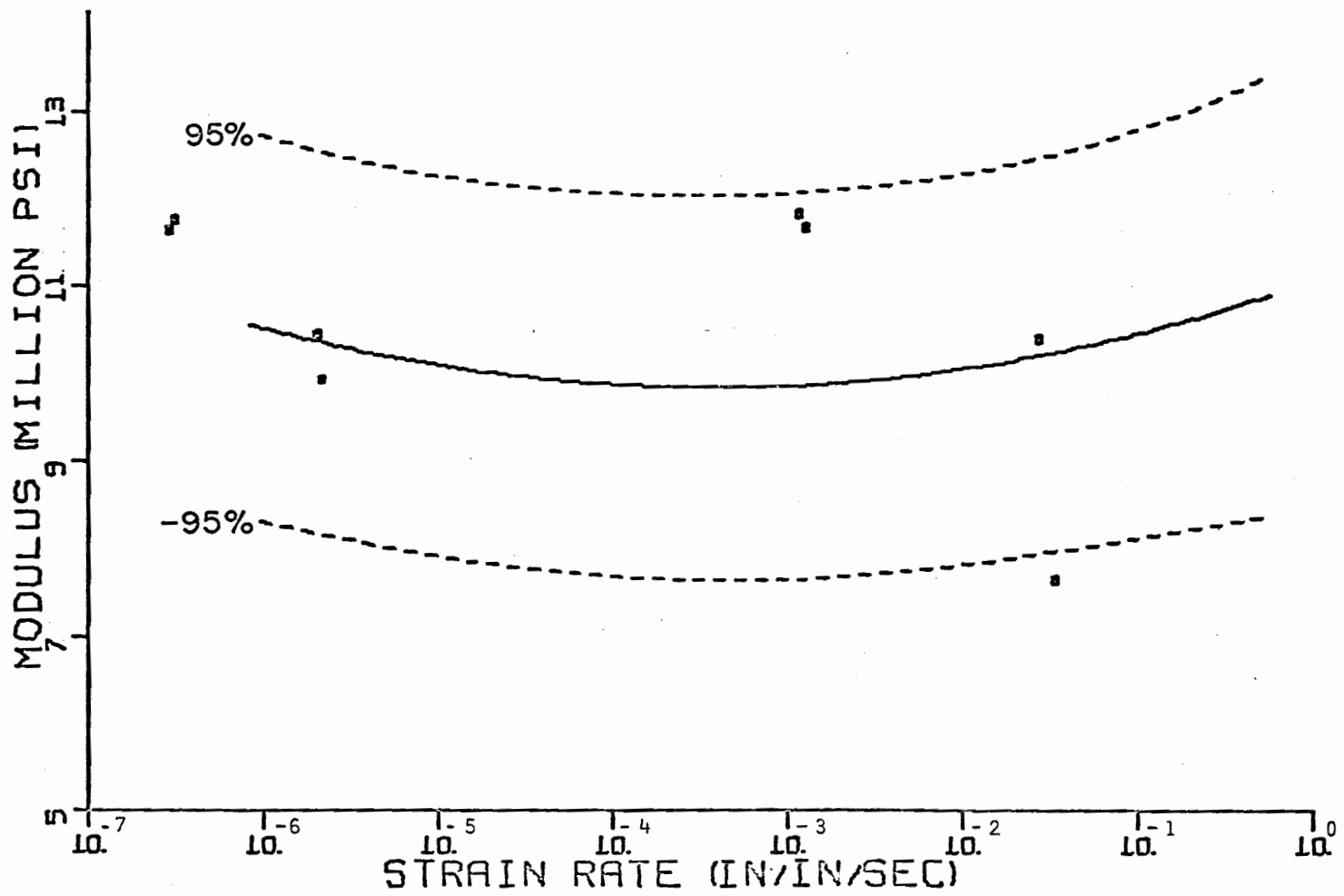


Figure 33. Probability Curves for the Initial Modulus of Graphite/Epoxy at -50°F as a Function of Strain Rate.

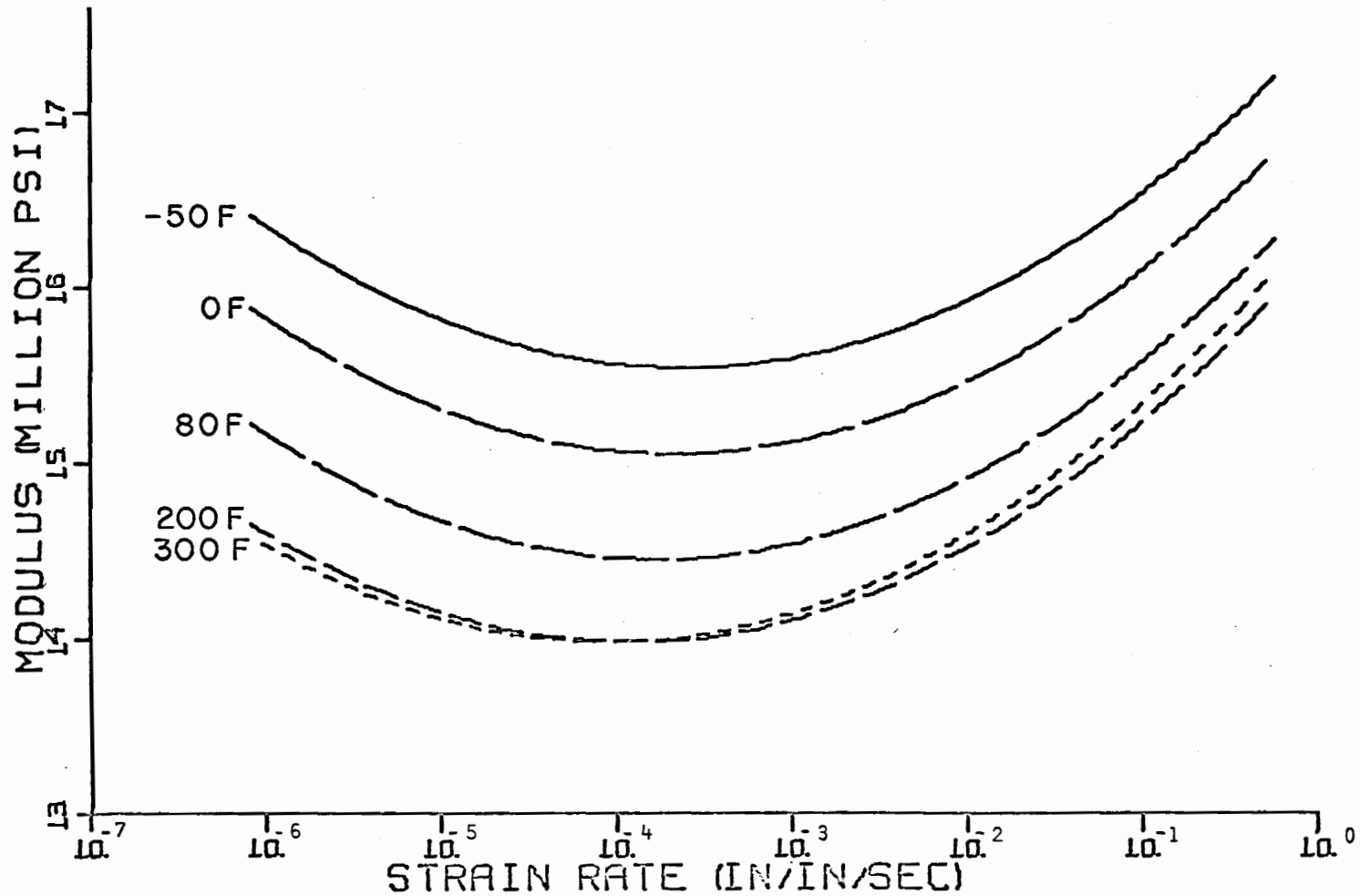


Figure 34. Constant-Temperature Initial Modulus Curves for Boron/Epoxy as a Function of Strain Rate.

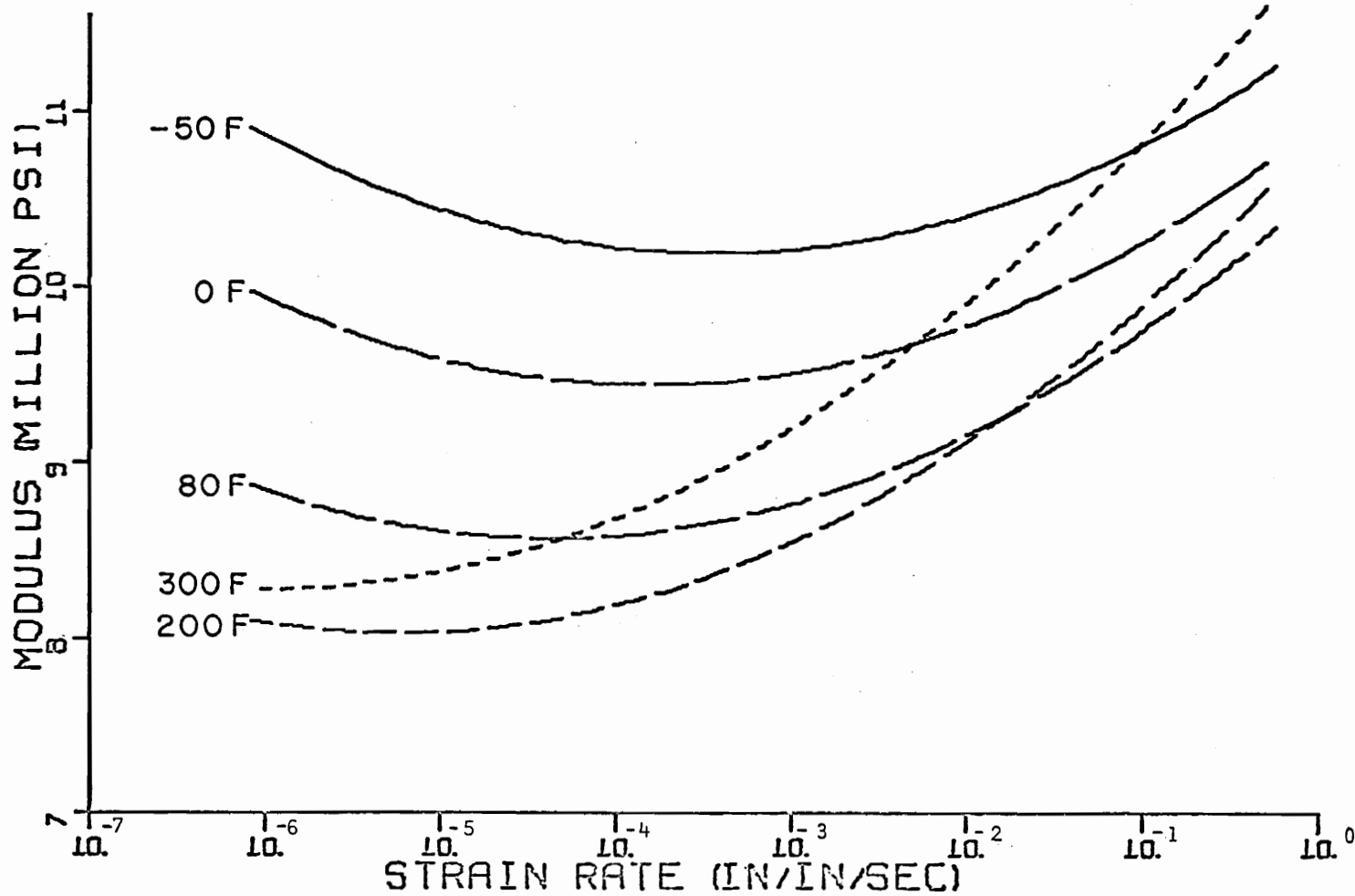


Figure 35. Constant-Temperature Initial Modulus Curves for Graphite/Epoxy as a Function of Strain Rate.

The strain rate experiments discussed earlier were carried to fracture and the temperature and strain-rate dependent strength has in each case been recorded.

In order to determine the influence of these variables on the ultimate strength of Boron/Epoxy and Graphite/Epoxy composites, response surface were fitted to these results also. The computer was programmed to choose the lowest order polynomial relation of the type given by Equation (3.1) with the maximum multiple correlation coefficient.

For both materials strain-rate independent relations were obtained. The fracture strength, S_u , of Boron/Epoxy is a linearly decreasing function of temperature, T , in degrees Fahrenheit

$$S_u = 1.13 \times 10^5 - 34T \quad (3.6)$$

For Graphite/Epoxy the ultimate strength, while also strain-rate independent, is a quadratic function of the temperature

$$S_u = 7.16 \times 10^4 - 1.19 \times 10^2 T + 5.63 \times 10^{-1} T^2 \quad (3.7)$$

Figures 36 and 37 show these relations in graphical form.

The Response Surface Methodology and Statistical conditioning of data were also used for Vibration Test results. Reference [99] provides a thorough discussion of the analysis. Plots of Response Surfaces for Storage and Loss Moduli as well as constant temperature plots are also included in that reference.

Due to insufficient data, no statistical conditioning was performed on creep test data.

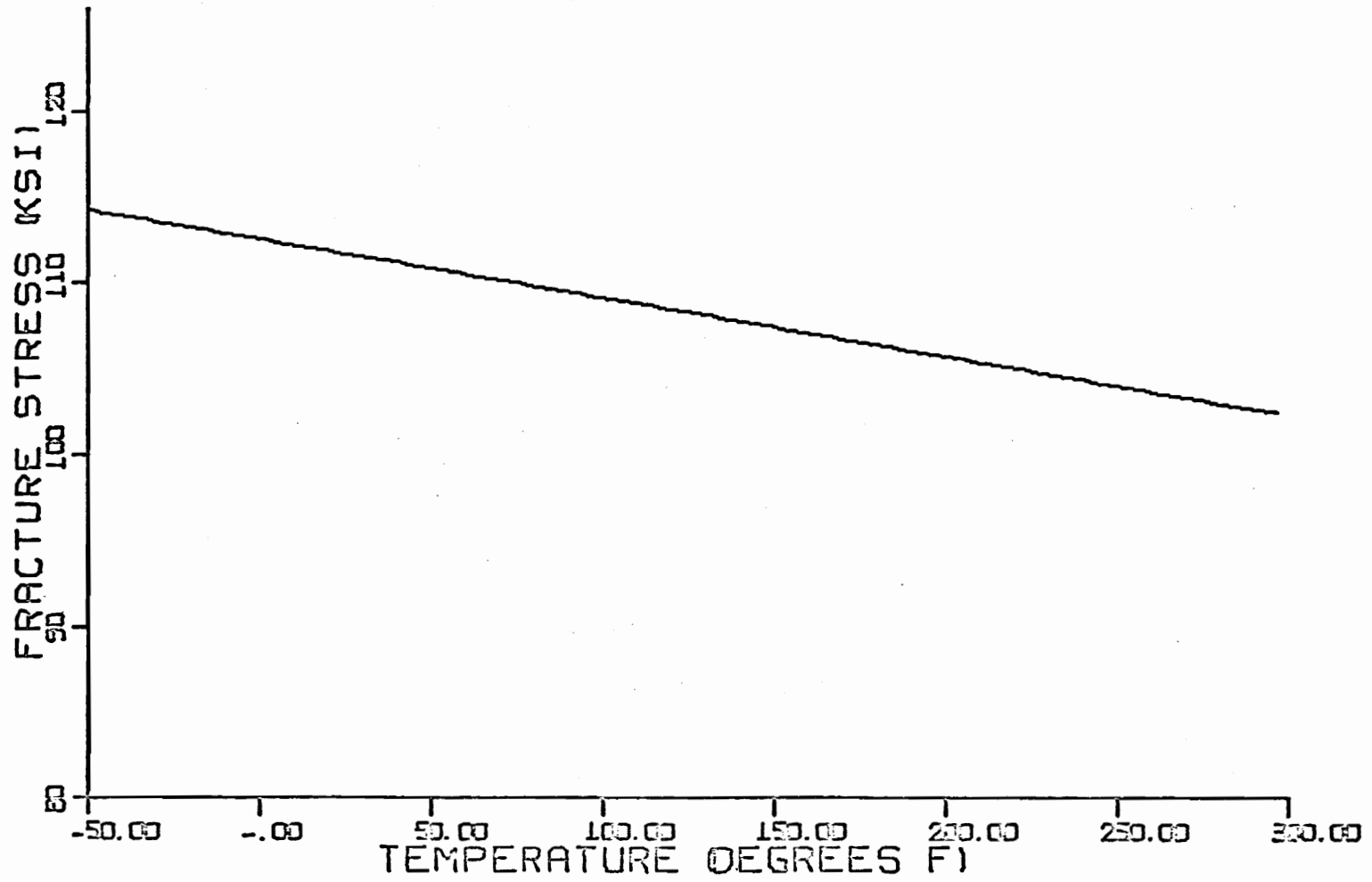


Figure 36. Fracture Strength as a Function of Temperature for Boron/Epoxy.

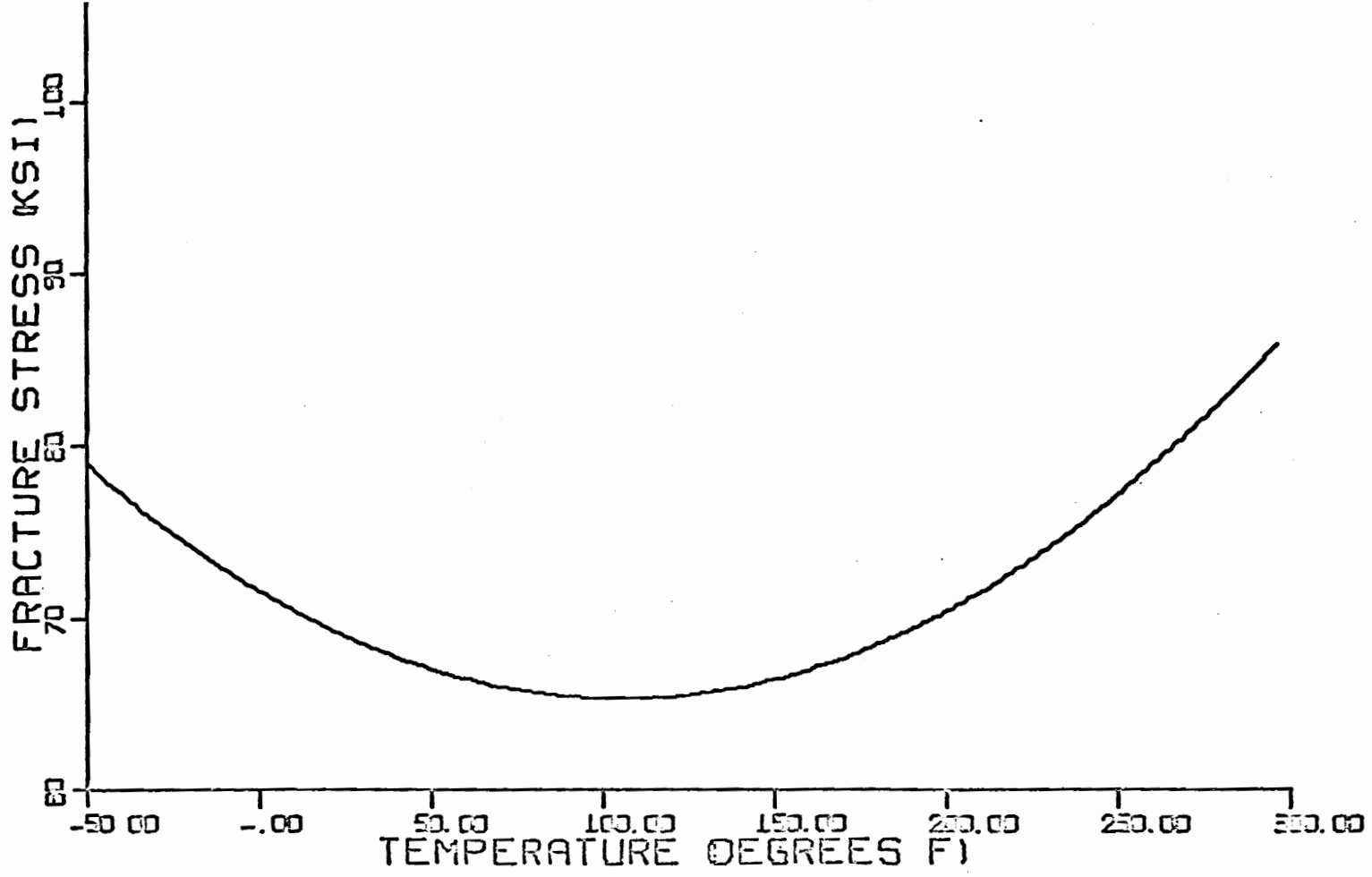


Figure 37. Fracture Strength as a Function of Temperature for Graphite/Epoxy.

IV. VISCOELASTIC CHARACTERIZATION

The purpose of carrying out viscoelastic characterization of advanced composites is two fold. The first aim is to use viscoelastic interconversion functions in order to utilize dynamic and constant strain rate tests in the prediction of long term behavior. The second one is to understand time-dependent effects on these materials.

The difficulty of understanding the elastic behavior of these anisotropic materials is further complicated by considering time dependence.

In order to understand this behavior, the first logical step would be to use well developed linear viscoelastic relations. The well founded viscoelastic approaches like time-temperature superposition, mechanical model representation, integral equation formulations have been tried to accomplish the stated objectives. Valuable simplifications afforded by approximate interrelations between viscoelastic functions have also been used.

Time-Temperature Superposition.

The time-temperature superposition principle is an extremely powerful tool in the study of viscoelastic properties of polymers. It affords a valuable simplification by separating the effect of the two variables of time and temperature on which the viscoelastic properties depend.

Although the time-temperature superposition principle was originally developed on an empirical basis, it can be developed as a logical sequence of the kinetic theory of polymers. Kinetic theory shows that the ratio of the relaxation times at two different temperatures can be expressed as [9]

$$a_T = \frac{\tau}{\tau_0} = \left(\frac{\zeta}{\zeta_0} \right) \frac{\rho_0 T_0}{\rho T} \quad (4.1)$$

where a_T is defined as a shift function and ζ is the viscosity of the polymer.

If written in terms of the stress-relaxation moduli, time-temperature superposition can be stated as,

$$E(t', T_0) = \frac{\rho_0 T_0}{\rho T} E(t = a_T t', T) \quad (4.2)$$

which implies that the relaxation modulus at temperature T_0 and time t' can be obtained from the relaxation modulus measured at temperature T and time t . On a plot of modulus vs. logarithmic time, this amounts to a vertical shift of magnitude $\rho_0 T_0 / \rho T$ and a horizontal shift of $\log a_T$. Equation (4.2) is for the relaxation modulus, but it is equally applicable to other viscoelastic functions.

The use of shift functions results in a method of extrapolation in which suitable results obtained at various temperatures can be superimposed by horizontal and vertical translation to form a master curve at a given reference temperature. Such a curve covers a wider time range than could be achieved by using data from a single

temperature. Thus, the effect of temperature is to divide or multiply the time scale by a constant, a_T .

A simplified procedure to determine a_T is discussed later.

There is no theoretical justification to extend time-temperature superposition into the glassy range. However, Smith [31], Lohr [28-29], Gauchel [51] and several others have shown its applicability. According to Ferry [9],

Below T_g , although long range configurational changes take place exceedingly slowly, more rapid viscoelastic responses exist which are attributed to a variety of local backbone and side chain motions and cover a very wide spectrum of relaxation times. Such motions can certainly not be described in terms of a monomeric friction coefficient. However, if it is assumed that all the relaxation times concerned with a particular type of motion have the same temperature dependence, reduced variables can be applied to the glassy zone in the region where the response is dominated by this motion as a separate calculation.

Time-temperature superposition has also been used for the extrapolation of other data such as maximum tensile strength, strain at maximum stress, and maximum strain for different polymer systems by many investigators. In commenting on the subject, Krokosky [49] states that

The fact that time-temperature superposition can be carried out on apparently unrelated data emphasizes the fundamental nature of the process. Time-temperature superposition has been verified experimentally for certain types of materials, but there is as yet no complete theory to explain why it works.

Determination of Softening Temperature.

Since the cure temperature for both composite systems was 350°F, it was used as an upper temperature limit. However, transverse forced vibration tests were performed to determine the softening temperature. A similar concept was used by Schapery [68] and Schwarzl [98] to ensure that their operating range was below the glass transition temperature. Schwarzl [98] refers to softening temperature as the logarithmic midpoint of the modulus decrease which is close to the glass transition temperature. Impedance vs. frequency curves at different temperatures were obtained as shown in Figure 38 for Boron/Epoxy Specimens. A minimum time of 30 minutes was allowed to stabilize the temperature of the specimen. A sharp drop in anti-resonance frequency and hence the modulus was observed between temperatures of 350° and 375°F. A similar trend was observed for Graphite/Epoxy. As a result, all tests were conducted below 350°F to avoid any softening effects and to be within the glassy region.

Temperature Shift Parameters.

The response surfaces developed in Chapter III can be utilized to determine temperature shift parameters within the context of viscoelastic theory. This in turn will indicate the possible amount of test acceleration that may be obtained by variations of temperature for fiber reinforced epoxy based composites. To establish shift parameters for the complex modulus, the method is outlined

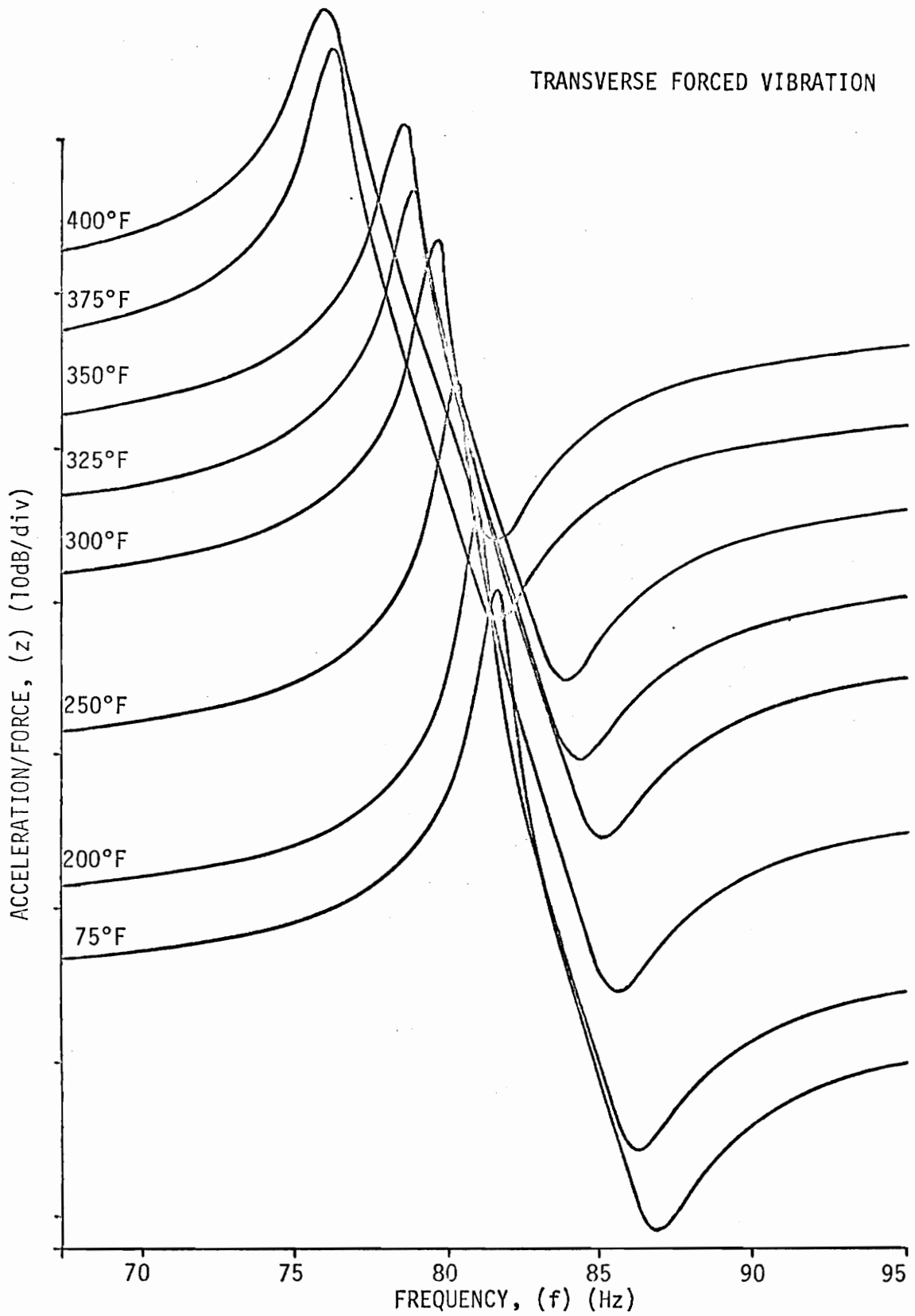


Figure 38. Determination of Softening Temperature for Boron/Epoxy Composite.

here. For a complete discussion see reference [94].

For a constant reference temperature denoted by T_r , the elastic modulus, E_r , is a quadratic function of strain-rate only (Fig. 39), Eq. (3.3) can be written in the form

$$E_r(\dot{\epsilon}) = A_r + B_r \ln \dot{\epsilon} + D \ln^2 \dot{\epsilon} \quad (4.3)$$

where $A_r = A + \frac{C}{T_r} + \frac{E}{T_r^2}$ and $B_r = B + \frac{F}{T_r}$

The coordinates of the minimum point on the curve described by Eq. (4.3) may be obtained by differentiation

$$\ln \dot{\epsilon}_{r_{\min}} = -\frac{B_r}{2D}, \quad E_{r_{\min}} = A_r - \frac{B_r^2}{4D} \quad (4.4)$$

The stationary point may be found in a similar form for an arbitrary temperature. The difference

$$\ln \dot{\epsilon}_{\min} - \ln \dot{\epsilon}_{r_{\min}} = \frac{\ln \dot{\epsilon}_{\min}}{\dot{\epsilon}_{r_{\min}}} = \ln a_T \quad (4.5)$$

is the horizontal temperature shift parameter

$$\ln a_T = -\frac{F}{2C} \left(\frac{1}{T} - \frac{1}{T_r} \right) \quad (4.6)$$

while the difference in moduli

$$\ln E_{\min} - \ln E_{r_{\min}} = \left(C - \frac{BF}{2D} \right) \left(\frac{1}{T} - \frac{1}{T_r} \right) + \left(E - \frac{F^2}{4D} \right) \left(\frac{1}{T^2} - \frac{1}{T_r^2} \right) \quad (4.7)$$

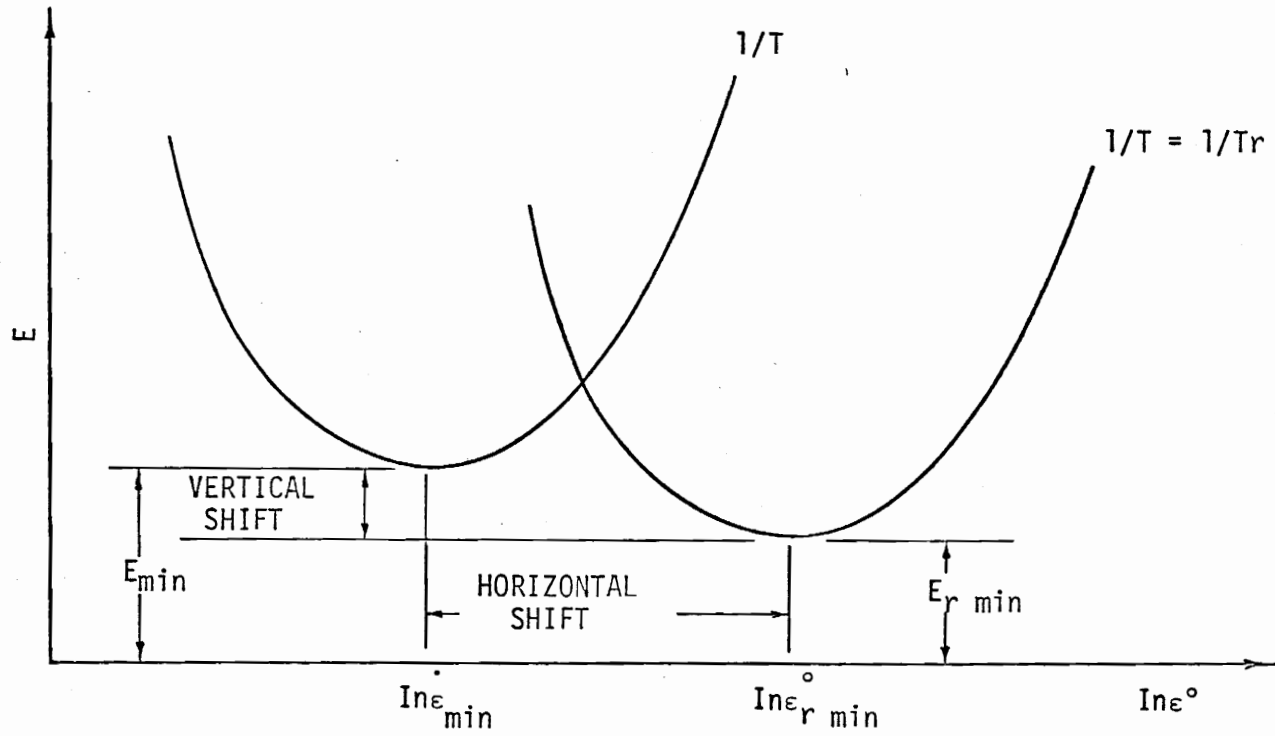


Figure 39. Horizontal and Vertical Shift.

is a vertical shift. Both parameters are functions of temperature and of the coefficients listed in Table 1. Eq. (4.6) shows that $\ln a_T$ exists only if the coefficient F of the interaction terms, $(\ln \epsilon)T$, exists. As mentioned in Chapter III, this term accounts for the skewness of the elliptic contours of Figures 28 and 29. A large angle between the coordinate axes and the axes of the ellipses indicate significant horizontal shift (Fig. 29). While a small angle shows that little if any temperature shifting is possible (Fig. 28).

The above procedure allows the construction of master curves of the Elastic Modulus and damping ratio as a function of frequency at one reference temperature. Horizontal and vertical shift parameters computed from Eqs. (4.6) and (4.7) are used for shifting and joining of successive curves obtained at various temperatures and thereby eliminating errors in judgement. Master curves obtained in the above manner for Elastic Modulus and damping ratios for Boron/Epoxy and Graphite/Epoxy at 80°F (300°K) reference temperatures are shown in Figures 40 to 43. As discussed before, the Elastic Modulus of Graphite/Epoxy shows significant horizontal shift as compared to that of Boron/Epoxy. A similar trend is observed for the damping ratio but to a lesser extent.

The master curves for storage and loss moduli of Boron/Epoxy and Graphite/Epoxy are reported in Reference [94].

Temperature Dependence of Shift Factor.

Once master curves are constructed, it would be appropriate to investigate the temperature dependence of empirically derived

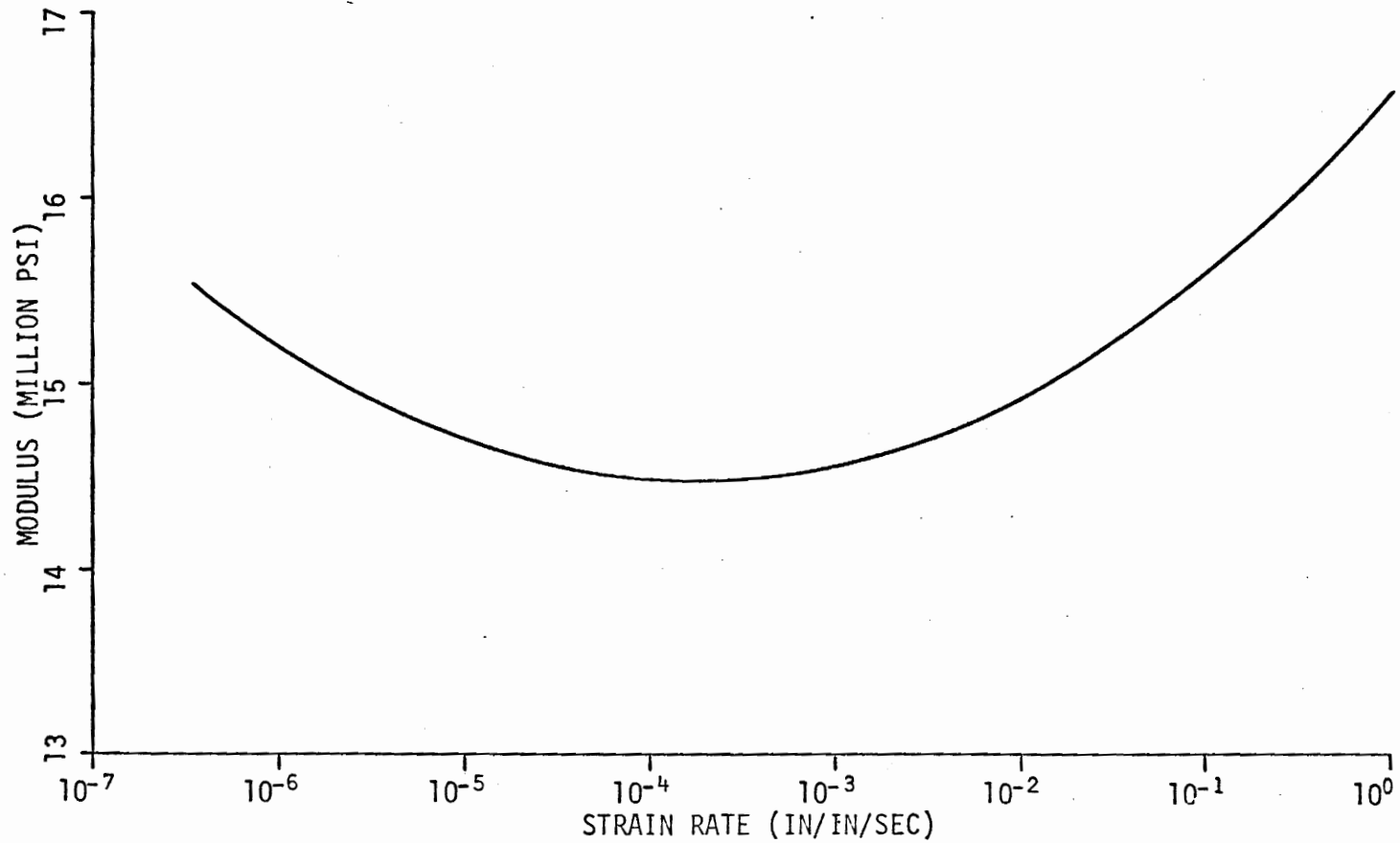


Figure 40. Master Curve for the Initial Modulus of Boron/Epoxy for a Reference Temperature of 80°F (300°K).

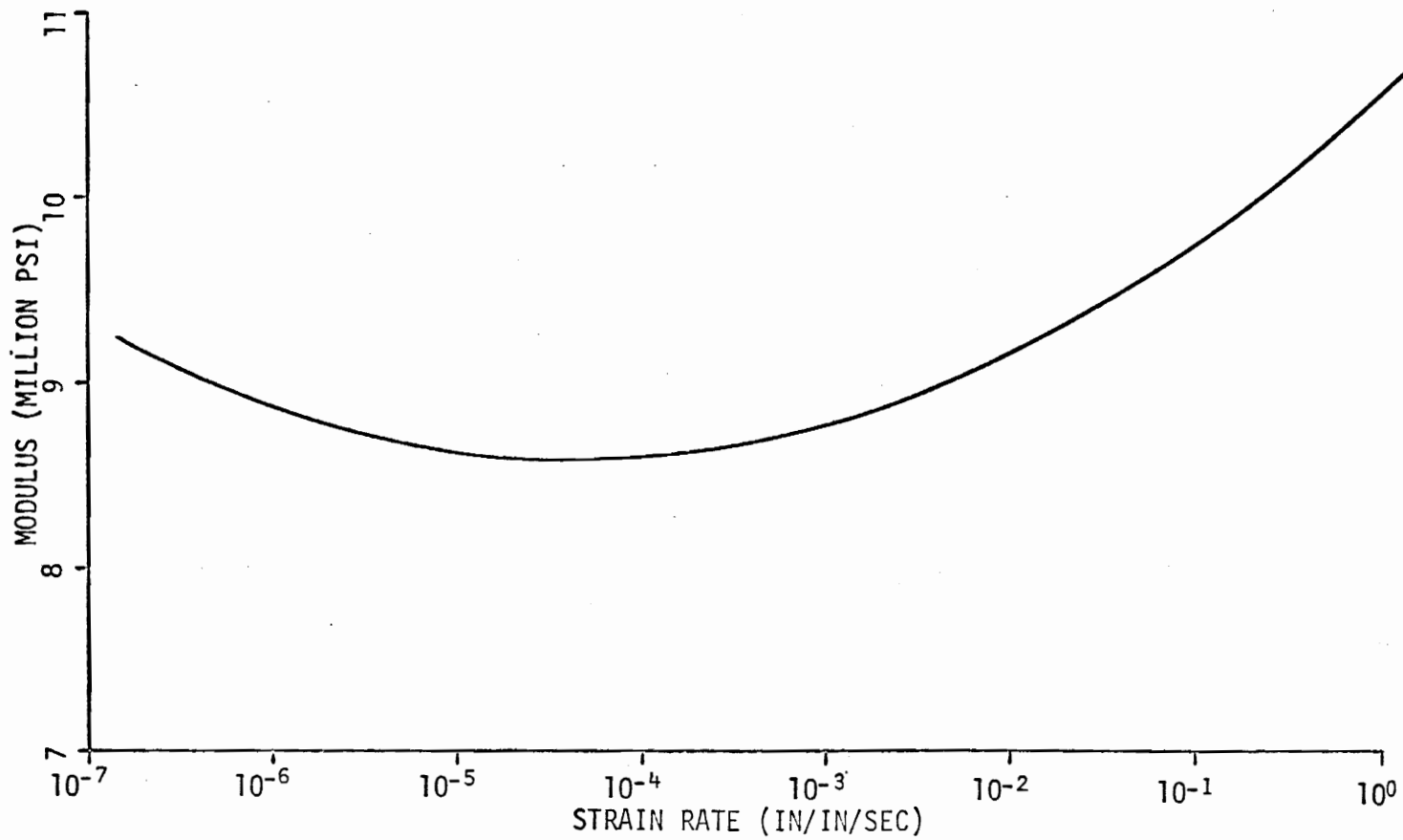


Figure 41. Master Curve for the Initial Modulus of Graphite/Epoxy for a Reference Temperature of 80°F (300°K).

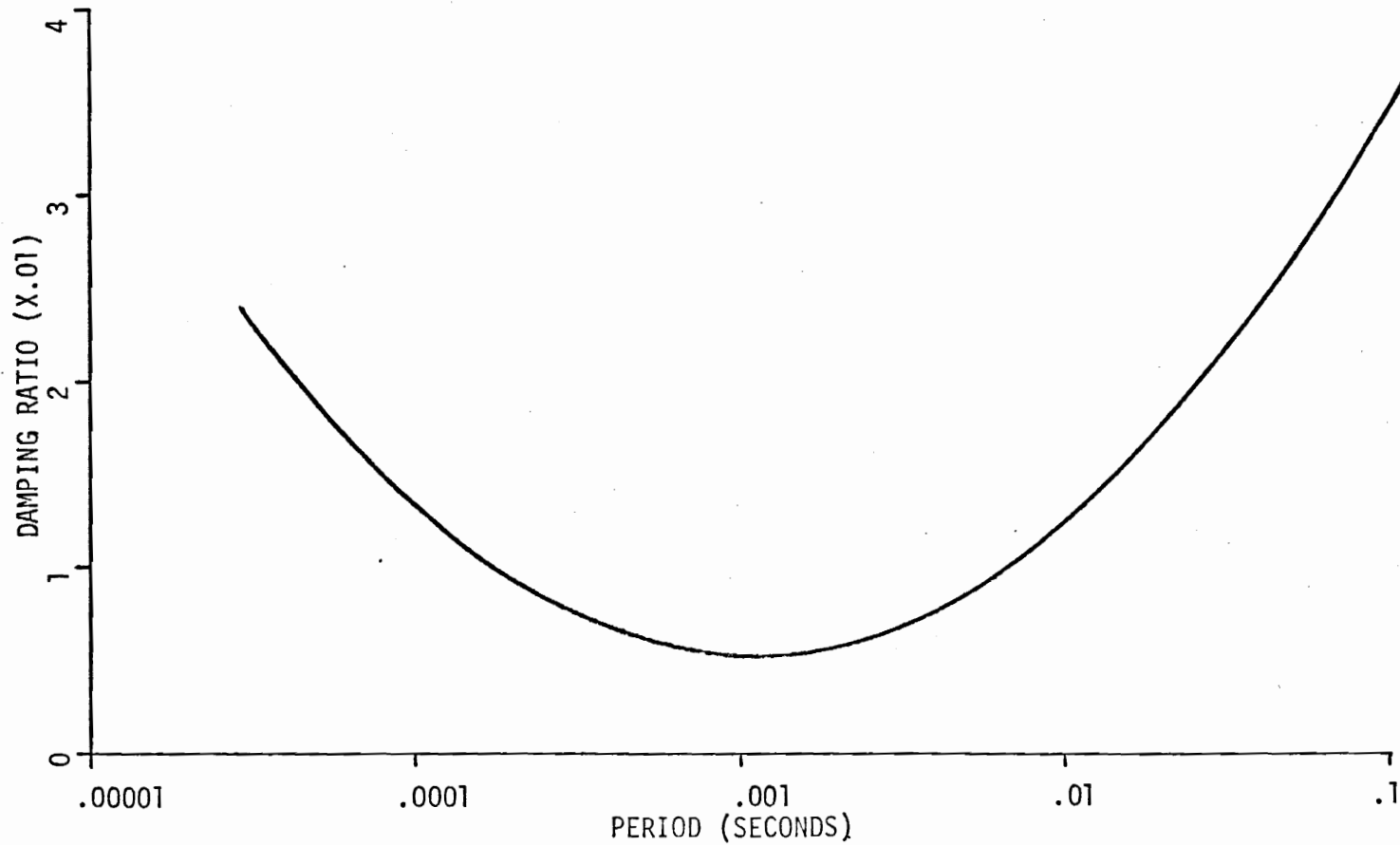


Figure 42. Master Curve for the Damping Ratio of Boron/Epoxy for a Reference Temperature of 80°F (300°K).

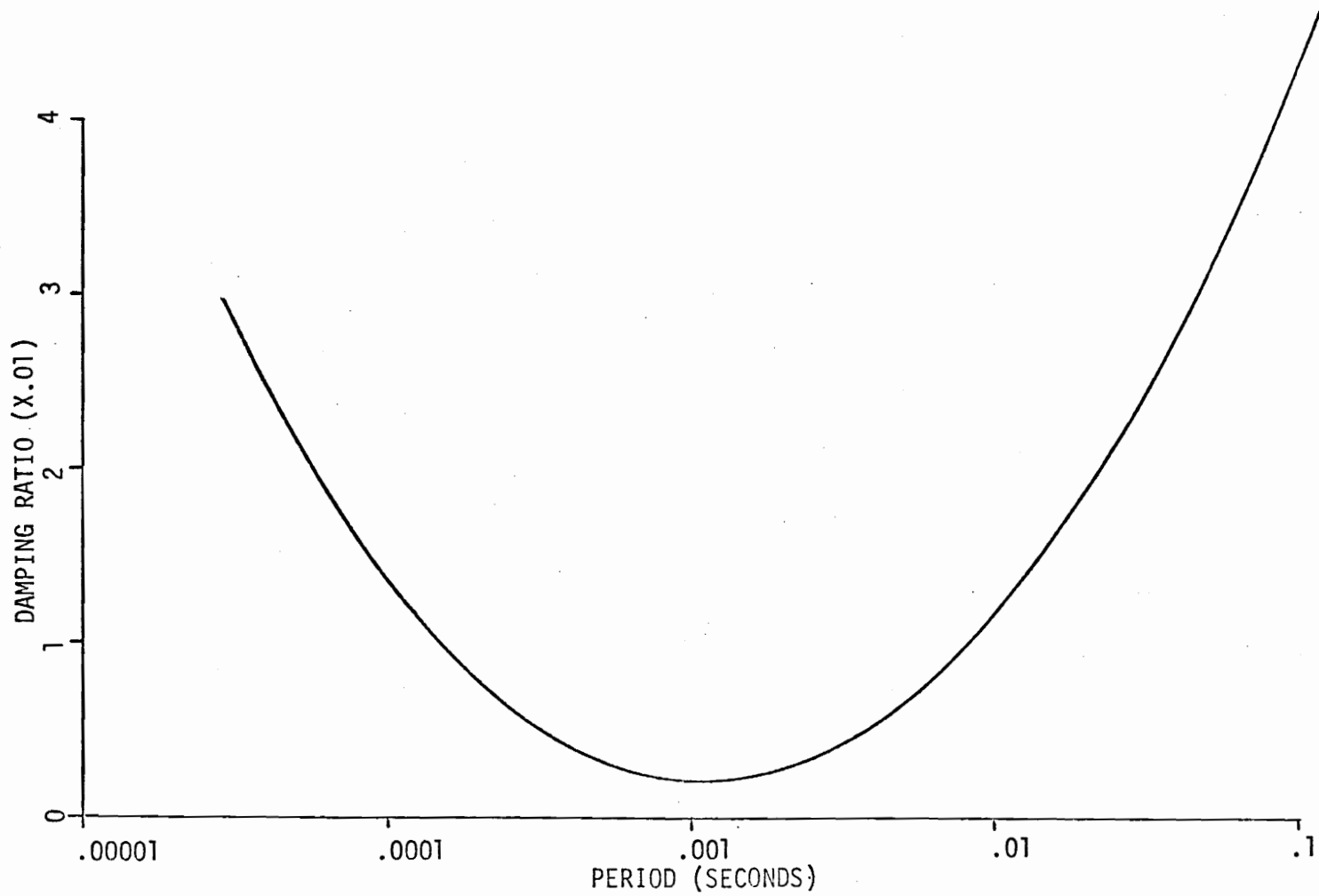


Figure 43. Master Curve for the Damping Ratio of Graphite/Epoxy for a Reference Temperature of 80°F (300°K).

shift factors. As discussed before, the relationship between temperature and time could be represented by a shift-factor a_T , which is the ratio of the time-scale at an arbitrary temperature relative to the time scale at a reference temperature T_r . It is a measure of the internal viscosity of a material.

In amorphous solids two types of time and temperature dependence are observed. At higher temperatures relaxation processes are stronger and it has been shown that a_T for amorphous polymers above their glass temperature can be represented by the WLF equation [12].

$$\log a_T = \frac{-8.86 (T - T_r)}{101.6 + T - T_r} \quad (4.8)$$

where T_r is a reference temperature empirically chosen so that equation (4.8) fits experimentally determined values of a_T . For polymeric bodies Eq. (4.8) is an approximate universal relation when T_r is taken as $50^\circ\text{C} + T_g$. The constants have been shown to vary rather slightly from polymer to polymer. A more general relationship is given by

$$\log a_T = \frac{C_1 (T - T_r)}{C_2 + T_1 - T_r} \quad (4.9)$$

where C_1 and C_2 are determined from the experiment. The Kinetic theory should be applicable if the measured shift function satisfies Eq. (4.9).

For viscoelastic response in the glassy region an Arrhenius type of dependence is usually observed. The shift factor a_T for this type of response is given by

$$\log a_T = \frac{\Delta H}{2.303R} \left(\frac{1}{T} - \frac{1}{T_R} \right) \quad (4.10)$$

ΔH is the activation energy in Kcal/mole.

R is the universal gas constant.

T is the absolute temperature in °K.

To characterize this kind of behavior when $\log a_T$ is plotted against $1/T$, it should give a straight line whose slope is equal to $\Delta H/2.303R$, and an intercept of $1/T_R$.

There is no unique definition of activation energy for WLF temperature dependence [12]. An apparent activation energy ΔH_a is often defined as

$$\Delta H_a = 2.303R \frac{d \log a_T}{d (1/T)} \quad (4.11)$$

This apparent activation energy increases with decrease in T up to about the glass temperature and thereafter decreases, where the WLF equation is no longer valid. This shows that the intermolecular forces and energy barriers which control the response to deformation are not the same over the whole temperature range studied.

Comparison of Eq. (4.10) with (4.6) gives,

$$\Delta H = \frac{-RF}{2C} \quad (4.12)$$

Thus Activation Energy can be directly obtained from the regression coefficients listed in Table 1 if an Arrhenius type of temperature dependence is established.

The temperature shift factor, a_T , for Boron/Epoxy and Graphite/Epoxy systems determined from various tests methods are plotted in Figures 44 through 49. The plots of $\log a_T$ vs. $1/T$ yield straight lines as expected in the glassy region. The values of ΔH for different tests along with regression coefficients are listed in Table 2.

The values obtained for activation energy are of the right order of magnitude. Sutherland [32] has reported 6-12 Kcal/mole for 3 different Epon 828 formulations in glassy range. For uni-directional phenolic glass laminates, Tsai [66] obtained $\Delta H = 7.85$ Kcal/mole. The opposite sign for loss modulus is not understood at the present.

The regression analysis was performed with a reference temperature in degrees Rankine to compare Graphite/Epoxy results with that of Shapery [45] and Sims [69]. Shapery obtained shift parameters, a_T , for strain response from creep tests. The Graphite/Epoxy system he used was HT-S/ERLA 2256 with 60% volume percent fiber content with orientation of $\pm 45^\circ$ to that of loading. He reported the activation energy of this system to be 35 Kcal/g-mole/ $^\circ R$. The flat slope of the $\log a_T$ vs. $1/T$ plot for the material investigated here seems to be physically reasonable because it contains fibers in the loading direction also; this makes the composite more elastic. The two

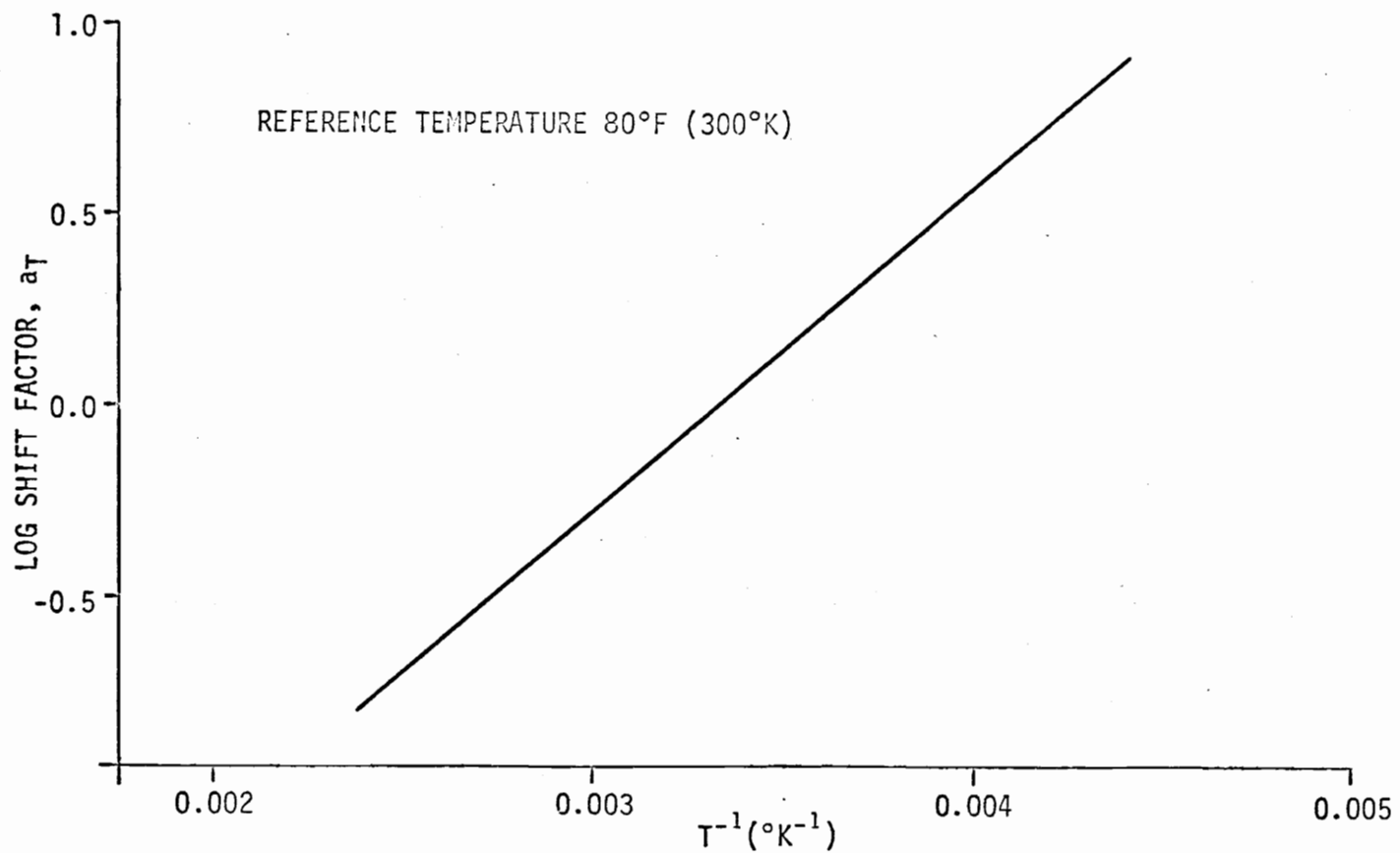


Figure 44. Temperature Shift Factor, a_T , for the Storage Modulus of Boron/Epoxy vs. Inverse Temperature.

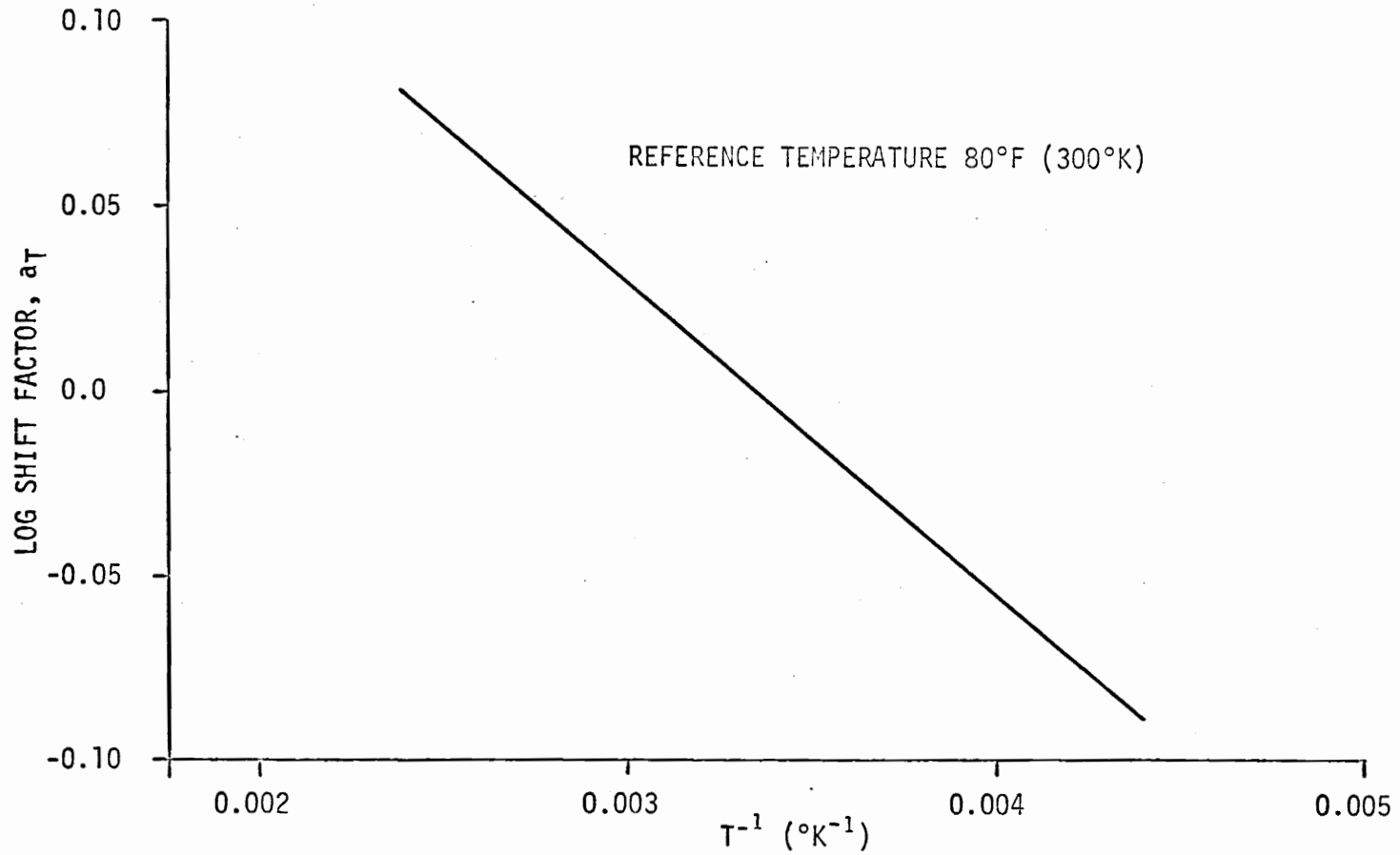


Figure 45. Temperature Shift Factor, a_T , for the Loss Modulus of Boron/Epoxy vs. Inverse Temperature.

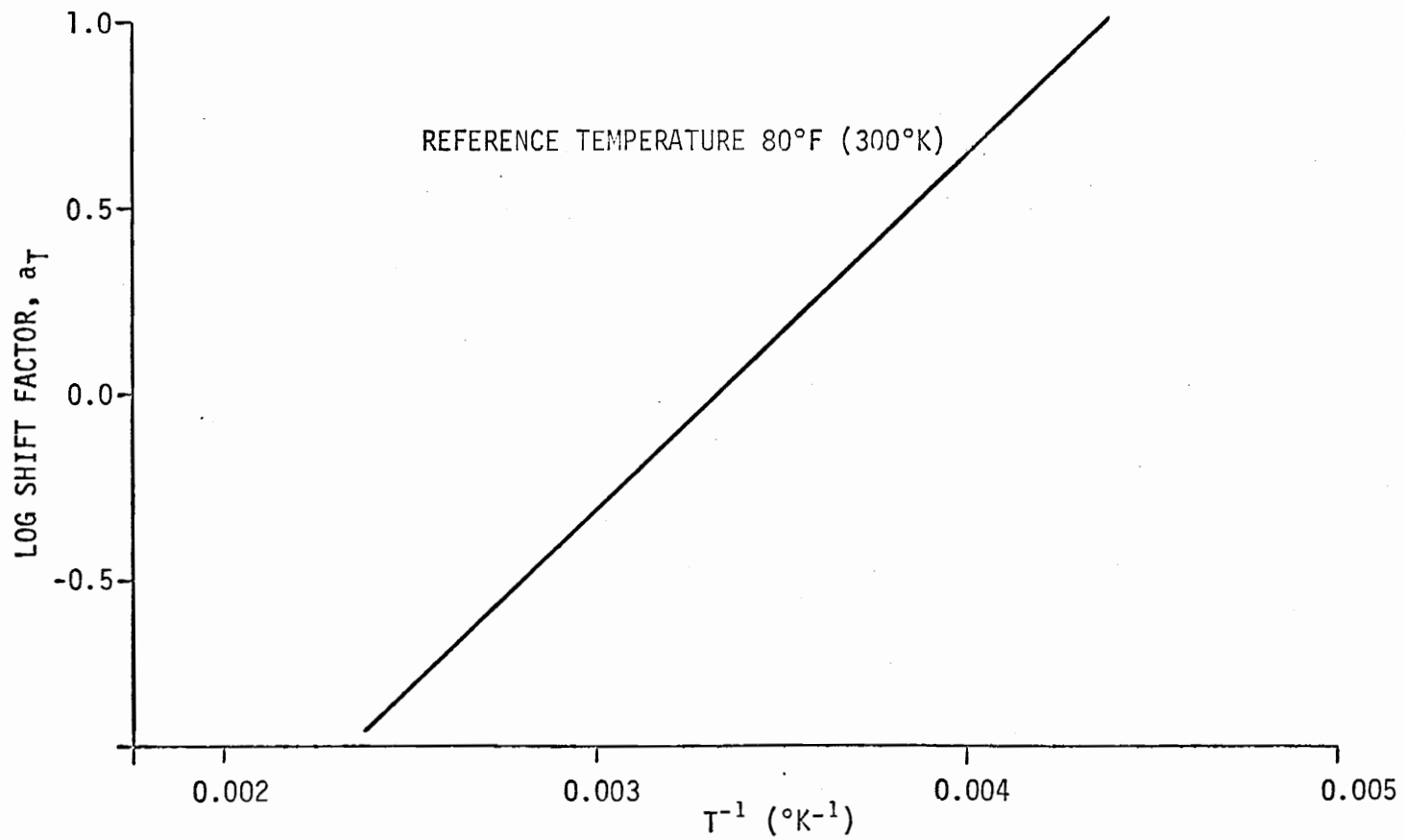


Figure 46. Temperature Shift Factor, a_T , for the Storage Modulus of Graphite/Epoxy vs. Inverse Temperature.

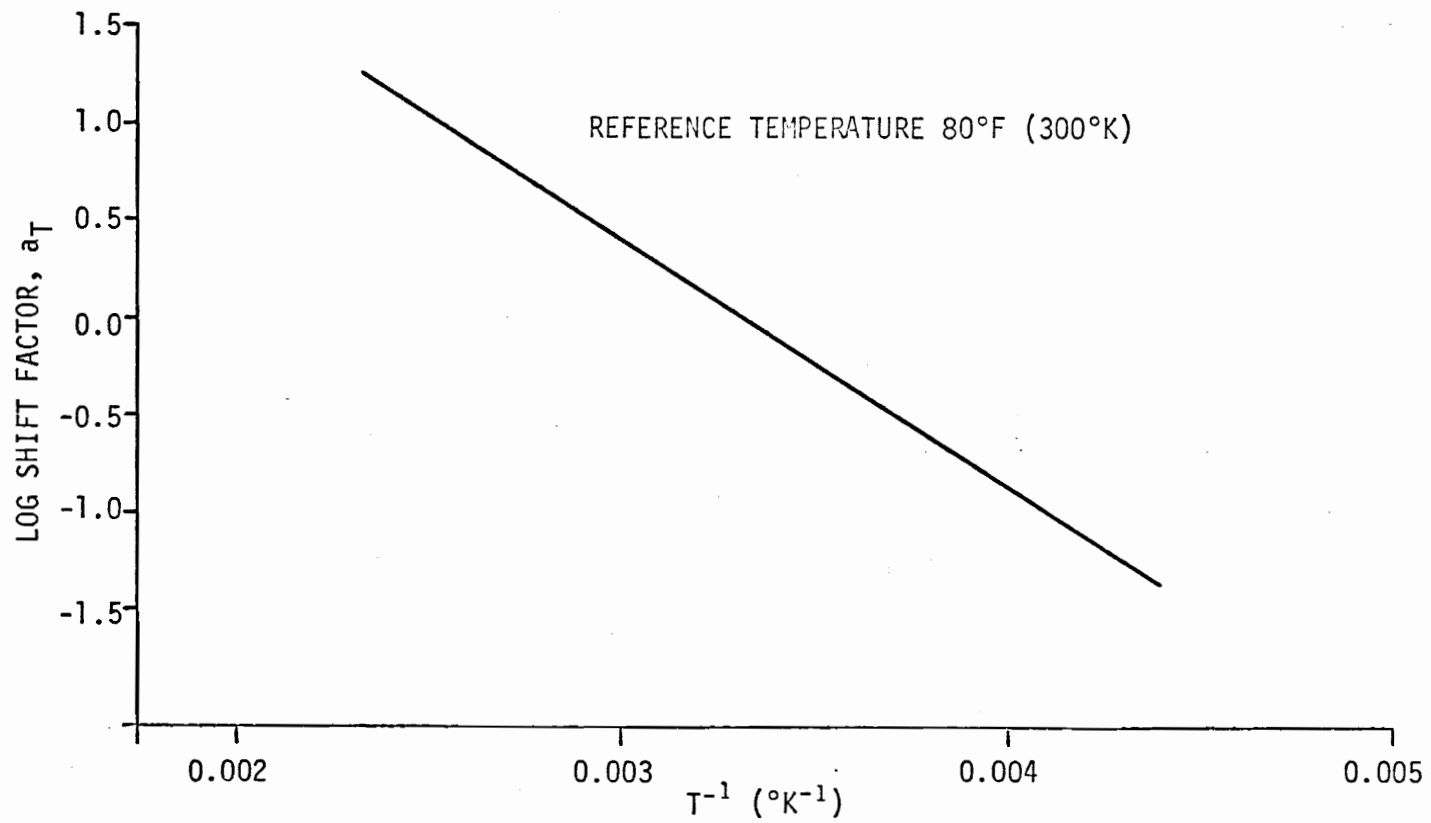


Figure 47. Temperature Shift Factor, a_T , for the Loss Modulus of Graphite/Epoxy vs. Inverse Temperature.

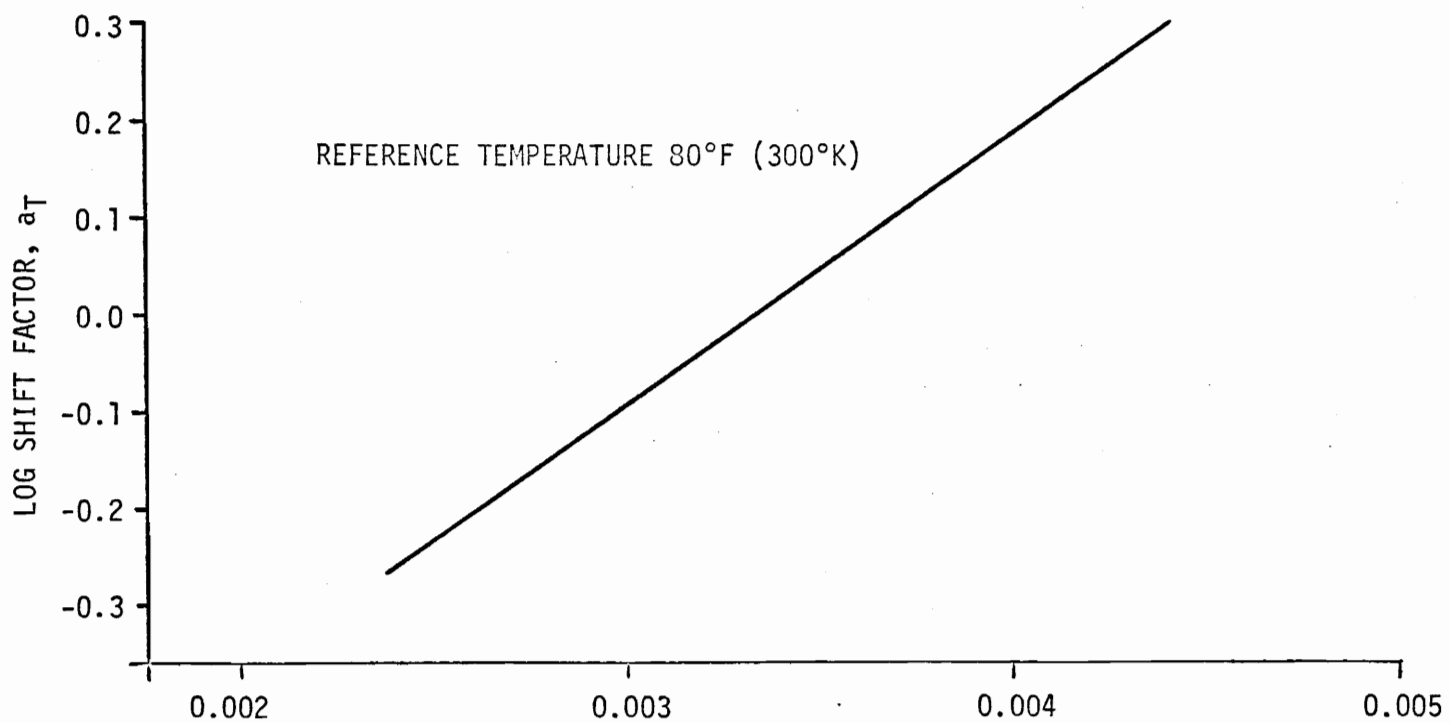


Figure 48. Temperature Shift Factor, a_T , for the Initial Modulus of Boron/Epoxy vs. Inverse Temperature.

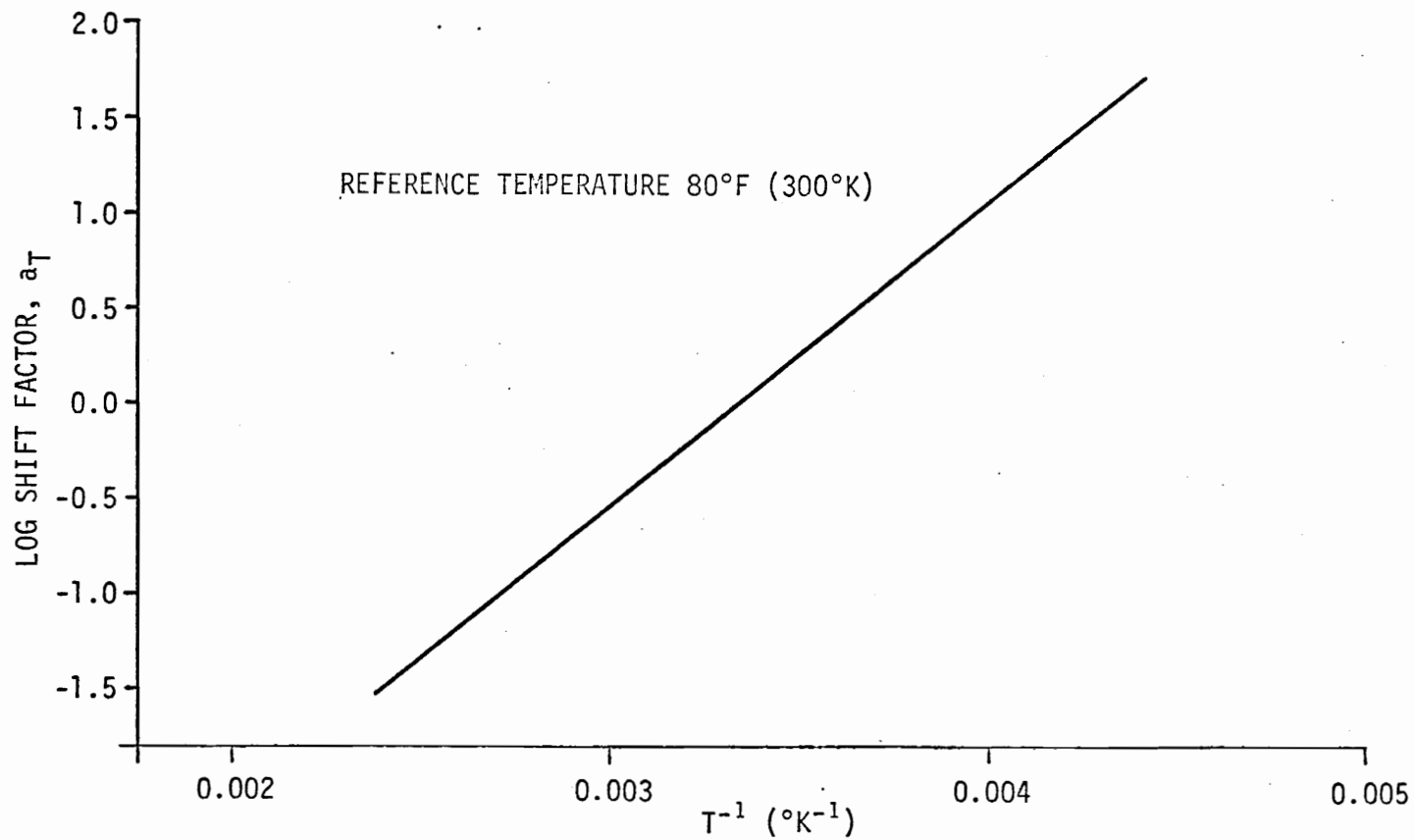


Figure 49. Temperature Shift Factor, a_T , for the Initial Modulus of Graphite/Epoxy vs. Inverse Temperature.

Table 2

DETERMINATION OF ACTIVATION ENERGY FROM REGRESSION COEFFICIENTS

Material	Function	F	C	$\Delta H(\text{Kcal/mole})/^{\circ}\text{K}$
Boron/Epoxy	Storage Modulus	-8.927	2.313×10^{-3}	3.834
	Loss Modulus	4.413×10^1	1.139×10^{-1}	-0.385
	Elastic Modulus	-3.538×10^7	2.751×10^4	1.278
Graphite/Epoxy	Storage Modulus	-7.657	1.743×10^{-3}	4.364
	Loss Modulus	9.022×10^1	1.495×10^{-1}	-0.600
	Elastic Modulus	-1.269×10^8	1.736×10^4	7.262

plots are compared in Figure 50.

The thermal coefficients of expansion for fiber and epoxy were used together with the law of mixtures to compute an approximate variation of the relative density with temperature change. The order of magnitude of the change in density for Boron/Epoxy at 300°F was computed to be 1.3987×10^{-13} times density at 80°F. This was negligible compared to the vertical shift as shown in reference [94]. It is believed that the composite materials studied here have a vertical shift which results from some other mechanism than that which is normally valid for polymers.

Predicting Strain Rate and Creep Properties.

Mechanical Model Representation: One of the objectives of this investigation was to develop reliable characterization procedures for the particular composites under study in order to predict intermediate and long time behavior from short time accelerated test techniques.

One way to achieve the stated objective would be to characterize the damping behavior obtained from vibration tests and then to use this characterization to predict constant strain rate or creep response. It is, therefore, necessary to employ an appropriate analytical technique for interconverting dynamic and static or quasi-static data. As stated earlier, one such analytical tool is based on the theory of viscoelasticity. Such a theory could be either linear or nonlinear and could be approached either through the use of mechanical models or integral equations. In this chapter the

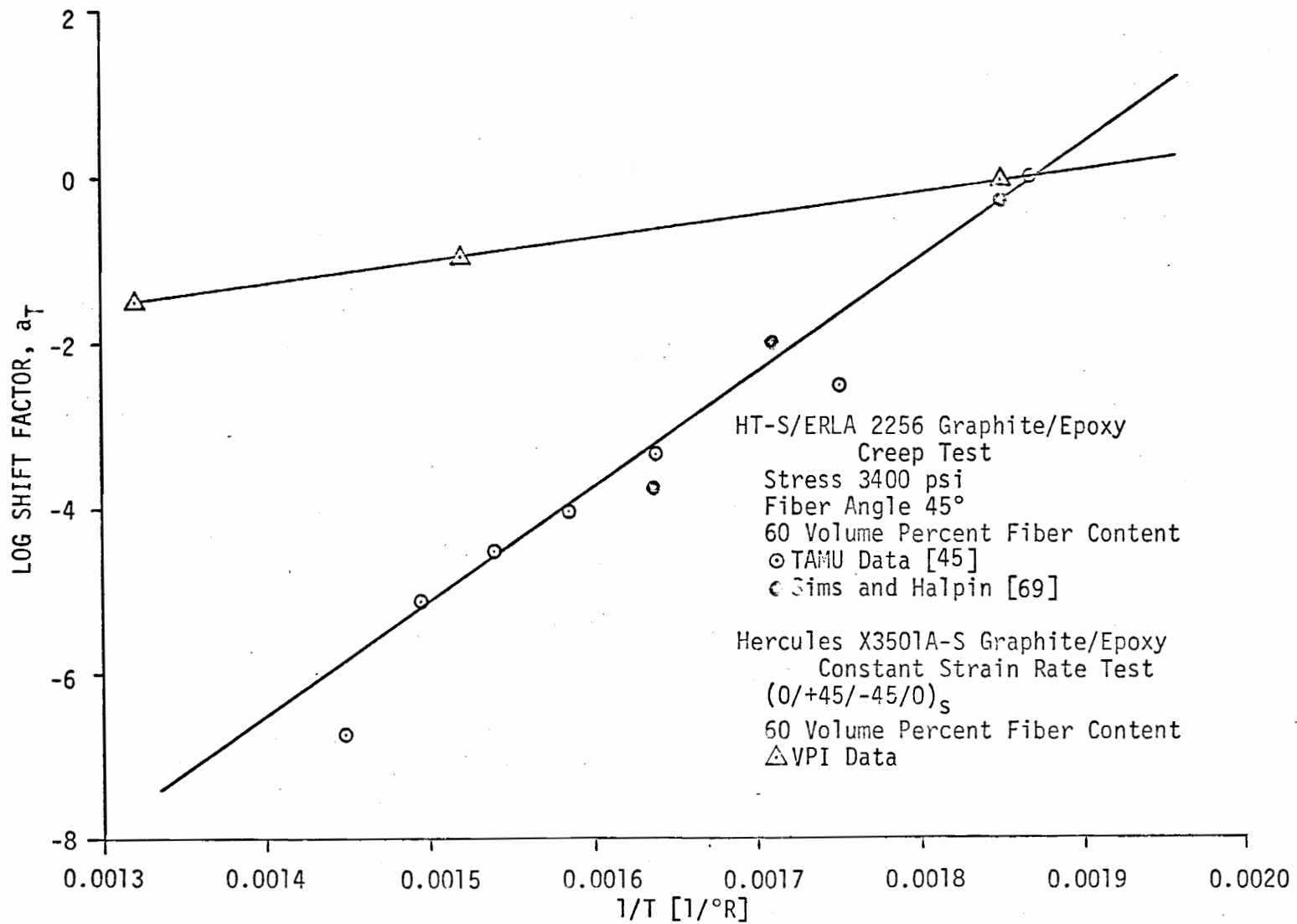


Figure 50. Temperature Shift Factor, a_T , vs. Inverse Temperature for Comparison of Graphite/Epoxy Systems.

mechanical model approach of linear viscoelasticity is reported. One reason for this approach is that quasi-static and dynamic properties for simple models are well known and makes conversion from one property to another relatively simple. Another, and perhaps more important reason, is that mechanical models have been used by metallurgists, polymer physicists, and materials scientists alike to explain damping behavior in both metals and nonmetals. Thus mechanical models can be a means to bring the many divergent points of view together with a common understanding. Indeed, the composite discussed here is a complex one consisting of eight plies with multiple fiber directions (i.e., 0° , $\pm 45^\circ$, 0)_S and a fiber content of about 60%. As a result, it is expected that damping behavior will be quite complex involving damping of the polymer matrix (below the T_g), the fibers, and interfacial effects. Because of these factors it is likely that the overall damping response will be a continuation of rate independent, quadratic and nonquadratic damping behavior of the fibers (Coulomb type) and rate dependent quadratic and nonquadratic damping of the matrix (viscous type) as discussed by Lazan and Shapery in references [35] and [67].

Figure 51 shows the vibration test results for Boron/Epoxy at room temperature. The data below a frequency of 1000 Hz is similar to that of aluminum presented by Schultz and Tsai [64] and Lazan [35]. The data above 1000 Hz is similar to that of a pure epoxy (below the T_g) presented by Schultz and Tsai [64]. The data in Figure 51 is typical of all the results from vibration

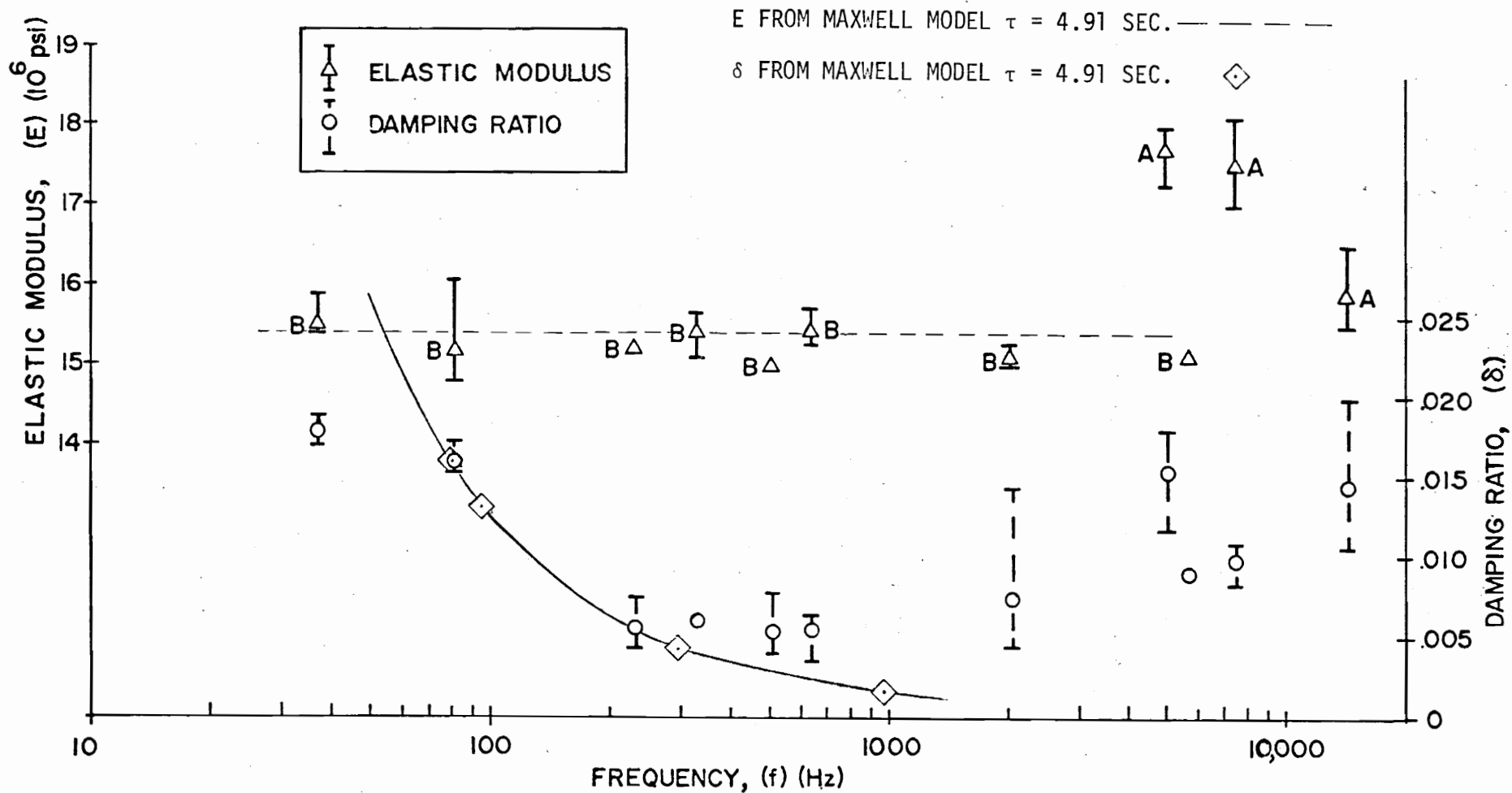


Figure 51. Maxwell Model Representation of Vibration Test Results on Boron/Epoxy Specimens at 80°F.

tests on both Boron/Epoxy and Graphite/Epoxy in all temperature regions and tends to support the view that damping behavior will be a complex combination of metal and polymer type response.

The complex modulus is defined as,

$$E^*(i\omega) = E'(\omega) + i E''(\omega) \quad (4.13)$$

or

$$E^*(i\omega) = E'(\omega)(1 + i\delta) \quad (4.14)$$

where

$$\delta = \frac{E''(\omega)}{E'(\omega)} \quad (4.15)$$

is the damping ratio. From Figure 51 it may be seen that the storage modulus is relatively insensitive to a variation in frequency; in comparison, the damping ratio (or loss modulus) is quite sensitive to frequency variations.

Using the relation,

$$E^*(i\omega) = \frac{\sum_{k=0}^m q_k (i\omega)^k}{\sum_{k=0}^m p_k (i\omega)^k} \quad (4.16)$$

which defines the complex modulus in terms of spring moduli and damper viscosities (or in terms of the coefficients of the differential equation connecting stress to strain for linear viscoelastic materials), the storage modulus, loss modulus or damping ratio can easily be determined for various mechanical models. For example, a

Maxwellian material has the following storage and loss properties:

$$E'(\omega) = k \left[\frac{1}{1 + \left(\frac{1}{\omega\tau}\right)^2} \right] \quad \& \quad \delta = \frac{1}{\omega\tau} \quad (4.17)$$

where k and τ are the spring moduli and the relaxation time respectively. A Kelvin material has the storage and loss properties:

$$E'(\omega) = E \quad , \quad \delta = \tau\omega \quad (4.18)$$

Below 1000 Hz, the damping ratio data of Figure 51 is like that of a Maxwell material and above 1000 Hz it is similar to that of a Kelvin material.

Figure 52 shows constant strain rate (constant head rate) information for Boron/Epoxy at room temperature. For rates between 2.5×10^{-6} in/in/sec to 5.14×10^{-1} in/in/sec a relatively small amount of rate sensitivity is shown which is again typical of all the results for both Boron/Epoxy and Graphite/Epoxy at various temperature levels.

It is desirable to see if the rate data of Figure 52 can be predicted from the damping behavior of Figure 51. A Maxwellian representation shown in Figure 53(a) was used because the Kelvin type response above 1000 Hz is unlikely to effect the rate results appreciably.

Since this study was conducted earlier in the investigation, statistically conditioned data was not used.

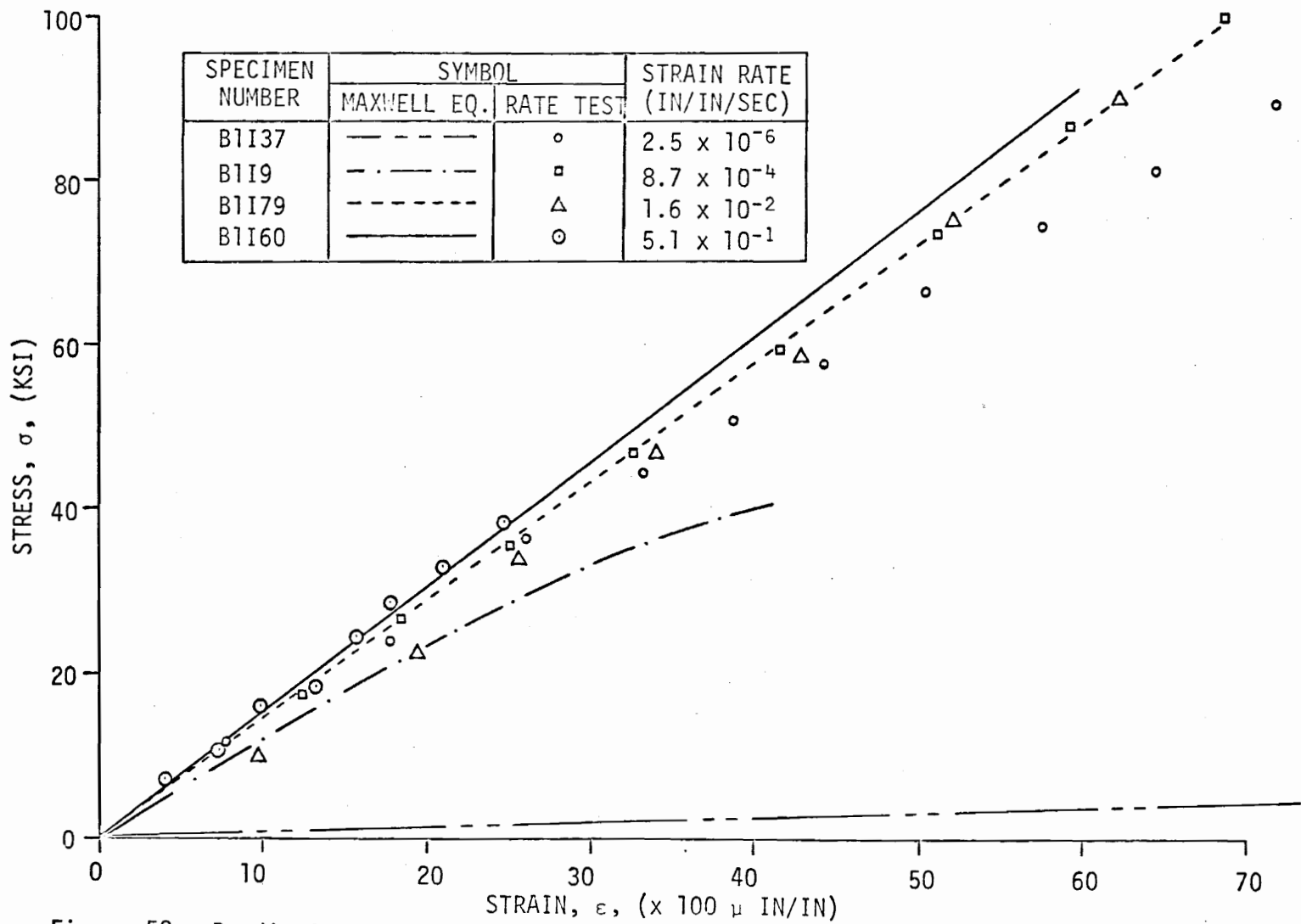
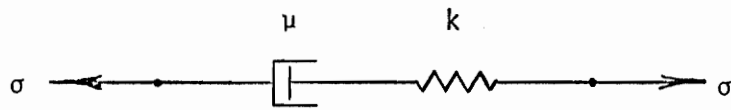
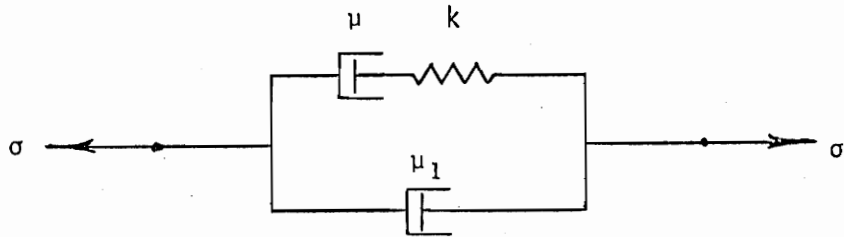


Figure 52. Prediction of Stress-Strain Curves at Various Strain Rates from Dynamic Test for Boron/Epoxy at 80°F Using Maxwell Model.



(a) Maxwell Model



(b) Triparameter Viscoelastic Model

Figure 53. Mechanical Model Representation.

Using the damping ratio for 80 Hz and the fact that the storage modulus varies little with frequency, (4.17) yields a relaxation time and a storage modulus of $\tau = 4.91$ sec and $k = 15.2 \times 10^6$ psi respectively. These values have been used to calculate the stress-strain curves shown superimposed on the data of Figure 52. As indicated previously, the response below 1000 Hz is nearly Maxwellian.

The strain rate behavior of a Maxwell material can easily be developed as follows

$$\sigma(\epsilon) = \tau k \dot{\epsilon} (1 - e^{-\epsilon/\tau \dot{\epsilon}})$$

$$\frac{d\sigma}{d\epsilon} = k e^{-\epsilon/\tau \dot{\epsilon}} \quad (4.19)$$

$$\left. \frac{d\sigma}{d\epsilon} \right|_{\epsilon \rightarrow 0} \rightarrow k$$

Since, τ and k are known from vibration data then, for a given $\dot{\epsilon}$, stress can now be computed for different strain levels. The stress strain curves obtained from Eq. (4.19) for different strain rates are plotted in Figure 52. They are superimposed on experimental curves. At the higher two rates they follow the experimental curves reasonably well, but at low rates the predictions are poor.

Triparameter Viscoelastic Model: Damping behavior as shown in Figure 51 agreed with Maxwell behavior only up to 1000 Hz. Above 1000 Hz damping increases again. A triparameter model whose damping

behavior is qualitative similarity to experimental observations was tried next. Lazan [35] has presented damping properties for different linear mechanical models. A triparameter viscoelastic model with two dissipators (Figure 53(b)) showed the required damping properties. It has an equivalent configuration to that of a three parameter fluid model.

Its constitutive equation is given by

$$p_0 \sigma + p_1 \dot{\sigma} = q_1 \dot{\epsilon} + q_2 \ddot{\epsilon} \quad (p_1 q_1 > q_2)$$

$$\text{where } p_0 = 1 \quad p_1 = \frac{\mu}{k} \quad (4.20)$$

$$q_1 = \mu + \mu_1 \quad \text{and} \quad q_2 = \frac{\mu \mu_1}{k}$$

μ , μ_1 and k are viscosity coefficients for dashpots and spring as shown in Figure .

The Complex Modulus for this model could be shown to have the form:

$$E^*(i\omega) = \frac{(p_1 q_1 - p_0 q_2) \omega^2}{p_0^2 + p_1^2 \omega^2} + i \frac{(p_0 q_1 + p_1 q_1 \omega^2) \omega}{p_0^2 + p_1^2 \omega^2} \quad (4.21)$$

therefore the damping ratio is expressed as

$$\begin{aligned} \delta &= \frac{(q_1 + p_1 q_2 \omega^2)}{(p_1 q_1 - q_2) \omega} \quad (4.22) \\ &= \frac{q_1}{(p_1 q_1 - q_2) \omega} + \frac{p_1 q_1 \omega}{(p_1 q_1 - q_2)} \\ &= \frac{C_1}{\omega} + C_2 \omega \end{aligned}$$

When these two lines are superposed, the resulting curve is fairly representative of damping data shown in Figure 51.

Substituting values of q_1 , q_2 and p_1 in Eq. (4.22) the damping ratio can be expressed in terms of model constants as

$$\delta = \frac{\{k^2(\mu + \mu_1) + \mu^2\mu_1\omega^2\}\omega}{k\mu^2\omega^2} \quad (4.23)$$

and the Storage Modulus, which is the real part of Eq. (4.21) becomes

$$E' = \frac{k\mu^2\omega^2}{k^2 + \mu^2\omega^2} \quad (4.24)$$

Various methods were tried to determine the model constants k , μ and μ_1 in order to approximate actual material properties.

The constants were obtained by simultaneous solutions of equations (4.23) and (4.24) by choosing ten values of E' and one of δ and vice versa for different frequencies. When substituted back into damping expression, it failed to represent the measured values. Limiting values of E' were also used with the same result.

The least square fit method, which was also tried by several investigators including Schapery [17] as a model fitting technique to measured values of material properties, was employed next. Expressions for a least square curve fit were derived for Eq. (4.23) using Cramer's rule,

$$B \sum_{i=1}^N \frac{1}{\omega_i^2} + NC = \sum_{i=1}^N \frac{\delta_i}{\omega_i} \quad (4.25)$$

and

$$C \sum_{i=1}^N \omega_i^2 + NB = \sum_{i=1}^N \delta_i \omega_i \quad (4.26)$$

where $B = \frac{\mu + \mu_1}{k^2}$ and $C = \frac{\mu_1}{k}$

Measured values of damping at eleven different points on the statistically conditioned damping curve shown in Figure 54 were used to determine constants B and C and hence μ , μ_1 and k. When these values were substituted into equation (4.23) values obtained for different frequencies gave a fair quantitative representation of measured damping ratios, Figure 54. A similar procedure was also tried for the storage modulus but because its analytic expression did not resemble experimental values, constants obtained from damping ratios were used.

Values for k, μ and μ_1 computed from Eqs. (4.25) and (4.26) were determined as,

$$k = 15.56 \times 10^6 \text{ psi}$$

$$\mu = 37.99 \times 10^6 \text{ psi-sec.}$$

$$\mu_1 = 17.76 \text{ psi-sec.}$$

For constant strain rate, the constitutive equation (4.20) is reduced to

$$\sigma + \frac{\mu}{k} \dot{\sigma} = (\mu + \mu_1) \dot{\epsilon} \quad (4.27)$$

using the initial condition $\sigma = 0$ when $t = 0$. With the relation

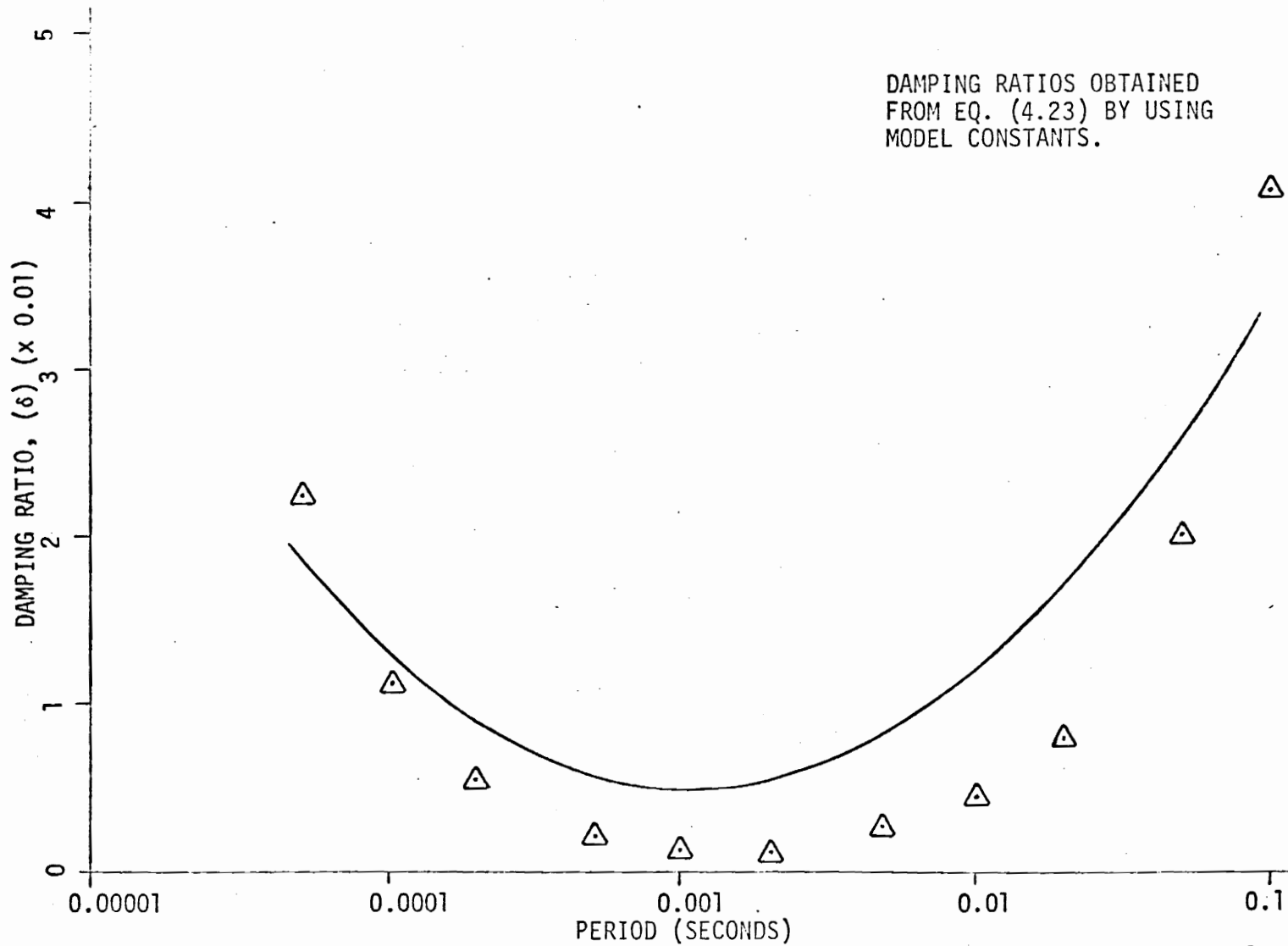


Figure 54. Least Square Fit to Determine Constants of Triparameter Viscoelastic Model from Vibration Test Results on Boron/Epoxy Specimens at 80°F.

$\frac{\mu}{k} = \dots$, and solving the above differential equation,

$$\sigma = (\mu + \mu_1) \dot{\epsilon} \{1 - e^{-t/\tau}\} \quad (4.28)$$

is obtained. Since, $\dot{\epsilon} = \frac{\epsilon}{t}$ substituting t in equation (4.28) yields a stress-strain relation for the above model.

$$\sigma(\epsilon) = (\mu + \mu_1) \dot{\epsilon} \{1 - e^{-\epsilon/\dot{\epsilon}\tau}\} \quad (4.29)$$

Using the values of k and μ , τ becomes equal to 2.4415 secs. as compared to 4.91 secs. reported earlier for a Maxwell model.

Constant strain rate curves have been drawn using the values for μ , μ_1 , k and τ given above and are superimposed on the experimental curves shown in Figure 55. Again, it can be seen that the procedure works reasonably well for high rates but not at all for the very low rates. Since the material behavior is complex, simple mechanical models may not be able to represent the material response.

Interconversion by Integral Equation.

Many investigators [22, 68, 70] have reported that the creep compliance obeys a power law for the advanced composite systems. If this assumption is valid for composites investigated here, the results of creep tests, constant loading tests, and dynamic tests can be interconverted using linear viscoelastic theory.

Sims and Halpin [69] derived interconversion formulae for constant load rate tests. Their results were modified here for constant strain rate tests. A brief derivation is presented, more

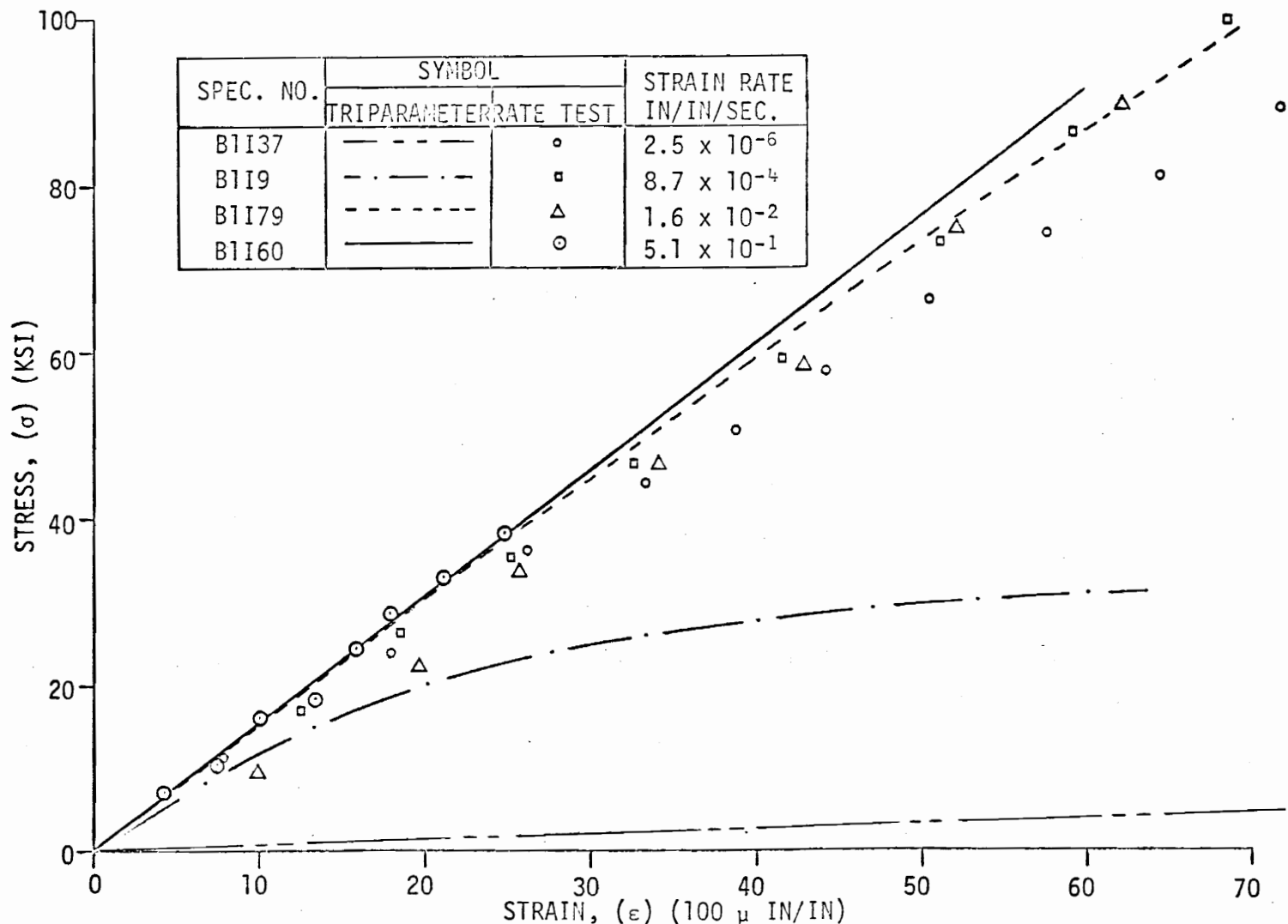


Figure 55. Prediction of Stress-Strain Curves at Various Strain Rates from Dynamic Tests for Boron/Epoxy at 80°F Using Triparameter Model.

detail can be obtained from the above reference.

For isothermal, uniaxial loading under plane state of stress, the creep compliance function, $D(t)$, is related to strain by,

$$\epsilon(t) = \int_{-\infty}^t D(t - \tau) \frac{\partial \sigma}{\partial \tau} d\tau \quad (4.30)$$

If the dynamic loading is of the form

$$\sigma(t) = \sigma_0 e^{i\omega t}$$

Eq. (4.30) becomes,

$$\epsilon(t) = i\omega\sigma_0 \int_{-\infty}^t D(t - \tau) e^{i\omega\tau} d\tau \quad (4.31)$$

Substituting $t - \tau = u$ and dividing by the stress $\sigma(t)$

$$\frac{\epsilon(t)}{\sigma(t)} = i\omega \int_0^{\infty} D(u) e^{-i\omega u} du \quad (4.32)$$

The exponential term in Eq. (4.32) could be expressed in trigonometric form

$$\frac{\epsilon(t)}{\sigma(t)} = i\omega \int_0^{\infty} D(u) [\cos \omega u - i \sin \omega u] du \quad (4.33)$$

The real part of Eq. (4.33) is a storage compliance,

$$D'(\omega) = \omega \int_0^{\infty} D(u) \sin \omega u du \quad (4.34)$$

and the imaginary part of Eq. (4.33) is a loss compliance

$$D''(\omega) = \omega \int_0^{\infty} D(u) \cos \omega u \, du \quad (4.35)$$

If creep compliance can be assumed to obey a power law for a step function input,

$$D(t) = at^b \quad (4.36)$$

where $a > 0$ and $0 < b < 1$, and an initial load at $t = 0$ is assumed, substituting Eq. (4.36) into Eq. (4.34) and Eq. (4.35)

$$D'(\omega) = \omega \int_0^{\infty} at^b \sin \omega t \, dt \quad (4.37)$$

and

$$D''(\omega) = \omega \int_0^{\infty} at^b \cos \omega t \, dt \quad (4.38)$$

are obtained.

$D'(\omega)$ and $D''(\omega)$ can be explicitly evaluated by using the relationship,

$$\int_0^{\infty} e^{-au} u^b \, du = \frac{\Gamma(b+1)}{a^{b+1}} \quad (4.39)$$

where $\Gamma(b+1)$ is the Gamma function.

If $a = i\omega$, then,

$$e^{-au} = e^{-i\omega u} = \cos \omega u - i \sin \omega u$$

and

$$a^{-(b+1)} = -i(\omega)^{-(b+1)} \left(\cos \frac{b\pi}{2} - i \sin \frac{b\pi}{2} \right) \quad (4.40)$$

Also can be expressed as,

$$-iD' + D'' = a\omega \int_0^{\infty} e^{-i\omega t} t^b dt \quad (4.41)$$

Performing the integration indicated in (4.41) by using relationships (4.39) and (4.40) and equating real and imaginary parts gives,

$$|D'| = (a\omega^{-b} \cos \frac{b\pi}{2}) \Gamma(1+b) \quad (4.42)$$

and

$$|D''| = (a\omega^{-b} \sin \frac{b\pi}{2}) \Gamma(1+b) \quad (4.43)$$

The complex compliance $D^*(\omega)$ is obtained by using known relationship

$$D^*(\omega) = |D'| - i |D''| \quad (4.44)$$

Substituting (4.42) and (4.43) in Eq. (4.44) and simplifying gives,

$$D^*(\omega) = a(i\omega)^{-b} \Gamma(1+b) \quad (4.45)$$

The above derivation could be checked by taking Laplace transform of creep compliance.

Again, assuming a power law for the creep compliance and using relations between creep compliance and relaxation modulus in Laplace Transform Space.

$$\bar{D}(t) \cdot \bar{E}(t) = \frac{1}{s^2} \quad (4.46)$$

Assuming a power law form for compliance,

$$\bar{D}(t) = \frac{a\Gamma(b+1)}{p(b+1)}$$

$$\bar{E}(t) = \frac{p(b-1)}{a\Gamma(b+1)}$$

inverting back to t space, and using the relation,

$$\frac{1}{\Gamma(b+1)\Gamma(b-1)} = \frac{\sin b\pi}{ab\pi} (t)^{-b}$$

It can be shown [69] that

$$E(t) = \frac{\sin b\pi}{ab\pi} (t)^{-b} \quad (4.47)$$

If a stress free loading history is assumed before $t = 0$, stresses are expressed by the integral relation

$$\sigma(t) = \int_0^t E(t-\tau) \frac{\partial \epsilon}{\partial \tau} d\tau \quad (4.48)$$

for a constant strain rate,

$$\epsilon(t) = Kt \quad (4.49)$$

where K is a constant and

$$\frac{\partial \epsilon}{\partial t} = K \quad (4.50)$$

Substituting in Eq. (4.48)

$$\sigma(t) = K \int_0^t E(t - \tau) d\tau \quad (4.51)$$

by letting $u = t - \tau$ yields

$$\sigma(t) = K \int_0^t E(u) du \quad (4.52)$$

by substituting $E(u)$ from Equation (4.47) in (4.52),

$$\sigma(t) = K \frac{\sin b\pi}{ab\pi} \int_0^t u^{-b} du \quad (4.53)$$

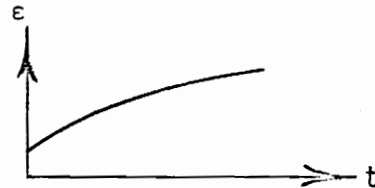
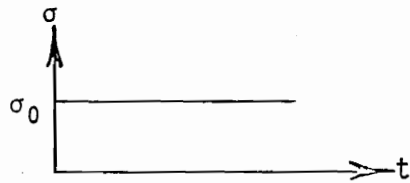
is obtained.

Solution of the above definite integral yields a stress-strain relationship for constant strain rate.

$$\sigma(t) = K \frac{\sin b\pi}{ab\pi} \left[\frac{t^{(1-b)}}{(1-b)} \right] \quad (4.54)$$

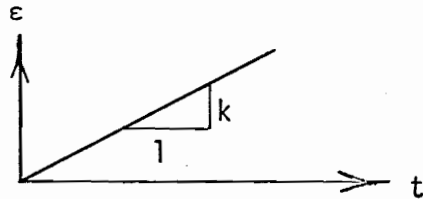
Thus, if the constants of the power law form of the creep compliance are known, the viscoelastic response of a composite material could be determined or alternatively dynamic tests can be used to determine constants a and b to predict constant strain rate and creep test results. Interconversion formulae are summarized in Figure 56.

To predict constant strain rate and creep behavior, a and b were determined from dynamic tests. Storage moduli values computed earlier can be converted to storage compliance as



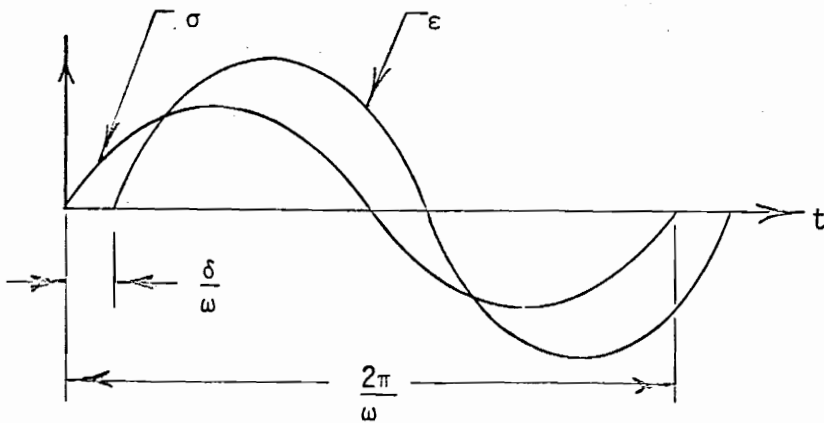
CREEP TEST

$$D(t) = \frac{\sin b\pi}{b\pi} \frac{1}{E(t)} = a t^b$$



CONSTANT STRAIN RATE TEST

$$\sigma(t) = K \frac{\sin b\pi}{ab\pi} \left[\frac{t(1-b)}{(1-b)} \right]$$



DYNAMIC TEST

$$D^*(\omega) = a\Gamma(b+1)(i\omega)^{-b}$$

$$D'(\omega) = a\Gamma(b+1) \omega^{-b} \cos \frac{b\pi}{2}$$

$$D''(\omega) = a(b+1) \omega^{-b} \sin \frac{b\pi}{2}$$

$$\delta = \tan \left(\frac{b\pi}{2} \right)$$

Figure 56. Viscoelastic Interconversion Relations.

$$|D'| = \frac{1/|E'|}{1 + \tan^2 \delta} \approx 1/|E'| \quad (4.55)$$

if $\delta \ll 1$

If equation (4.43) is divided by (4.42),

$$\delta = \tan \left(\frac{b\pi}{2} \right) \quad (4.56)$$

is obtained.

Since damping ratios are experimentally determined, constant b could be found from equation (4.56). For a given b and $|D'|$, a can be computed using equation (4.42).

For a given temperature, a and b values can be obtained as a function of frequency using regression coefficients from equation (3.3).

Since damping ratio shows a frequency dependence, constant b also varies substantially at different frequencies while a is relatively constant. The plot of variation of a and b with $t = 1/\omega$ is shown in Figure 57. Values of a and b were computed at different times to obtain stresses at constant strain rates using equation (4.54):

$$\sigma(t = 1/\omega) = K \frac{\sin b\pi}{ab\pi} \left[\frac{t(1-b)}{(1-b)} \right]$$

The stress-time curve (or stress-strain curve at constant strain rate) predicted from the above equation is compared with experimental curve for Boron/Epoxy at 300°F for a strain rate of

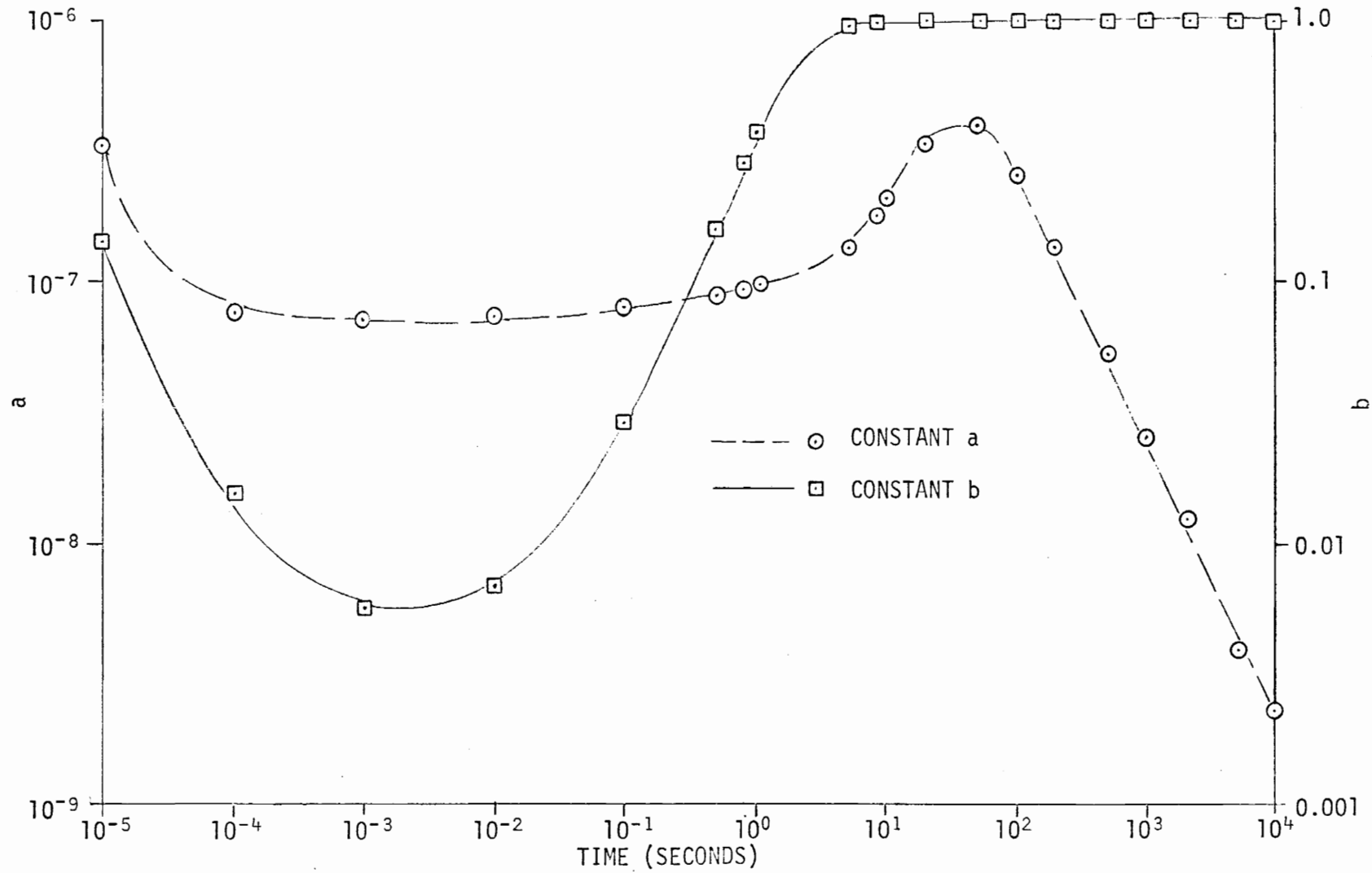


Figure 57. Variation of Constants a and b with Time, for Boron/Epoxy at 300°F as Obtained from Dynamic Tests.

0.257 in/in/sec in Figure 58. The experimental curves are averaged for at least two individual tests. The figure shows that the predicted values compare very well. Since the equation obtained by regression analysis becomes physically incensitent with observed phenomena beyond the experimental range, damping and storage modulus values were extrapolated.

Stress-time curves were obtained from the extrapolation for the three low rates are in good agreement with experiments. The discussion about this behavior is explained in the next chapter. Predicted curves for Graphite/Epoxy at 80°F at two different strain rates are shown in Figures 60 and 61.

Extrapolated values of a and b from Storage Modulus and damping ratio of Boron/Epoxy at 300°F were used to compute the creep compliance at 10^5 and 10^6 secs. using the power law, equation (4.36). They are plotted together with experimental points in Figure 69. Here again, experimental and predicted values were within 10%. The discrepancy might be due to the fact that while statistically conditioned dynamic data was used to compute a and b , the comparison is made with single creep test results. In closure, this approach seems to be working well for predicting strain rate and creep behavior.

Numerical Integration Method

In an effort to calculate one experimentally observable viscoelastic function from another, numerical solutions of various

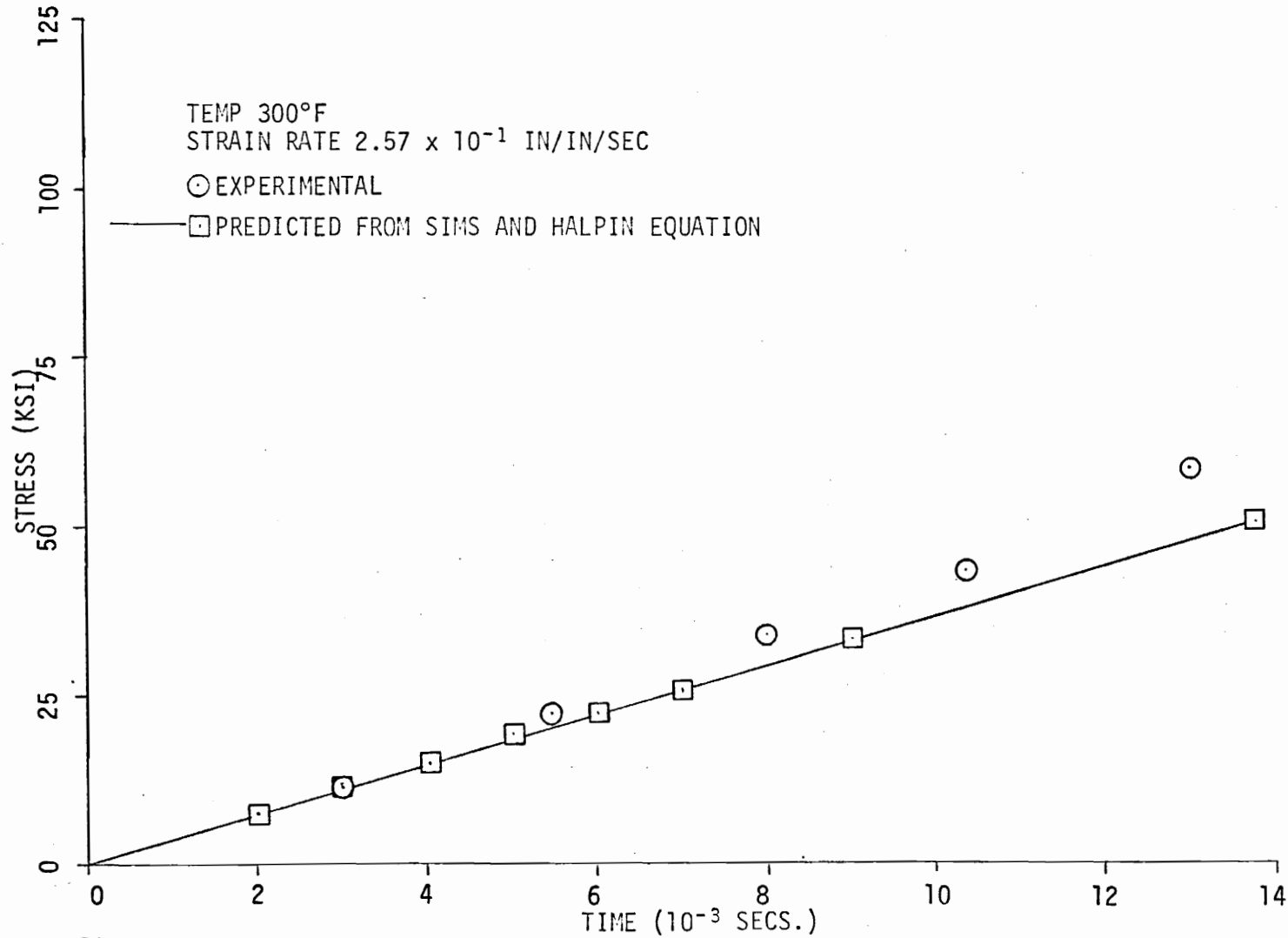


Figure 58. Prediction of Stress-Strain Curve at a Constant Strain Rate from Dynamic Tests by Sims and Halpin Equation [69] for Boron/Epoxy.

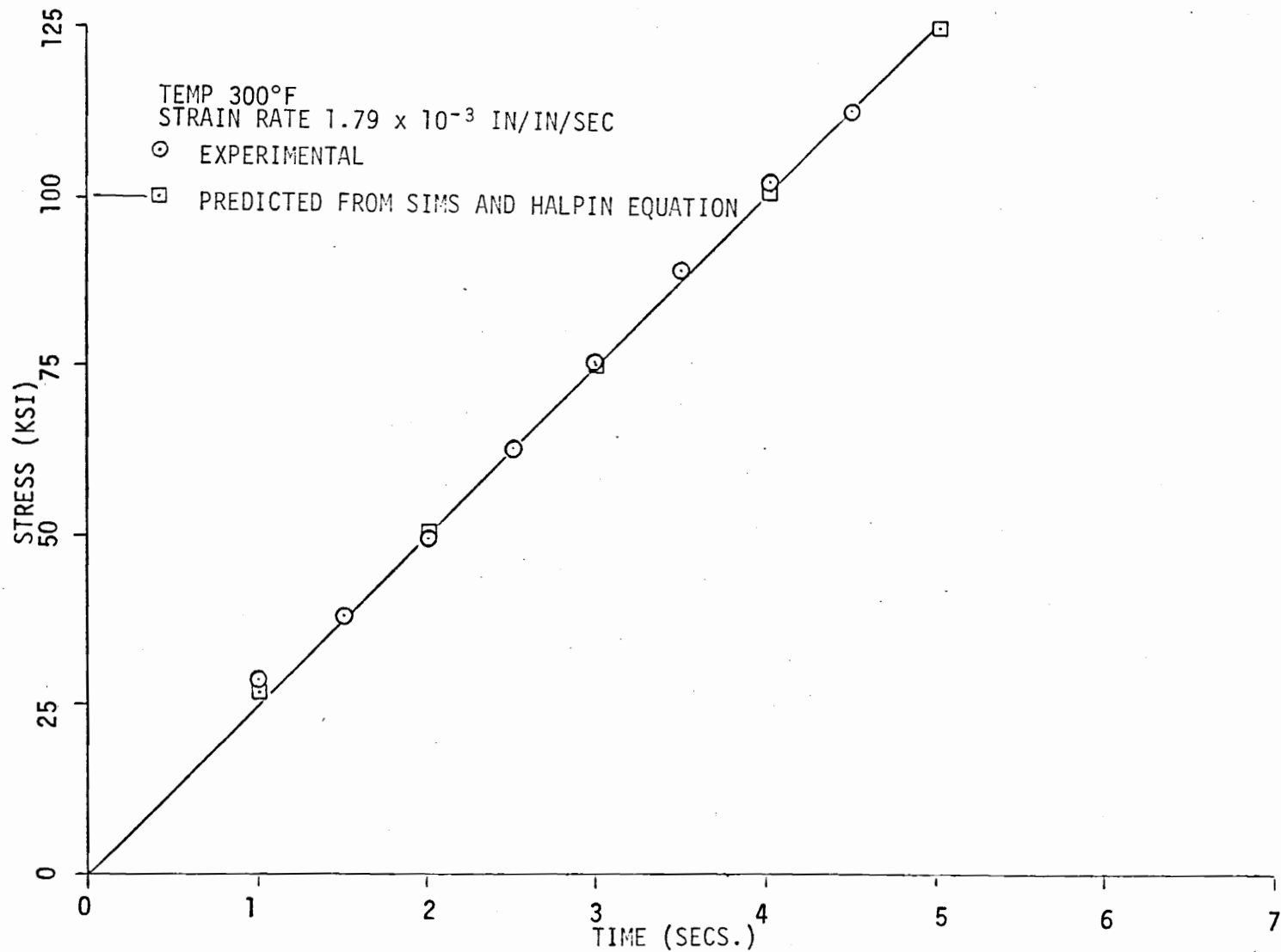


Figure 59. Prediction of Stress-Strain Curve at a Constant Strain Rate from Dynamic Tests by Sims and Halpin Equation [69] for Boron/Epoxy.

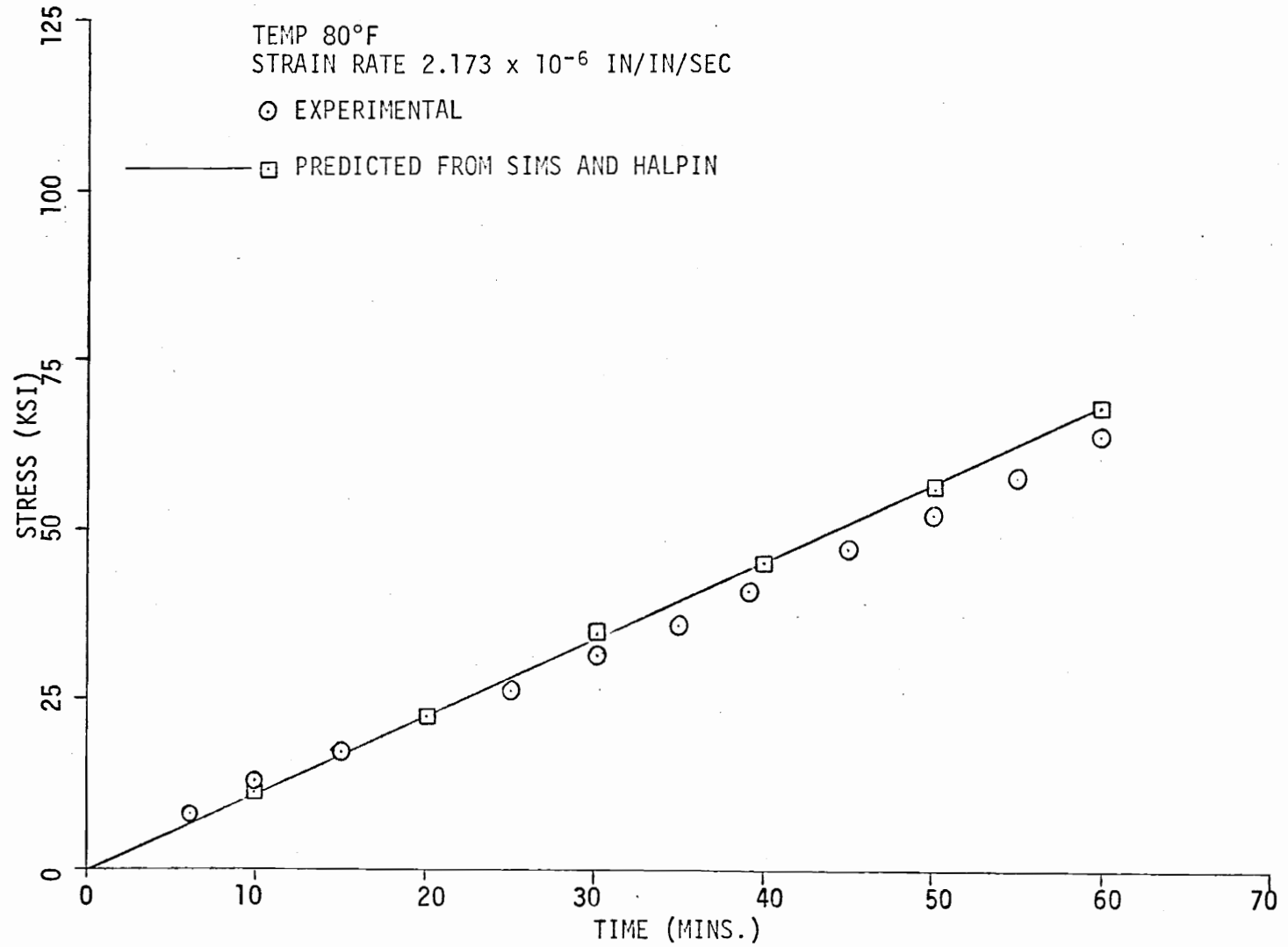


Figure 60. Prediction of Stress-Strain Curve at a Constant Strain Rate from Dynamic Tests by Sims and Halpin Equation [69] for Graphite/Epoxy.

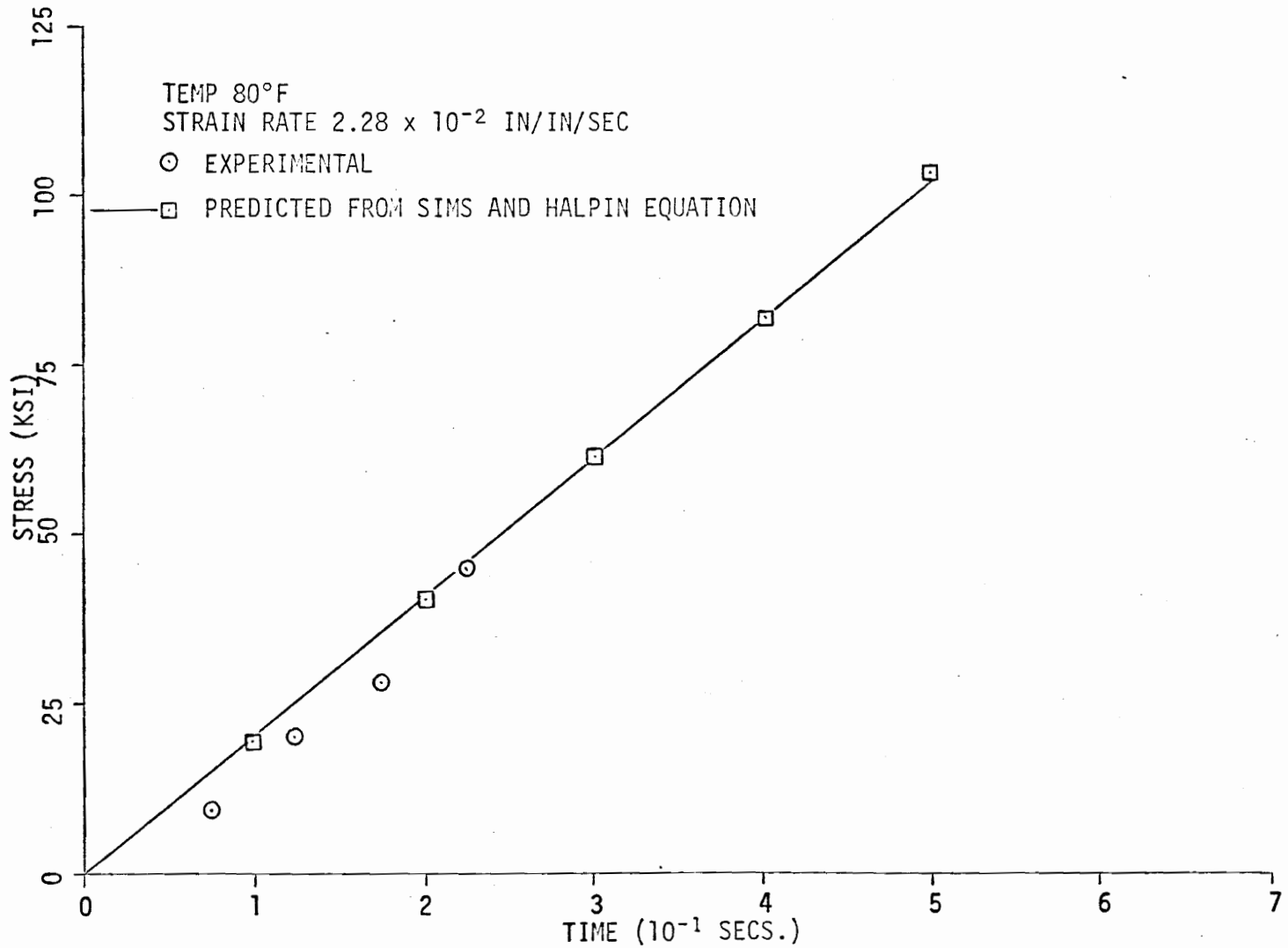


Figure 61. Prediction of Stress-Strain Curve at a Constant Strain Rate from Dynamic Tests by Sims and Halpin Equation [69] for Graphite/Epoxy.

integral interrelations could also be tried. The components of the complex dynamic modulus are related to the relaxation modulus by the Fourier transform relationships,

$$E(t) = E_e + \frac{2}{\pi} \int_0^{\infty} \left[\frac{E'(\omega) - E_e}{\omega} \right] \sin \omega t \, d\omega \quad (4.57)$$

or where E_e is Equilibrium Modulus

$$E(t) = E_e + \frac{2}{\pi} \int_0^{\infty} \frac{E''(\omega)}{\omega} \cos \omega t \, d\omega \quad (4.58)$$

Equation (4.57) can be rewritten by carrying out the integration of the second term in the integrand, using $E_e = E'(0) = E(t) \Big|_{t \rightarrow \infty}$

$$E(t) = \frac{2}{\pi} \int_0^{\infty} \frac{E'(\omega)}{\omega} \sin \omega t \, d\omega \quad (4.59)$$

If complex modulus components were known over the full frequency range, the relaxation modulus could be numerically determined. Even though equation (4.59) involves $E'(\omega)$ over the entire frequency range, it is possible to obtain the relaxation function over a limited time range from complex modulus data over a limited frequency range [10]. This is possible because the relaxation function at a particular value of time is not equally dependent upon the complex modulus at all values of frequency, but rather has a weighted dependence through equation (4.59). Gottenberg and Christensen [82] used this method to obtain the relaxation modulus from the storage

modulus. In performing this calculation, it was required to demonstrate convergence of the Fourier integral over a finite frequency range. They had to extrapolate the high and low frequency ends of the experimental storage modulus curves. The problem of establishing convergence criteria and numerical stability of the storage modulus expression given by equation (3.3) was encountered in the present investigation also. In order to avoid this difficulty, approximate methods developed by Ninomiya and Ferry [19] were used to perform these calculations.

This approximate method has an analytical foundation based on the properties of the integrands of the corresponding exact equations. The imaginary parts of the complex moduli and compliances are related to relaxation and retardation spectra as follows:

$$E''(\omega) = \int_{-\infty}^{\infty} \frac{\omega\tau}{1 + \omega^2\tau^2} H d(\ln \tau), \quad (4.60)$$

$$D''(\omega) = \int_{-\infty}^{\infty} \frac{\omega\tau}{1 + \omega^2\tau^2} L d(\ln \tau) + \frac{1}{\omega\zeta}$$

where H is the relaxation spectrum and

L is the retardation spectrum, ζ is the steady flow viscosity, τ is relaxation time in Eq. (4.60) and retardation time in Eq. (4.61).

The kernel function or intensity function $K_I(\omega\tau)$ is the same for both equations and it gives a curve symmetrical about its maximum of 0.500 at $\omega\tau = 1$ and tends to zero on both sides when plotted against

$\log \omega\tau$. Its area above the $\log \omega\tau$ axis is equal to $\pi/2$.

The difference between the relaxation modulus, $E(t)$, and the real part of the complex modulus, $E'(\omega)$, is related to the relaxation spectrum, H , by

$$E'(\omega) - E(t)|_{t=1/\omega} = \int_{-\infty}^{\infty} \left[\frac{\omega^2\tau^2}{1 + \omega^2\tau^2} - e^{-(1/\omega\tau)} \right] H \, d \ln \tau \quad (4.62)$$

and for the compliance by

$$\begin{aligned} -D'(\omega) + D(t)|_{t=1/\omega} &= \int_{-\infty}^{\infty} \left[\frac{\omega^2\tau^2}{1 + \omega^2\tau^2} - e^{-(1/\omega\tau)} \right] L \, d \ln \tau \\ &+ \frac{1}{\omega\zeta} \end{aligned} \quad (4.63)$$

Again the intensity functions are the same for both equations and are denoted by $K_D(\omega\tau)$. K_D has a maximum of 0.196 at $\omega\tau = 2.24$ and its area is equal to Euler's constant, 0.5772.

When both K_D and K_I are plotted against $\log \omega\tau$, it is possible to obtain a curve which superposes exactly on K_D by shifting K_I vertically and horizontally on a log-log plot. Thus,

$$K_D(\omega\tau) \approx a_1 K_I(b_1\omega\tau) \quad (4.64)$$

where a_1 and b_1 are constants which correspond to vertical and horizontal shift factors.

Then the approximate formulas of relaxation modulus and creep compliance obtained from dynamic functions can be shown to be of form [19]

$$E'(\omega) - E(t) \Big|_{t=1/\omega} \approx a_1 E''(a_1 \omega) \quad (4.65)$$

and

$$-D'(\omega) + D(t) \Big|_{t=1/\omega} \approx a_1 D''(a_1 \omega) \quad (4.66)$$

where, a , assumes values

$$0.367 < a_1 < 0.446.$$

The difference can be further minimized by the condition:

$$\frac{\partial}{\partial a_1} \left\{ \int_{-\infty}^{\infty} [K_D(\omega\tau) - a K_I(a\omega\tau)]^2 d \ln \tau \right\} = 0 \quad (4.67)$$

from which $a_1 = 0.384 \approx 0.40$. By adding higher order terms, the approximate formulas can be improved as follows:

$$K_D(\omega\tau) \approx 0.40 K_I(0.40\omega\tau) - 0.014 K_I(10\omega\tau) \quad (4.68)$$

$$E(t) = E'(\omega) - 0.40 E''(0.40\omega) + 0.014 E''(10\omega) \Big|_{\omega=1/t} \quad (4.69)$$

and

$$D(t) = D'(\omega) + 0.40 D''(0.40\omega) - 0.014 D''(10\omega) \Big|_{\omega=1/t} \quad (4.70)$$

Eqs. (4.69) and (4.70) require values of dynamic functions at three different frequency levels.

Equation (3.1) of the response surface for the storage and loss modulus as functions of time and temperature could be written as

$$\ln E'(\omega) = A + B \ln t + \frac{C}{T} + D (\ln t)^2 + \frac{E}{T^2} + F \frac{\ln t}{T}$$

or

(4.71)

$$\ln E''(\omega) = A + B \ln t + \frac{C}{T} + D (\ln t)^2 + \frac{E}{T^2} + F \frac{\ln t}{T}$$

The coefficients of Eq. (4.71) are given in Table 3. For a constant temperature, Eq. (4.71) can be written in the form,

$$\ln E'(\omega) =_{t=1/\omega} A' + B' \ln t + C' (\ln t)^2$$

and

(4.72)

$$\ln E''(\omega) =_{t=1/\omega} D' + E' \ln t + F' (\ln t)^2$$

where A' , B' , C' , D' , E' and F' are constants. They can be further reduced to the form,

$$E'(\omega=1/t) = e^{(A' + B' \ln t + C' (\ln t)^2)}$$

and

(4.73)

$$E''(\omega=1/t) = e^{(D' + E' \ln t + F' (\ln t)^2)}$$

Substituting equations (4.73) into Eq. (4.69), $E(t)$ can be expressed directly in terms of regression coefficients and can be

Table 3
 THE COEFFICIENT OF EQ. (4.71) FOR $1/T$ IN DEGREES KELVIN AND $\dot{\epsilon}$
 IN INCHES/IN/SEC.

	Boron/Epoxy		Graphite/Epoxy	
	E'	E''	E'	E''
A	16.030	16.575	16.090	15.942
B	3.709×10^{-2}	1.334	4.323×10^{-2}	1.673
C	2.313×10^{-3}	1.139×10^1	1.742×10^{-3}	1.495×10^{-1}
D	1.285×10^2	-5.00×10^2	0	0
E	-2.109×10^3	1.210×10^5	-4.7131×10^3	1.019×10^5
F	-8.926	4.413×10^1	-7.657	9.0×10^1

determined at different times and temperatures. This computation can be performed with ease compared to tedious integrations involved in the solution of Equation (4.59).

The plots for comparison of storage and relaxation moduli for both materials at 80°F and 300°F are shown in Figures 62 and 63. $E(t)$ and $E'(\omega)$ are both measures of stored elastic energy, and a dynamic measurement at a frequency ω is qualitatively equivalent to a transient one at $t = 1/\omega$ [9]. As seen from the figures, they are approximately mirror images if plotted on the same axis with $t = 1/\omega$. Physically, it can be argued that the shape of these curves is little different and $E'(1/t) > E(t)$ at all times. This again can be observed in Figures 62 and 63. Physical bounds on the equation for $E'(\omega)$ required that $E(t)$ be computed only up to 10^{-2} seconds which fell within the experimental observations.

The heredity integral form of the stress-strain relation is expressed as

$$\sigma(t) = \int_{-\infty}^t E(t - \tau) \frac{d\varepsilon}{d\tau} d\tau \quad (4.74)$$

If a stress free state is assumed prior to $t = 0$, the lower limit of integration can be replaced by zero.

$$\sigma(t) = \int_0^t E(t - \tau) \frac{d\varepsilon}{d\tau} d\tau \quad (4.75)$$

Now, if $t - \tau = u$, for constant strain rate,

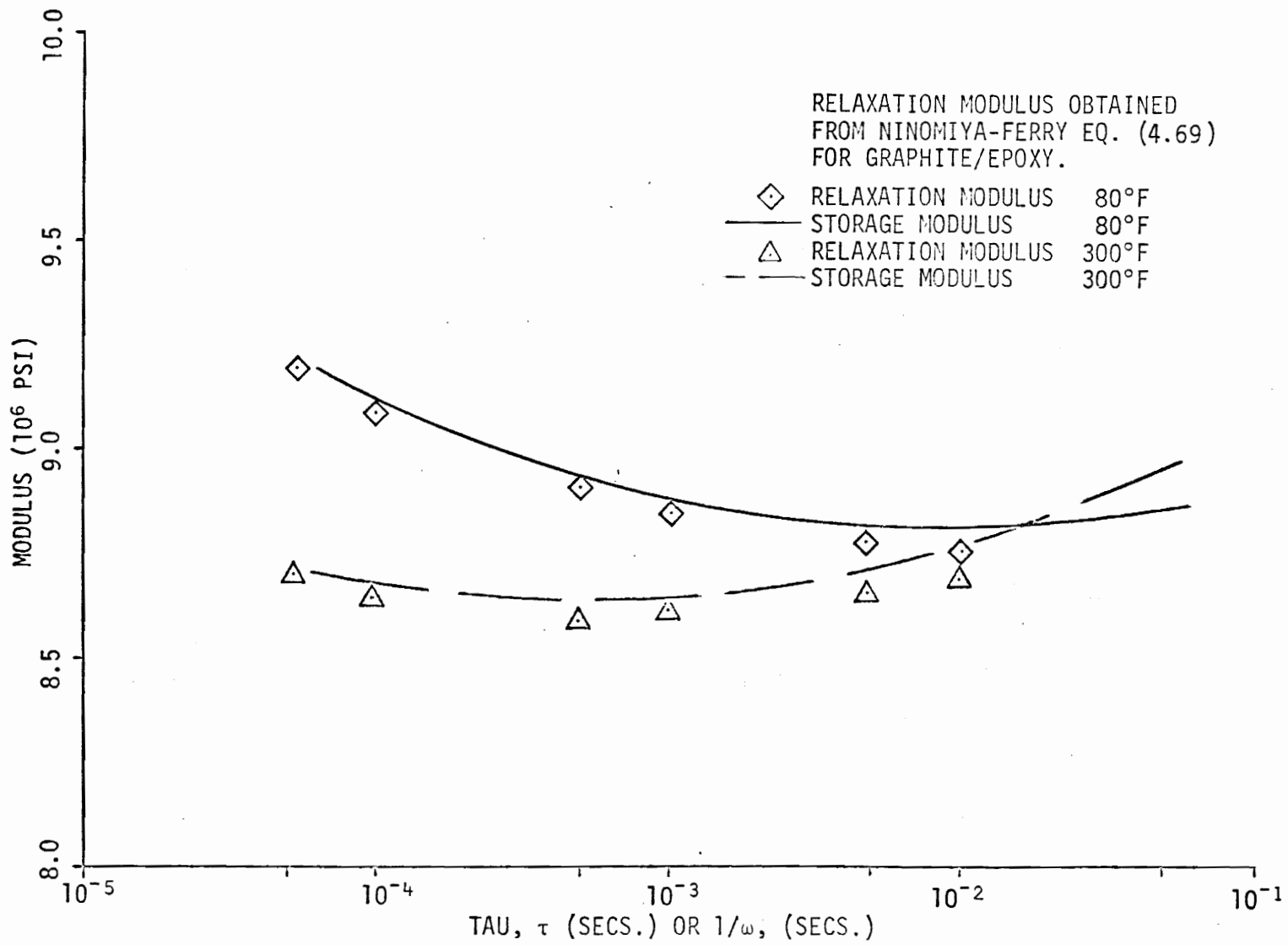


Figure 62. Comparison of Storage and Relaxation Moduli for Graphite/Epoxy.

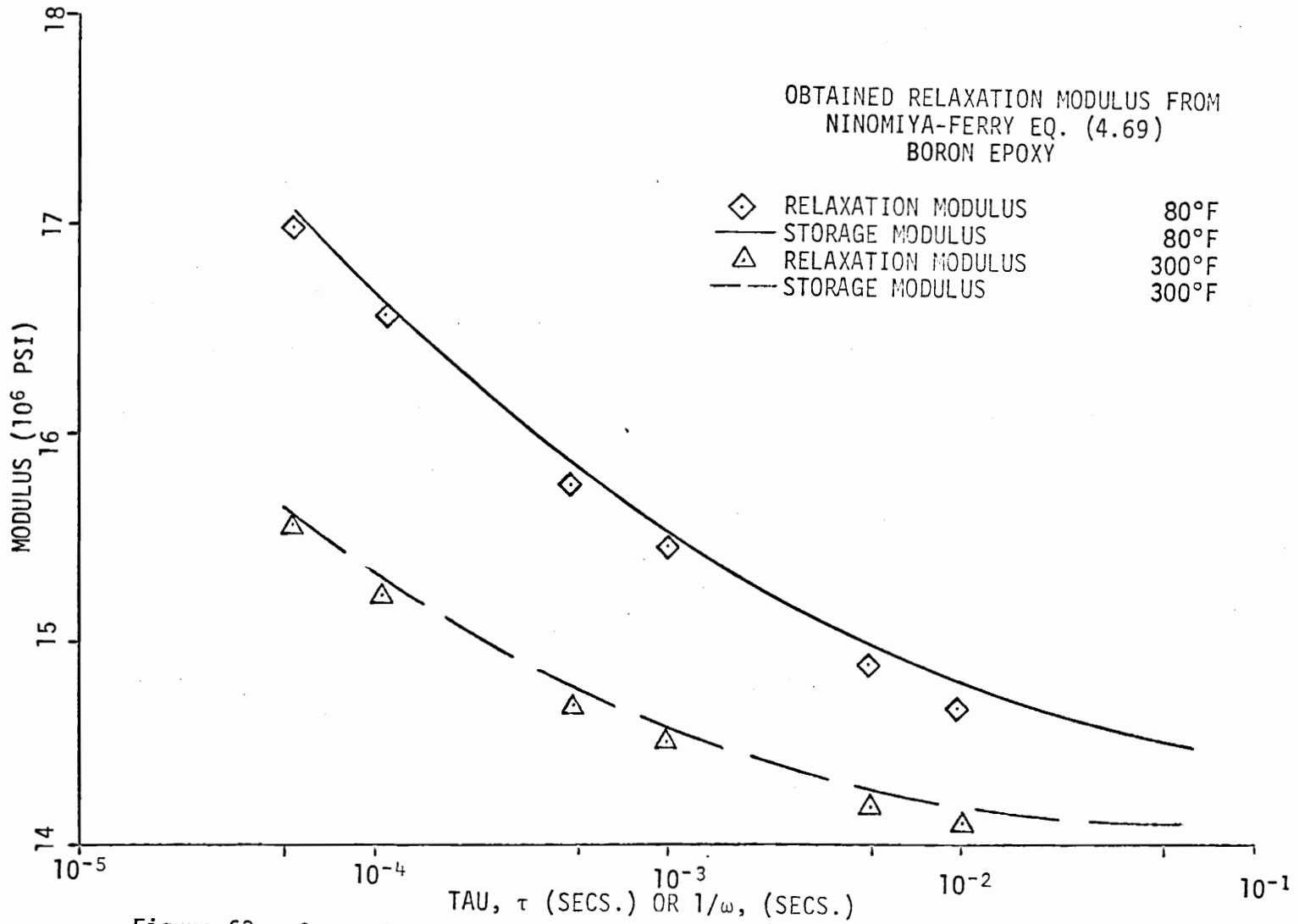


Figure 63. Comparison of Storage and Relaxation Moduli for Boron/Epoxy.

$$\sigma = \dot{\epsilon} \int_0^t E(u) du \quad (4.76)$$

Equation (4.76) can be solved by numerical integration, using expressions for the integrand, $E(t)$, from equations (4.69) and (4.72). In performing this integration the lower limit was taken as 0.00005, the point where extrapolation of $E'(\omega)$ was fairly valid. The stress-time curves at different strain rates were obtained for Boron/Epoxy and Graphite/Epoxy at different temperatures. Figures 64 through 67 show the comparison of experimental and predicted curves at two different temperatures and strain rates for both materials. They bear out the validity of this method of interconversion. Figure 66 did show the deviation of predicted behavior from experimental curves. This difference is tracable to the fact that the strain rate was not constant throughout the test because of some inertia effect in the testing system.

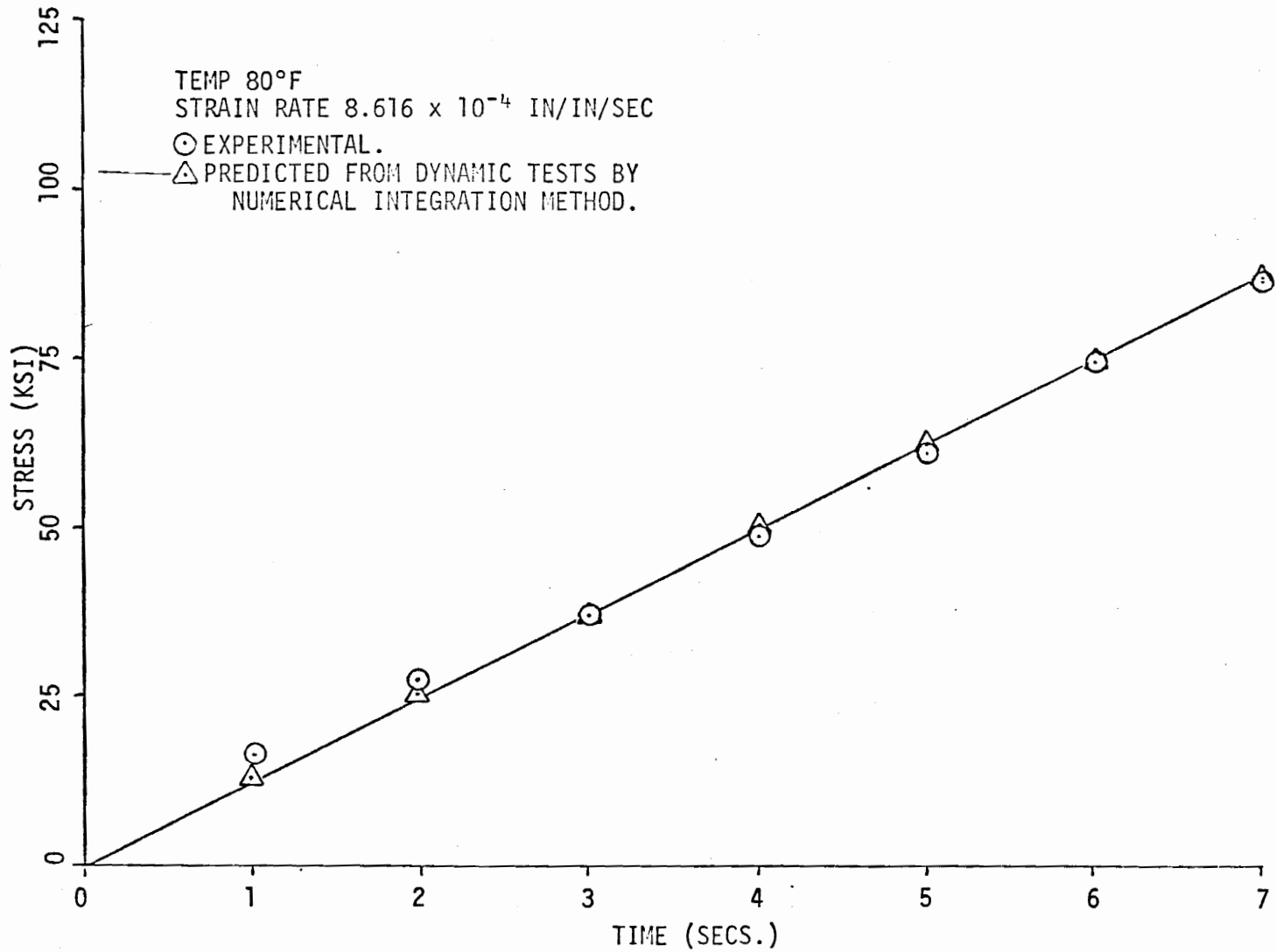


Figure 64. Prediction of Stress-Strain Curve at a Constant Strain Rate from Dynamic Tests by Numerical Integration Method for Boron/Epoxy.

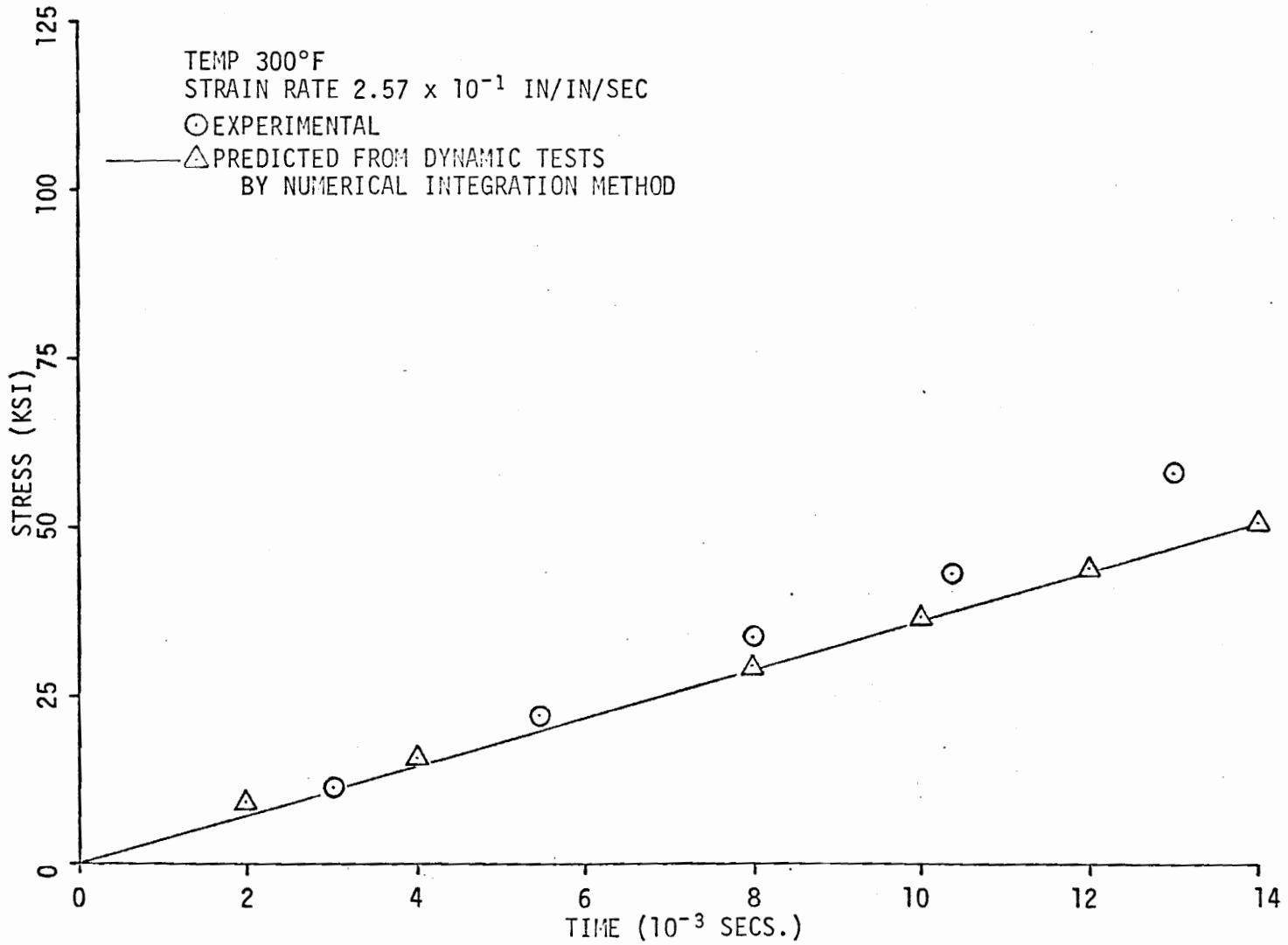


Figure 65. Prediction of Stress-Strain Curve at a Constant Strain Rate from Dynamic Tests by Numerical Integration Method for Boron/Epoxy.

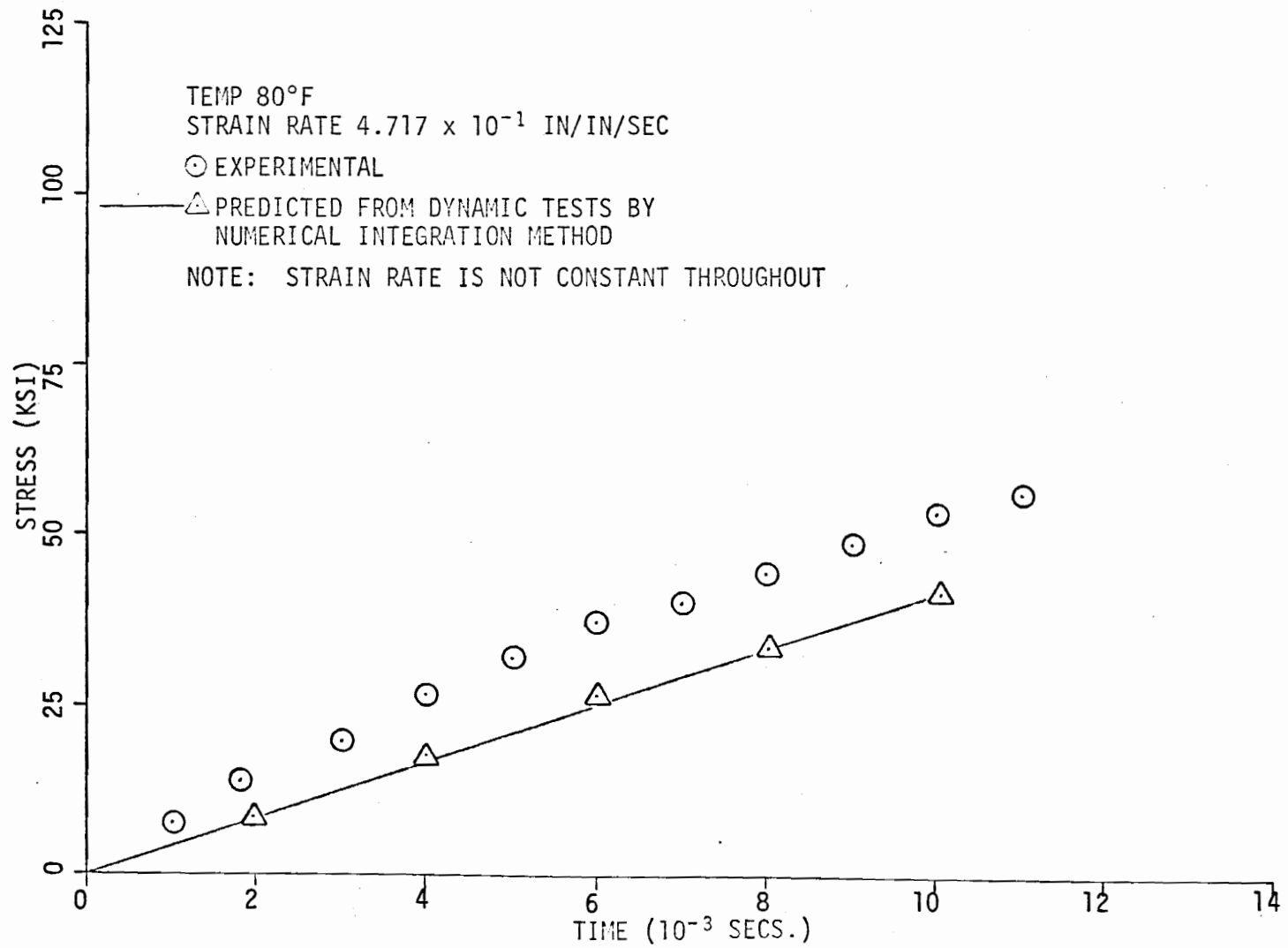


Figure 66. Prediction of Stress-Strain Curve at a Constant Strain Rate from Dynamic Tests by Numerical Integration Method for Graphite/Epoxy.

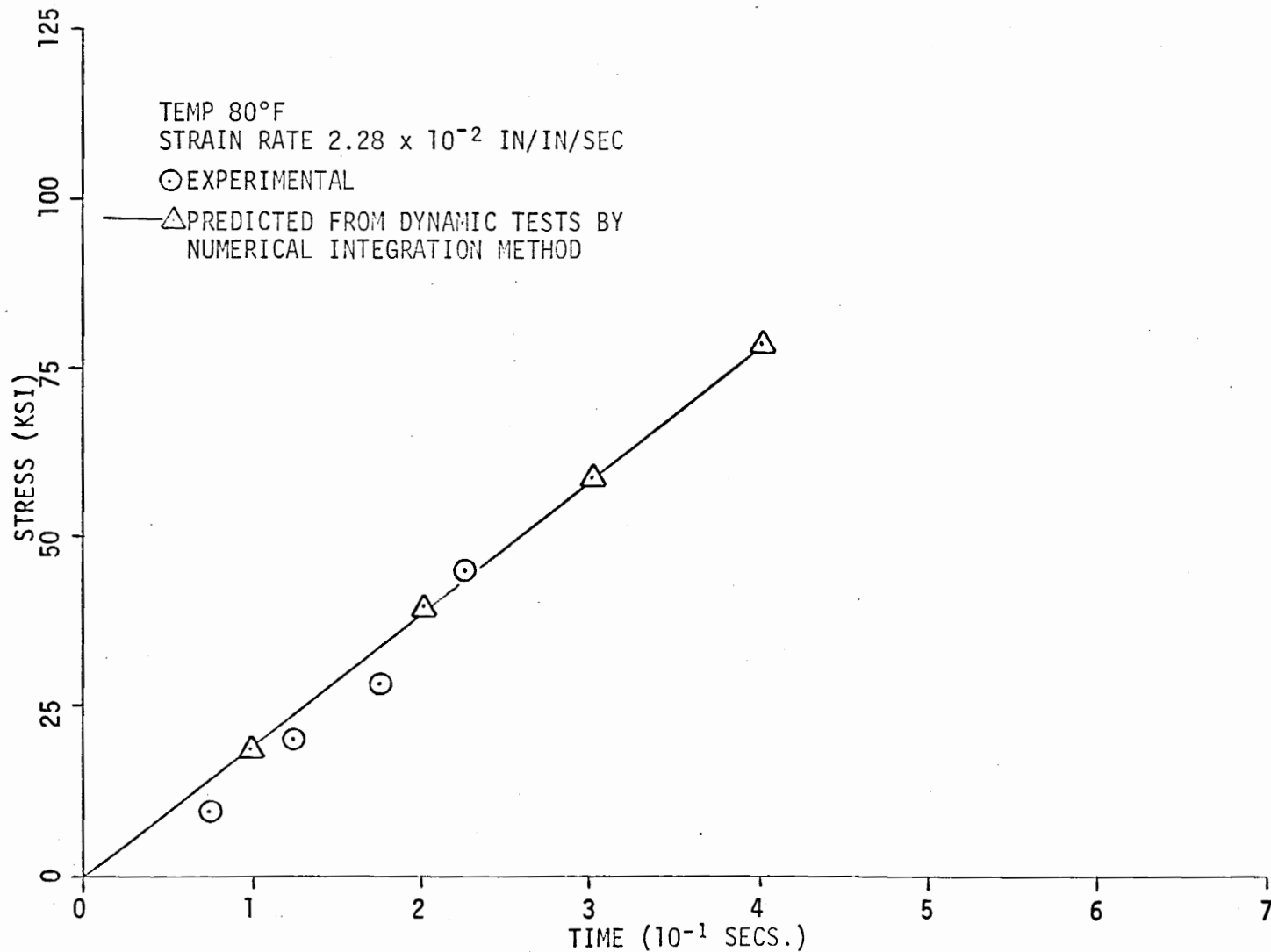


Figure 67. Prediction of Stress-Strain Curve at a Constant Strain Rate from Dynamic Tests by Numerical Integration Method for Graphite/Epoxy.

V. DISCUSSION AND CONCLUSIONS

Viscoelastic characterization of the advanced composites studied reveals some important facts. It has been shown in the previous chapter that the time and temperature effects can be related by the "method of reduced variables" for each loading condition. A different shifting procedure is however required for each test. For the time-temperature superposition principle to be valid the same shift factor should apply independently of the type of test used, and if the material is thermorheologically simple its temperature dependence should be completely described by the shift factor.

Krokosky [49] has reported that the a_T value for pure asphalt obtained experimentally was a function of the type of test. Similar findings are also reported in this study. The stress dependence in the shift factor was also noted by Moehlenpah [26].

The difference observed in shift factors and activation energy computed from their storage and loss modulus is unexplainable at the moment. However, Leaderman's [13] comments might give some insight.

There are several cases reported in the literature of dynamic data for amorphous polymers where the same set of values of a_T did not give smooth master curves of the storage and loss components of the reduced dynamic response function. These discrepancies may be due in part to the inadequacy of the absolute temperature as the reduction factor, since the elasticity of real polymer chains is not due entirely to entropy change.

Another possible reasoning may be that, while storage modulus reflects the gross properties of the material, loss modulus reflects microlevel properties through the damping ratio. Shapery [67] has shown that damping of dynamic response is quite sensitive to even small nonlinearities at the local level. However, to make a rational judgement detailed study is indicated.

It is interesting to note that Boron/Epoxy has been found to be temperature dependent but experiments conducted over a range of five decades of strain-rate indicate very little strain-rate dependence. The ultimate strength of the material shows no strain rate sensitivity at all, while it shows a linear relationship with temperature as seen in Figure 36.

Graphite/Epoxy exhibits a temperature and strain rate dependent stiffness but its ultimate strength (Figure 37) similarly to Boron/Epoxy does not show any strain rate effects. The stiffness of Graphite/Epoxy exhibits more temperature (time) dependence than Boron/Epoxy.

Though the use of the time-temperature superposition principle is restricted to each test method, a significant amount of acceleration can be achieved by varying the temperature for each type of test, as seen by master curves plotted in Figures 40 through 43.

Damping behavior of a material is dependent on test conditions as well as on micro- and macromechanisms. As seen earlier, simple mechanical models may not be able to simulate the complex damping

phenomenon observed in these materials. While these models may be operative in certain frequency and strain rate domains, they are not useful in the range of practical interest. The Maxwell model showed a good fit for damping behavior at frequencies below 1000 Hz and predicted higher strain rates. The three parameter viscoelastic models did cover damping behavior over a wide range of frequencies in a qualitative way but its storage modulus relationship did not resemble actual material behavior.

Due to the presence of elastic fibers in the direction of loading there may be different controlling mechanisms operative at the micro-level which may be exhibited in the damping mechanism. Some damping may be rate dependent (matrix effect) and some may be rate independent (fiber effect) depending on the range of stress amplitude, strain rate, frequency, temperature and other test and environmental conditions. In order to represent such a behavior, models which incorporate both rate-dependent (viscous damping) and rate-independent (Coulomb damping) features need to be tried.

Lazan [35] has reported that such a modified Maxwell model has proved very effective in using vibration data to predict the long term creep response of concrete. Such a model may explain the complex damping behavior of the composites being investigated.

The applicability of integral equations and the numerical integral method to interconvert dynamic data to high strain rate and creep tests have been demonstrated in the previous chapter. The convenience with which the regression equation obtained from curve

fitting of experimental data can be used in above methods shows its importance in the present analysis. However, it should be used with care because beyond certain bounds the regression equation deviates from the known physical behavior of the material. When the equation (3.1) for the damping ratio was used beyond the experimentally observable range, physically inconsistent high values of damping were obtained. The validity of this equation below 10 Hz became questionable. The same observation was made at higher frequencies (i.e., 20,000). But here the behavior was reasonable up to 100,000 Hz.

Thus, it was found necessary to restrict the use of the regression equations within these bounds. The effect of these equations on the values of a's and b's shown in Figure 57 beyond experimental range can be easily seen. Since the lower two rates and part of the third highest rate fell beyond the range of dynamic experiments it was necessary to assume constant a's and b's to predict the stress-strain curves. The good agreement between predicted and experimental values did establish the basis for such extrapolation.

To use numerical integral techniques, relaxation moduli were also assumed to be constant beyond 10^{-2} secs. When integrated between $t = 0$ and $t = 1/\omega$, they did predict experimental stress-strain curves reasonably well. The corresponding extrapolated values of storage modulus were also used to compute a's for the integral equation method. This gave a check on the extrapolated values.

To put this concept in proper perspective relaxation moduli obtained from all three tests are plotted on the same Figure 68. The overlapping region between dynamic tests and the high strain rate test is also shown. These points were used directly to predict the stress-strain curve at the highest rate. This establishes the validity of the regression equation within the experimental range. A single creep test was used to obtain a relaxation modulus as direct inversion from creep compliance. Figure 68 does give a complete picture of behavior of stress-relaxation at 300°F for Boron/Epoxy over eleven decades. Since creep data was not available at room temperature, they were not plotted. The dotted lines on the figure 68 show the trend of the curves if the regression equation is used beyond 10^{-2} secs.

Figure 69 shows the creep compliance for Boron/Epoxy as obtained from dynamic, strain rate and creep tests. The creep compliance within the range 10^{-1} to 10^3 secs. was obtained from the relaxation modulus by simple inversion which were, in turn, obtained by extrapolation. Creep compliance was also computed from assumed constant values of a and b. The values are plotted in Figure 69. The calculated values agree with experimental values within 10%. This again enhances the validity of the extrapolated values.

The same reasoning is applied in dealing with Graphite/Epoxy to obtain Figure 70. Since no creep data was available, it is not shown on the plot.

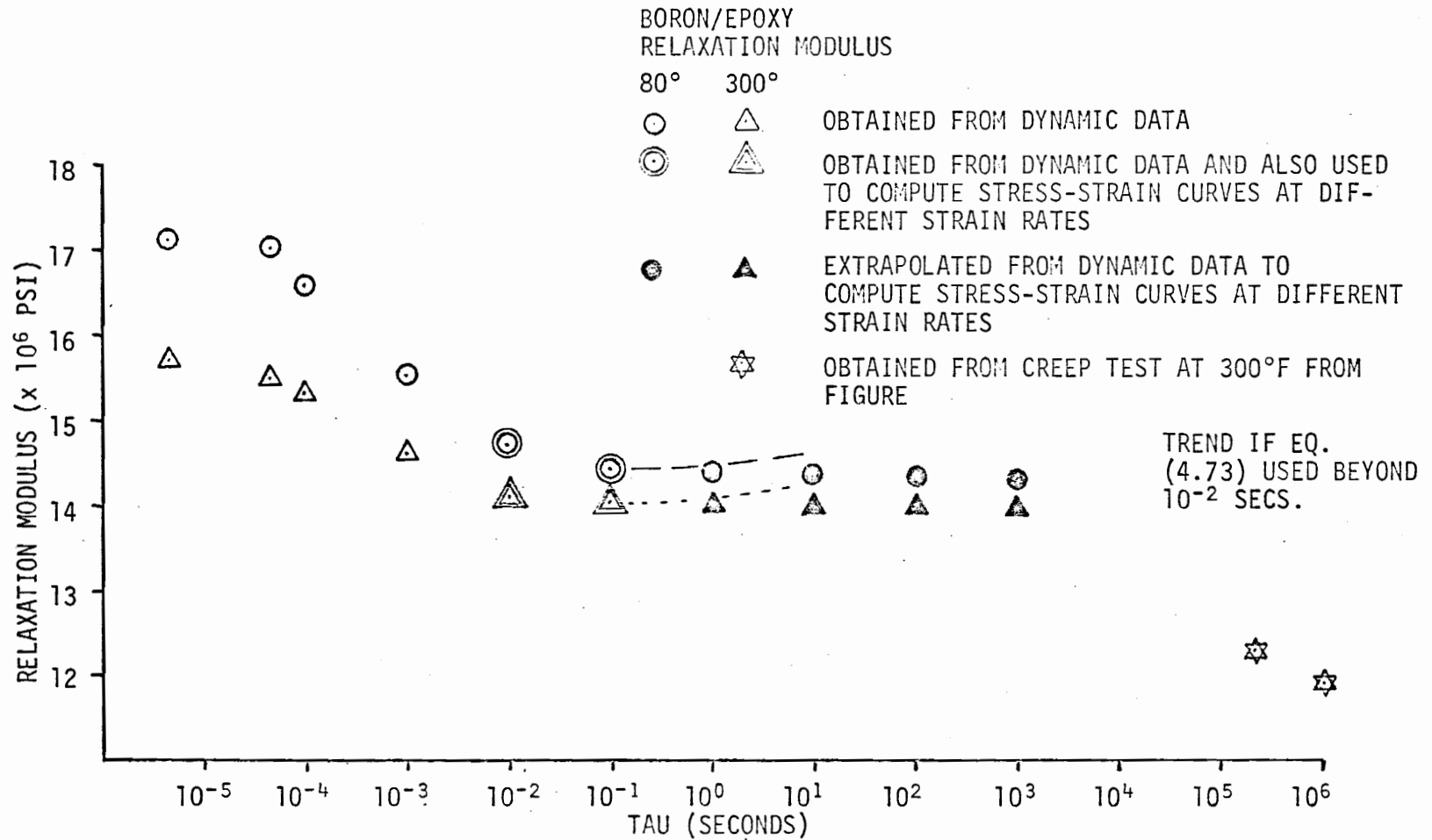


Figure 68. Relaxation Modulus for Boron/Epoxy Obtained from Dynamic, High Strain Rate and Creep Test.

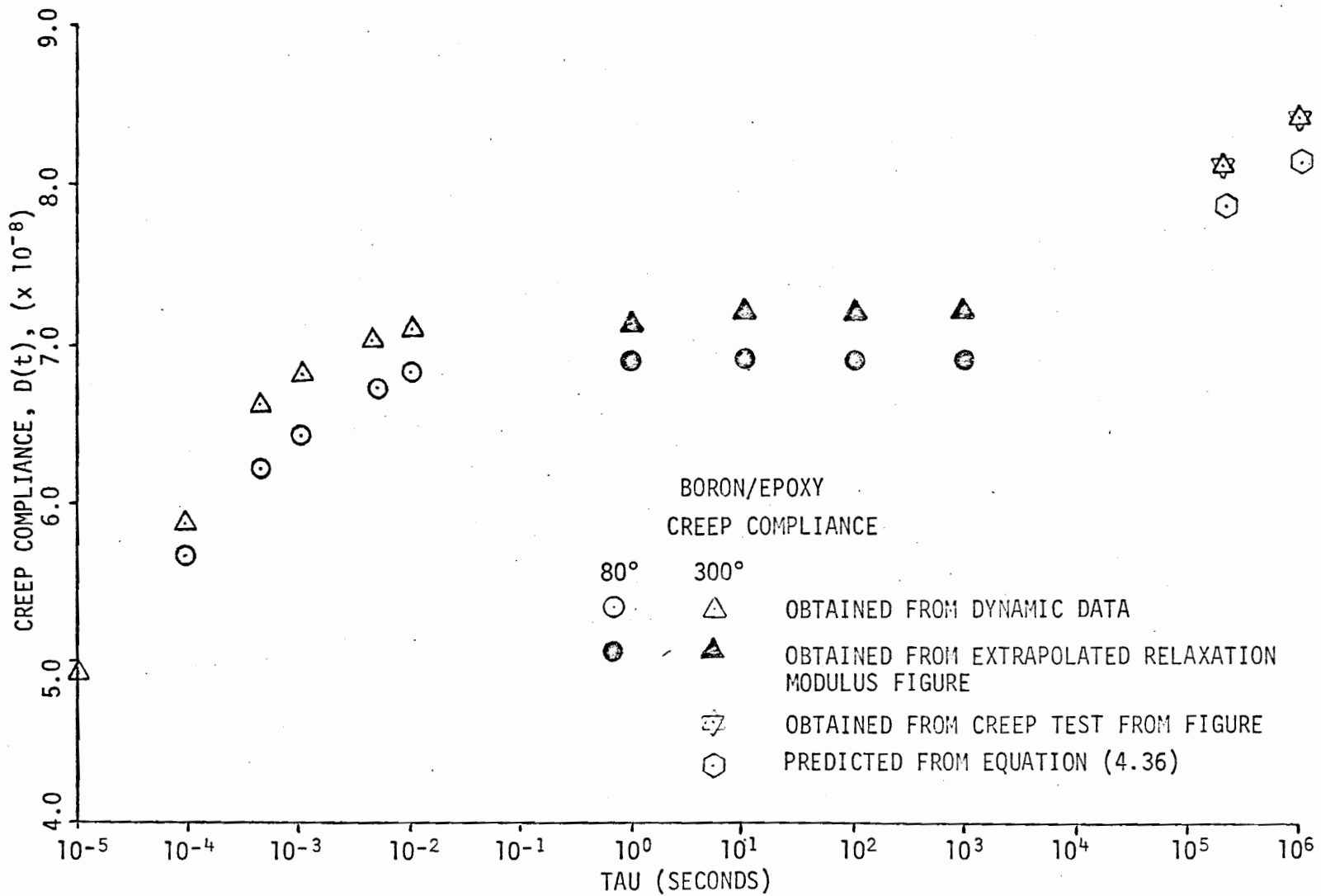


Figure 69. Creep Compliance for Boron/Epoxy Obtained from Dynamic, High Strain Rate and Creep Test.

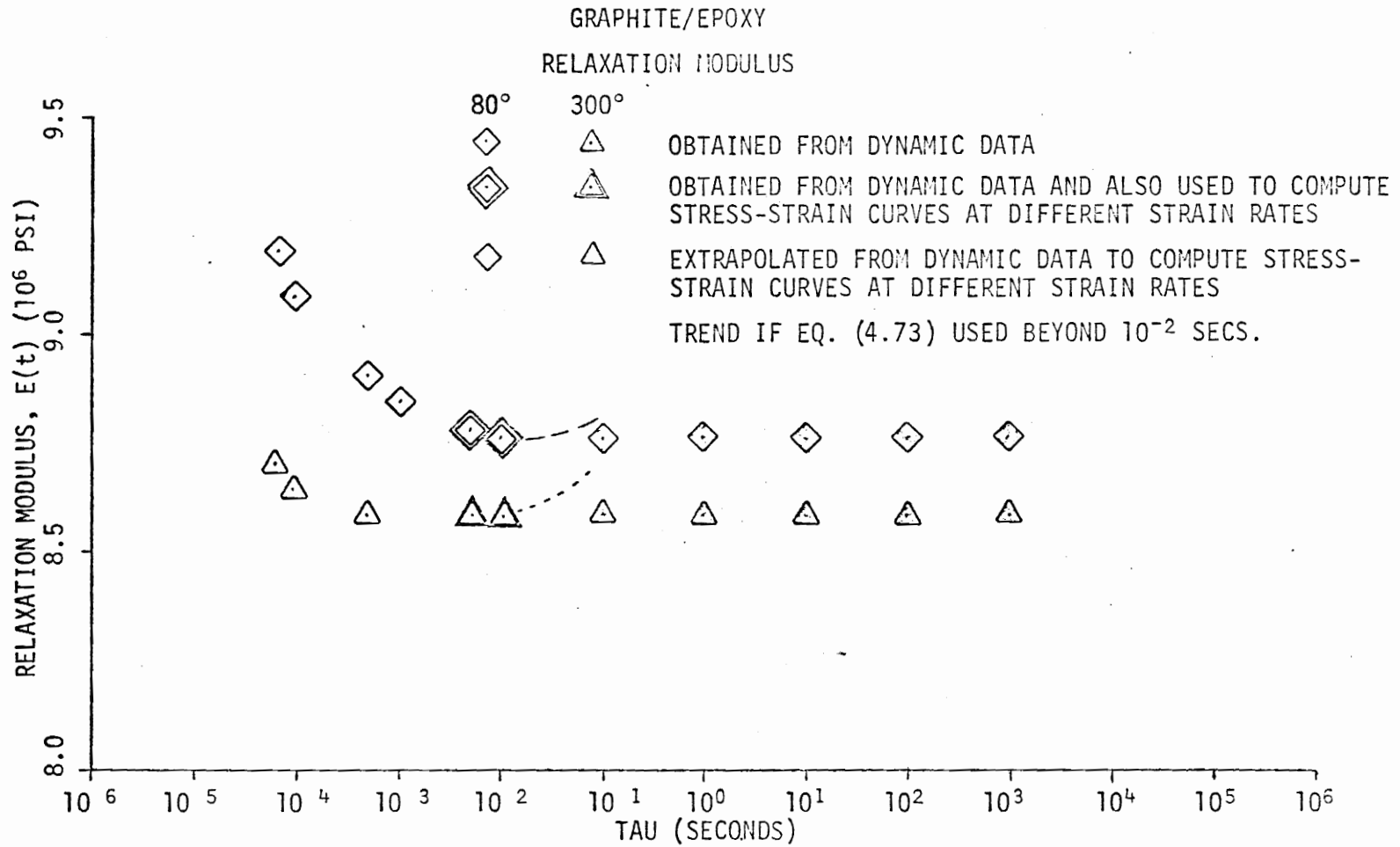


Figure 70. Relaxation Modulus for Graphite/Epoxy Obtained from Dynamic, High Strain Rate and Creep Test.

Thus, if used with physical reasoning, the regression equation could be of considerable value.

In conclusion, the following inferences could be drawn from this investigation:

1. Due to large scatter in experimental data, typical in advanced composites, statistical conditioning is required to analyze the test results. The equation for the regression analysis and the constants can be conveniently used to perform viscoelastic analysis. It has been shown that horizontal and vertical shift parameters can be obtained from these equations.
2. Time-temperature shifting procedure can be applied to individual tests. However, further study is needed to understand the discrepancies observed in shift factors and activation energy under different loading conditions for the composites under study.
3. It is seen from the shift factors that for a particular type of test significant test, acceleration may be obtained for Graphite/Epoxy while little if any acceleration can be achieved for Boron/Epoxy by variation of the test temperatures.
4. Both Boron/Epoxy and Graphite/Epoxy show strain rate independent ultimate strengths. While Boron/Epoxy displays a linear dependence on temperature, quadratic dependence is observed for Graphite/Epoxy.

Simple mechanical models fail to represent actual material behavior in the range of practical interest. Models which incorporate rate dependent and rate independent behavior could be used to simulate such phenomena.

In closure, it would be appropriate to quote Lockett [89] on the subject.

The validity of a particular theory should be judged as much by its ability to model real behavior as by its mathematical rigour. It is as much the duty of the theoretician to assist in simplifying and applying these theories as it is the duty of the experimentalist or designer who wishes to use them.

VI. REFERENCES

1. Aklonis, J. J., et al., "Introduction to Polymer Viscoelasticity," Wiley-Interscience, 1972.
2. Flugge, W., "Viscoelasticity," Blaisdell Publishing Company, 1967.
3. Gross, B., "Mathematical Structure of the Theories of Viscoelasticity," Hermann & Cie, Editeurs, 1953.
4. Tobolsky, A. V. and Mark, H. F., "Polymer Science and Materials," Wiley-Interscience, 1971.
5. Nielsen, L. E., "Mechanical Properties of Polymers," Reinhold Publishing Co., 1962.
6. Ward, I. M., "Mechanical Properties of Solid Polymers," pp. 196-224, Wiley-Interscience, New York, 1971.
7. Bergen, J. T., "Viscoelasticity, Phenomenological Aspects," Academic Press, New York, 1960.
8. McClintock, F. A. and Argon, A. S., "Mechanical Behavior of Materials," Addison-Wesley, Massachusetts, 1966.
9. Ferry, J. D., "Viscoelastic Properties of Polymers," John Wiley & Sons, New York, 1970.
10. Christensen, R. M., "Theory of Viscoelasticity--An Introduction," Academic Press, New York, 1971.
11. Vincent, P. I., "Mechanical Properties of High Polymers: Deformation," Physics of Plastics, (ed. Ritchie, P. D.), The Plastics Institute, London, 1965.
12. Halpin, J. C., "Introduction to Viscoelasticity," Composite-Materials Workshop, ed. Tsai, S. W., Halpin, J. C. and Pagano, N. J., Technomic Publishing Inc., Stanford, Conn., 1968.
13. Leaderman, H., "Some Aspects of the Mechanical Properties of High Polymers," Proceedings of the Conference on the Mechanical Behavior of Wood, Berkeley, California, 1962.
14. Schmitz, J. V., "Testing of Polymers," Interscience Publishers, New York, 1965.

15. Kolsky, H., "Experimental Studies of the Mechanical Behavior of Linear Viscoelastic Solids," *Mechanics and Chemistry of Solid Propellants Proceedings of the 4th Symposium on Naval Structural Mechanics*, O.N.R., Lafayette, Indiana, 1965.
16. Bland, D. R., "Model Fitting to Measured Values of Complex Modulus or Compliance," Chapter 6, *Theory of Linear Viscoelasticity*, Pergamon, Oxford, 1960.
17. Schapery, R. A., "A Simple Collocation Method for Fitting Viscoelastic Models to Experimental Data," GALCIT SM 61-23A Report, 1961.
18. Gottenberg, W. G., and Christensen, R. M., "An Experiment for Determination of the Mechanical Property in Shear for a Linear, Isotropic Viscoelastic Solid," *Int. J. Engng. Sci.*, Vol. 2, pp. 45-57, 1964.
19. Ninomiya, K., and Ferry, J. D., "Some Approximate Equations Useful in the Phenomenological Treatment of Linear Viscoelastic Data," *J. of Colloid Science*, Vol. 14, pp. 36-48, 1959.
20. Catsiff, E., and Tobolsky, A. V., "Stress-Relaxation of Polyisobutylene in the Transition-Region (1, 2)," *J. Colloid Sci.*, Vol. 10, pp. 375, 1955.
21. Schwarzl, F. R., "On the Interconversion of Linear Viscoelastic Functions with Special Application to Shear Behavior in the Glass-Rubber Transition Region," *Deformation and Fracture of High Polymers*, (H. Kausch, et al., eds.), Plenum Press, New York, 1973.
22. Schapery, R. A., "A Method of Viscoelastic Stress Analysis Using Elastic Solutions," Vol. 279, No. 4, 1965, pp. 268-289.
23. Schapery, R. A., "Approximate Method of Transform Inversion for Viscoelastic Stress Analysis,"
24. Christensen, R. M., "Restrictions Upon Viscoelastic Relaxation Functions and Complex Moduli," *Transactions of the Society of Rheology*, Vol. 16, pp. 603-614, 1972.
25. Brinson, H. F., "Mechanical and Optical Viscoelastic Characterization of Hysol 4290," *Experimental Mechanics*, Dec. 1968.

26. Moehlenpah, A. E., Isai, O., and Dibendetto, A. T., "The Effect of Time and Temperature on the Mechanical Behavior of a 'Plasticized' Epoxy Resin Under Different Loading Modes," *Journal of Applied Polymer Science*, Vol. 13, pp. 1231-1245, 1969.
27. McLellan, D. L., "Prediction of Stress-Strain Behavior at Various Strain Rates and Temperatures," *Applied Polymer Symposia*, No. 12, 1969.
28. Lohr, J. J., "Yield Stress Master Curves for Their Glass Transition Temperatures," *Transactions of the Society of Rheology*, Vol. 9, No. 1, 1965.
29. Lohr, J. J., "Time-Temperature-Strain Rate Equivalence for Various Engineering Thermoplastics," *Applied Polymer Symposia*, 1965.
30. Smith, T. L., "Viscoelastic Behavior of Polyisobutylene Under Constant Rates of Elongation," *J. Polymer Science*, Vol. 20, pp. 89-100, 1956.
31. Smith, T. L., "Stress-Strain-Time-Temperature Relationships for Polymers," *A.S.T.M. S.T.P.* 325, 1962.
32. Sutherland, H. J. and Lingle, R., "An Acoustic Characterization of Polymethyl Methacrylate and Three Epoxy Formulations," *J. Appl. Phys.*, Vol. 43, No. 10, October 1972.
33. McCrum, N. G., and Pogany, G. A., "Time-Temperature Superposition in the α Region of an Epoxy Resin," *J. Macromol. Sci.-Phys.*, B4(1), pp. 109-126, March, 1970.
34. Andrews, E. H. and Reed, P. E., "Deformation of Cross-Linked Polymers Below T_g ," *Deformation and Fracture of High Polymers*, (H. Kausch, et al., eds.), Plenum Press, New York, 1973.
35. Lazan, B. J., "Damping of Materials and Members in Structural Mechanics," Pergamon Press, London, 1968.
36. Heller, R. A. and Nicholas, T., "Determination of the Complex Shear Modulus of a Filled Elastomer from a Vibrating Sandwich Beam," *Experimental Mechanics*, Vol. 24, No. 1, p. 110, 1967.
37. Heller, R. A., and Nederveen, C. J., "Comparison of Complex Moduli Obtained from Forced and Free Damped Oscillations," *Transactions of the Society of Rheology*, Vol. 11, No. 1, 1967.

38. Meinecke, E. A., and Clark, R. C., "Mechanical Properties of Polymeric Foams," Technomic Publication, Westport, Conn., 1973.
39. Christensen, R. M., "Viscoelastic Properties of Heterogeneous Media," *J. Mech. Phys. Solids*, Vol. 17, 1969.
40. Hashin, Z., "The Elastic Moduli of Heterogeneous Materials," *J. of Applied Mechanics*, pp. 143-150, 1962.
41. Hackett, R. M., "Viscoelastic Stresses in a Composite System," *Polymer Engineering and Science*, Vol. 11, No. 3, pp. 220-225, May 1971.
42. Halpin, J. C., and Pagano, N. J., "Observations on Linear Anisotropic Viscoelasticity," *J. of Composite Materials*, Vol. 2, No. 1, Jan. 1968.
43. Mechanics and Chemistry of Solid Propellants, Proceedings of the Fourth Symposium on Naval Structure Mechanics, Pergamon Press, Lafayette, April 1965.
44. Baltrukonis, J. H., "The Dynamics of Solid Propellant Rocket Motors," *Mechanics and Chemistry of Solid Propellants*, Proceedings of the Fourth Symposium on Naval Structural Mechanics, Lafayette, 1965.
45. Schapery, R. A., "Studies on the Nonlinear Viscoelastic Behavior of Solid Propellant," Texas A & M Report, MM 2803-73-2, May, 1973.
46. Schapery, R. A., "Recent Developments in the Nonlinear, Viscoelastic Characterization of Solid Propellant," *Solid Rocket Structural Integrity Abstracts*, Vol. 8, April, 1971, pp. 1-66.
47. Koh, S. L., "Problems in Nonlinear Viscoelasticity," *Mechanics and Chemistry of Solid Propellants*, Proceedings of the Fourth Symposium on Naval Structural Mechanics, Lafayette, Indiana, 1965.
48. Lockett, F. J., "Experimental Characterization of Nonlinear Viscoelastic Materials," *Mechanics and Chemistry of Solid Propellants*, Proceedings of the Fourth Symposium on Naval Structural Mechanics, Lafayette, Indiana, 1965.
49. Krokosky, E., "Behavior of Time Dependent Composite Materials," *Modern Composite Materials*, ed. Broutman, L. J. and Krock, R. H., Addison Wiley, 1967.

50. Terrel, R. L., Awad, I. S., and Foss, L. R., "Investigating Stress-Strain Characteristics of Asphalt-Treated Materials," Closed Loop, Magazine of Mechanical Testing, Fall/Winter 1973.
51. Gauchel, J. V., "The Viscoelastic Behavior of Epoxy-Glass Composites," Ph.D. Dissertation, Washington University, 1972.
52. Cessna, L. C., "Stress-Time Superposition of Creep Data for Polypropylene and Coupled Glass-Reinforced Polypropylene," Polymer Engineering and Science, Vol. 11, No. 3, pp. 211-219, May, 1971.
53. Pink, E., and Campbell, J. D., "An Investigation of Strain Rate Effects in a Reinforced Polymer," University of Oxford Report, Engineering Laboratory, Oxford, Report No. 1028/71, 1971.
54. Pink, E., and Campbell, J. D., "The Effect of Strain Rate and Temperature on the Deformation Behaviour of Reinforced and Unreinforced Epoxy Resin," University of Oxford Report, Engineering Laboratory, Oxford, Report No. 1040/72, 1972.
55. Schapery, R. A., "Stress Analysis of Viscoelastic Composite Materials," Journal of Composite Materials, Vol. 1, No. 3, 1967.
56. Lou, Y. C., and Schapery, R. A., "Viscoelastic Characterization of a Nonlinear Fiber Reinforced Plastic," J. Composite Materials, Vol. 5, April 1971.
57. Zakhariyev, G., et al., "A Rheological Model of Polymers and Glass Reinforced Plastics," Mekhanika Polimerov, No. 5, pp. 851-857, 1971.
58. Kokoshvili, S. M., Tamuzh, V. P., and Yanson, O. Yu., "Calculation of Relaxation Spectra from Dynamic Test Data," Mekhanika Polimerov, No. 2, pp. 349-353, March-April, 1971.
59. Bodner, S. R., and Lifshitz, J. M., "Experimental Investigations on the Dynamic Strength of Composites," Proceedings of the Fifth Symposium on Naval Structural Mechanics, Philadelphia, 1967.
60. Hashin, Z., et al., "Static and Dynamic Viscoelastic Behavior of Fiber Reinforced Materials and Structures," U.S. Army Aviation Material Laboratories, Fort Eustis, Va., Report No. 68-70, 1968.

61. Hashin, Zvi, "Viscoelastic Behavior of Fiber Reinforced Materials," Chapter 4.3, Theory of Fiber Reinforced Materials, NASA-CR-1974.
62. Calvit, H. H., Sutherland, H. J., and Willcox, M. G., "A Quasi-Static Investigation of Fiber Reinforced Materials," Ballistic Research Laboratories Report, No. 26, ENRL No. 1088, 1970.
63. Sutherland, H. J., and Calvit, H. H., "A Dynamic Investigation of Fiber-Reinforced Viscoelastic Materials," S.E.S.A. Spring Meeting, Detroit, Michigan, 1974.
64. Schultz, A. B., and Tsai, S. W., "Dynamic Moduli and Damping Ratios in Fiber Reinforced Composites," J. of Composite Materials, Vol. 2, No. 3, p. 368, July 1968.
65. Schultz, A. B., and Tsai, S. W., "Measurements of Complex Dynamic Moduli for Laminated Fiber-Reinforced Composites," J. of Composite Materials, Vol. 3, p. 434, July 1969.
66. Tsai, S. W., "Environmental Factors in the Design of Composite Materials," Mechanics of Composite Materials, Proceedings of the Fifth Symposium on Naval Structural Mechanics, Philadelphia, May 1967.
67. Schapery, R. A., "Viscoelastic Behavior and Analysis of Composite Materials," Texas A & M University, Mechanics and Materials Research Center, Report No. MM72-3, August 1972.
68. Schapery, R. A., et al., "Studies on the Viscoelastic Behavior of Fiber Reinforced Plastic," AFML-TR-73-179, July 1973 report.
69. Sims, D. F., and Halpin, J. C., "Methods for Determining the Elastic and Viscoelastic Response of Unidirectional Composite Materials," 1973, In Press.
70. Ericksen, R. H., "Room Temperature Creep of Borsic-Aluminum Composites," Metallurgical Transactions, Volume 4, July 1973.
71. Stinchcomb, W. W., et al., "Effects of Cyclic Frequency on the Mechanical Properties of Composite Materials," Virginia Polytechnic Institute and State University Report, VPI-E-73-25, 1973.
72. Laird, G. W., and Kingsbury, H. B., "A Method of Determining Complex Moduli of Viscoelastic Materials," Experimental Mechanics, March 1973.

73. Jones, E. R., et al., "Damping Measurements of a Controlled Composite Material," J. of Acoustical Society, August 1973.
74. Meyn, D. A., "Effect of Temperature and Strain Rate on the Tensile Properties of Boron-Aluminum and Boron-Epoxy Composites," ASTM, 3rd Symposium on Composite Materials, March 1973.
75. Chiao, T. T., et al., "Tensile Properties of an Ultrahigh-Strength Graphite Fiber in an Epoxy Matrix," A.S.T.M. Conference on Composite Reliability, Las Vegas, Nevada, April 1974.
76. Smart, J., and Williams, J. G., "A Comparison of Single-Integral Non-Linear Viscoelastic Theories," J. of Mech. of Phys. Solids, 1972.
77. Brinson, H. F., "Rate and Time Dependent Yield Behavior of a Ductile Polymer," VPI-E-72-23, Nov. 1972.
78. Brinson, H. F., and DasGupta, A., "The Strain Rate Behavior of Ductile Polymers," SESA Fall Meeting, 1973.
79. Christensen, R. M., "On Obtaining Solutions in Nonlinear Viscoelasticity," J. of Applied Mechanics, March 1968.
80. Davis, J. L., "Some Problems in Nonlinear Viscoelasticity," Fourth International Congress on Rheology, (E. H. Lee, Ed.), Part 2, John Wiley, 1963.
81. Distenfanso, N., and Todeschini, R., "Modeling, Identification and Prediction of a Class of Nonlinear Viscoelastic Materials," Int. J. Solids Structures, 1973.
82. Gottenberg, W. G., et al., "An Experimental Study of a Nonlinear Viscoelastic Solid in Uniaxial Tension," Transactions of the ASME, Sept. 1969.
83. Lou, Y. C., Schapery, R. A., "Viscoelastic Behavior of a Nonlinear Fiber-Reinforced Plastic," AFML-TR-68-90, Part II, April 1969.
84. Schapery, R. A., "On the Characterization of Nonlinear Viscoelastic Materials," Polymer Engineering and Science, Vol. 9, July 1969.
85. Schapery, R. A., "A Nonlinear Constitutive Theory for Particulate Composites Based on Viscoelastic Fracture Mechanics," Proc. of JANNAF Structures and Mechanical Behavior, April, 1974.

86. Schapery, R. A., "On a Thermodynamic Constitutive Theory and Its Application to Various Nonlinear Materials," Proceedings of the IUTAM Symposium East Kilbride, pp. 260-285, 1968.
87. Schapery, R. A., "A Theory of Non-Linear Thermoviscoelasticity Based on Irreversible Thermodynamics," Proceedings of Fifth U.S. National Congress of Applied Mechanics, A.S.M.E., pp. 511-530, 1966.
88. Hahn, H. T., and Tsai, S. W., "Nonlinear Elastic Behavior of Unidirectional Composite Laminae," J. of Composite Materials, Vol. 7, Jan. 1973.
89. Lockett, F. J., "Nonlinear Viscoelastic Solids," Academic Press, 1972.
90. Riven, R. S., "Some Remarks on the Mechanics of Nonlinear Viscoelastic Materials," Proceedings of the 14th International Congress on Rheology, Ed. by Onogi, S., University of Tokyo Press, 1969.
91. Heller, R. A.; Swift, G. W.; Stinchcomb, W. W.; Thakker, A. B.; and Liu, J. C., "Time and Temperature Dependence of Boron/Epoxy and Graphite/Epoxy Laminates," AFML-TR-73-261, Nov. 1973.
92. Heller, R. A., "Sixth Quarterly Progress Report," AFML, Dec. 1973.
93. Heller, R. A., Thakker, A. B., and Arthur, C. E., "Temperature Dependence of the Complex Modulus for Fiber Reinforced Materials," Composite Reliability Conference, April 1974.
94. Arthur, C. E., Heller, A. S., and Thakker, A. B., "A Response Surface for the Complex Modulus of Composite Materials," AFML-TR-74, April, 1974.
95. Snowden, J. C., "Vibration and Shock in Damped Mechanical Systems," Wiley, New York, 1968.
96. Barr, A. J., and Goodnight, J. H., "SAS, A User's Guide to the Statistical Analysis System," North Carolina State Univ., Raleigh, N.C., 1972.
97. Meyers, R.H., "Response Surface Methodology," Allyn Bacon, Boston, 1971.
98. Schwarzl, F. R., "On the Mechanical Properties of Unfilled and Filled Elastomers," Central Laboratory, T. No., Deft, Holland.

99. Heller, R. A., Heller, A. S., and Thakker, A. B., "Statistical Evaluation of Mechanical Properties for Composite Materials," ASCE, EMD Speciality Conference, Stanford, California, June 1974.

APPENDIX A

SPECIMEN PREPARATION AND PROCUREMENT

Layup Procedure for Boron/Epoxy and Graphite/Epoxy Specimens

Avco 55-05 boron and Hercules X3501A-S graphite tape were used as follows: 0°, -45°, +45°, 0°, +45°, -45°, 0° each angle measured from the longitudinal axis of the specimen. The specimens are 8 plies thick (.0434").

The layup procedure was generally as outlined in Paragraph 8.2.2.2.1 of "Structural Design Guide for Advanced Composite Applications" published by the Advanced Composites Division, Air Force Materials Laboratory, Wright-Patterson Air Force Base, Ohio. The differences between the procedure used and that outlined in Paragraph 8.2.2.2.1 are as follows:

1. The tool used was a flat metal plate with longitudinal boundary supports of metal .050 inches thick. Coroprene boundary supports were not used.
2. The surface of the tool was covered with a film of Tedlar rather than TX-1040.
3. The plies of boron and graphite were laid up directly on the tool rather than on a template. The glass fabric scrim cloth faced downward on all plies below the center line and upward above the outer line.

Curing Procedure and Quality Control Data
for Boron/Epoxy Specimen

The cure cycle recommended by Avco Corporation was used. (This is given on page 26 of Specification No. GM3004A from Grumman Aerospace Corporation) as follows:

Cure pressure: 50 ± 5 psi; vacuum level: during curing cycle 2 in. mercury max.; rate of temperature rise: $4-6^{\circ}\text{F}$ per minute; cure temperature: $350 \pm 10^{\circ}\text{F}$; cure time: 90 ± 5 minutes; cool down cycle: cool to below 125°F in no less than 40 minutes under full pressure; post cure cycle: 375° to 385° for 3 hours ± 10 minutes.

The panels were approximately 12 to 15 inches wide and 15 to 21 inches long. Quality control testing of the panels included a resin content and specific gravity determination on 25% of the panels and a flexural strength and modulus determination on another 25%.

Design objectives were as follows:

Fiber Volume	55-60%
Void Content	5% max.
Flexural Strength	110,000 p.s.i. min.
Flexural Modulus	14×10^6 p.s.i. min.

Flexure quality control tests were conducted on 1/2 in. wide specimens with a 1-1/2 in. span and a mid span load by Brunswick Corporation.

The data is given in Table A-1. The flexural modulus was computed using the simple linear beam deflection equation

$$y = \frac{P\ell^3}{48EI} \quad (\text{A-1})$$

Table A-1

QUALITY CONTROL DATA ON THE BORON/EPOXY PANELS

<u>Panel Iden.</u>	<u>Specific Gravity</u>	<u>Fiber Volume</u>	<u>Percent Voids</u>	<u>Flexural Strength</u>	<u>Flexural Modulus</u>
B	2.028	57.6	1.2	182,300	14.5 x 10 ⁶
C	2.030	58.4	2.0	169,900	14.2 x 10 ⁶
D	2.035	58.8	2.0	168,200	13.6 x 10 ⁶
F	2.040	61.1	4.2	Not Run	Not Run
G	1.979	55.8	3.0	174,800	17.2 x 10 ⁶
I	2.001	56.2	1.9	179,500	16.7 x 10 ⁶

Test specimens were routed from the panels using a slotted router coated with 60/80 diamond grit. This ensured minimum fiber breakout at the ends. The edges were kept parallel and the ends perpendicular to the fiber direction. The various specimens are shown in Figure 1.

Specimens Type I were affixed with end tabs of fiberglass cloth measuring 2.0 in. long by about 0.05 in. thick. The end tabs were attached with EPON 934 resin. A bevel of 30° was provided and end tabs were machined together with the specimens.

Curing Procedure and Quality Control Data
for Graphite/Epoxy Specimen

The cure cycle recommended by Hercules Corporation (Hercules Bulletin on X3501, dated 7/20/72) was used:

1. Insert the layup into room temperature autoclave and pull full vacuum.

2. Raise the laminate temperature at a rate of 5°F/minute.
3. When the part temperature reaches 280°F ± 5°F (approximately 45 ± 3 minutes), apply total of 100 psi (venting vacuum bag when full pressure is obtained).
4. Continue raising the laminate temperature at a rate of 5°F/minute until 350°F ± 5°F (approximately 10 ± 2 minutes) is reached.
5. When the laminate temperature reaches 350°F ± 5°F, cure 100 ± 5 minutes with 100 ± 5 psi.
6. Cool the laminate to 150°F or below under full pressure in 30 minutes or slower before removing it from the autoclave.

NOTE: Step 3 was based on 3" x 10" x 15 ply laminate. For different layups, the full pressure may be applied at different temperature in order to obtain desired fiber/resin volume ratio in the cured laminates.

Post Cure: Four hours at 400°F in an oven. (Recommend restraining the laminate between two rigid metal plates with clamps or weights.)

The panels were approximately 12 inches wide and 16 to 21 inches long. Quality control testing of the panels included a resin content and specific gravity determination on 25% of the panels and a flexural strength and modulus determination on another 25%.

Design objectives were as follows:

Fiber Volume	55-60%
Void Content	5% max.

Flexural Strength 50,000 psi min.

Flexural Modulus 8×10^6 psi min.

Quality control test procedures were the same as those used for Boron/Epoxy. The data is presented in Table A-2.

Table A-2

QUALITY CONTROL DATA ON THE GRAPHITE/EPOXY PANELS

<u>Panel Iden.</u>	<u>Specific Gravity</u>	<u>Fiber Volume</u>	<u>Percent Voids</u>	<u>Flexural Strength</u>	<u>Flexural Modulus</u>
A-10	Not Run	Not Run	Not Run	112,500	8.33×10^6
A	Not Run	Not Run	Not Run	Not Run	Not Run
B	1.53	53.5	2.2	134,100	9.52×10^6
C	Not Run	Not Run	Not Run	132,600	10.45×10^6
D	1.54	53.5	1.6	Not Run	Not Run

Specimens were prepared in a manner described for Boron/Epoxy and are shown in Figure 1. It has been observed that a great deal of warping was present in the early specimens.

After considerable discussion with Hercules, Grumman and Brunswick, it has been established that the suggested cure cycles require the use of only one metal plate under the layup and no plate above it. This arrangement produces an unsymmetrical heat sink which in spite of the careful cooling cycle in the autoclave is responsible for thermal gradients in the layup and causes warping of the panels.

When a second, identical, heat sink was placed on top of the layup, the warping was eliminated. Specimens were subsequently

manufactured in this manner.

APPENDIX B

DETERMINATION OF STORAGE MODULUS AND LOSS RATIO

The complex modulus, $E^*(\omega)$, is given by the relation

$$E^*(\omega) = E'(\omega) (1 + j \tan \delta) \quad (B.1)$$

where, δ is the loss ratio and $E'(\omega)$ is the real part, or storage modulus.

The imaginary part of the complex modulus (loss modulus), $E''(\omega)$ for small δ , is given by

$$E''(\omega) = E' \tan \delta \approx E' \delta \quad (B.2)$$

Due to large thickness to length ratios, the effects of shear were neglected and isotropic beam and bar theories were used to compute storage modulus.

For longitudinal vibrations, the relation between storage modulus and the frequency is

$$C^2 = \frac{E'(\omega)}{\rho} \quad (B.3)$$

where C is the wave speed.

For fixed-free boundary conditions, $E'(\omega)$ at first anti-resonance is computed from

$$E'(\omega) = 16 \ell^2 \rho f_1^2 \quad (B.4)$$

where ℓ is the length, ρ is the mass density and f_1 is the first anti-resonance frequency in Hertz.

The storage modulus for transverse vibration of a double cantilever beam driven by a sinusoidal force at the midpoint can be expressed as

$$E'(\omega) = \frac{48\pi^2 f_n^2 \rho}{h^2} \left[\frac{\ell}{2(na)} \right]^4 \quad (\text{B.5})$$

where h is the thickness of the beam.

References [94-95] give detailed discussions on the derivation of the above equations and values of parameter "na" ($na_1 = 1.8751$, $na_2 = 4.6941$, $na_3 = 7.8548$).

For small δ , the damping ratio at an anti-resonance can be determined from

$$\delta = \frac{\omega_2' - \omega_1'}{\omega_n} = \frac{f_2' - f_1'}{f_n} \quad (\text{B.6})$$

where f_n is the n^{th} anti-resonance frequency and f_2' and f_1' are the half power frequencies as shown in Figure 5. At the half power points the impedance is equal to 0.707 times its peak value at anti-resonance which on logarithmic scale is equivalent to 3dB.

APPENDIX C

TABULATION OF STRAIN RATE DATA

The experimental observations are listed in a computer print-out for each temperature (°F) in order of increasing strain rate (decreasing Fracture Time). Fracture Stress (FSTRES) and Stress are in psi while Fracture Time (FTIME) is in seconds. The procedure for obtaining these parameters is described under "rate tests."

Average strain rate is listed at the end of observations for each test.

BORON EPOXY STRAIN RATE DATA

SPEC.NO	TEMP	FSTRES	FTIME	STRAIN	STRESS
B1110	80.	115325.00	0.488E 04	0.00	0.00
B1110	80.	115325.00	0.488E 04	713.17	10526.32
B1110	80.	115325.00	0.488E 04	971.52	16253.87
B1110	80.	115325.00	0.488E 04	1130.30	21362.23
B1110	80.	115325.00	0.488E 04	1507.07	26315.79
B1110	80.	115325.00	0.488E 04	1803.10	32507.74
B1110	80.	115325.00	0.488E 04	2018.40	37925.70
B1110	80.	115325.00	0.488E 04	2368.26	44117.65
B1110	80.	115325.00	0.488E 04	2852.67	51083.59
B1110	80.	115325.00	0.488E 04	3229.44	58049.54
B1110	80.	115325.00	0.488E 04	3794.59	65015.48
B1110	80.	115325.00	0.488E 04	4117.54	72755.44
B1110	80.	115325.00	0.488E 04	4171.36	80495.38
B1110	80.	115325.00	0.488E 04	4507.76	88235.31
B1110	80.	115325.00	0.488E 04	5153.65	96749.25
B1110	80.	115325.00	0.488E 04	5718.80	103715.10

STRAIN RATE = 1.270E-06

B1150	80.	112951.80	0.480E 04	0.00	0.00
B1150	80.	112951.80	0.480E 04	886.50	15060.24
B1150	80.	112951.80	0.480E 04	1561.93	25602.41
B1150	80.	112951.80	0.480E 04	2364.00	36897.59
B1150	80.	112951.80	0.480E 04	3236.43	50451.81
B1150	80.	112951.80	0.480E 04	4277.71	65512.05
B1150	80.	112951.80	0.480E 04	5206.43	81325.31
B1150	80.	112951.80	0.480E 04	6402.50	97891.56

STRAIN RATE = 1.520E-06

B1155	80.	110248.30	0.489E 04	0.00	0.00
B1155	80.	110248.30	0.489E 04	547.22	7763.98
B1155	80.	110248.30	0.489E 04	848.19	10869.57
B1155	80.	110248.30	0.489E 04	1135.49	17080.75
B1155	80.	110248.30	0.489E 04	1450.14	21739.13
B1155	80.	110248.30	0.489E 04	1805.83	27950.31
B1155	80.	110248.30	0.489E 04	2188.89	33385.09
B1155	80.	110248.30	0.489E 04	2626.67	39596.27

BORON EPOXY STRAIN RATE DATA

SPEC.NO	TEMP	FSTRES	FTIME	STRAIN	STRESS
B1155	80.	110248.30	0.489E 04	3064.44	46273.29
B1155	80.	110248.30	0.489E 04	3529.58	52795.03
B1155	80.	110248.30	0.489E 04	4022.08	60559.01
B1155	80.	110248.30	0.489E 04	4541.94	68323.00
B1155	80.	110248.30	0.489E 04	5089.16	75931.69
B1155	80.	110248.30	0.489E 04	5650.07	83850.94
B1155	80.	110248.30	0.489E 04	6183.61	91614.94
B1155	80.	110248.30	0.489E 04	6771.87	99378.88
B1155	80.	110248.30	0.489E 04	7373.82	107764.00
STRAIN RATE =				1.540E-06	
B1152	80.	99099.13	0.750E 01	0.00	0.00
B1152	80.	99099.13	0.750E 01	1164.33	15015.02
B1152	80.	99099.13	0.750E 01	1927.17	28528.53
B1152	80.	99099.13	0.750E 01	2703.39	39039.04
B1152	80.	99099.13	0.750E 01	3640.20	52552.55
STRAIN RATE =				1.313E-04	
B1149	80.	111882.60	0.900E 01	0.00	0.00
B1149	80.	111882.60	0.900E 01	1245.62	18209.88
B1149	80.	111882.60	0.900E 01	1916.34	27006.17
B1149	80.	111882.60	0.900E 01	2491.24	37037.04
B1149	80.	111882.60	0.900E 01	3161.96	47067.90
STRAIN RATE =				7.910E-04	
B1153	80.	113650.80	0.902E 01	0.00	0.00
B1153	80.	113650.80	0.902E 01	1040.49	14285.71
B1153	80.	113650.80	0.902E 01	1775.77	25555.56
B1153	80.	113650.80	0.902E 01	2427.81	34920.64
B1153	80.	113650.80	0.902E 01	3190.84	46031.75
B1153	80.	113650.80	0.902E 01	4050.97	58730.16
B1153	80.	113650.80	0.902E 01	4994.35	71428.56
B1153	80.	113650.80	0.902E 01	5965.48	84920.63
B1153	80.	113650.80	0.902E 01	7075.33	99206.38

BORON EPOXY STRAIN RATE DATA

SPEC.NO	TEMP	FSTRES	FTIME	STRAIN	STRESS
STRAIN RATE =				8.840E-04	
B1I78	80.	106250.00	0.425E 00	0.00	0.00
B1I78	80.	106250.00	0.425E 00	793.42	6562.50
B1I78	80.	106250.00	0.425E 00	1586.84	18750.00
B1I78	80.	106250.00	0.425E 00	2380.25	29687.50
B1I78	80.	106250.00	0.425E 00	3173.67	42187.50
B1I78	80.	106250.00	0.425E 00	4165.44	56562.50
B1I78	80.	106250.00	0.425E 00	6148.99	85937.50
B1I78	80.	106250.00	0.425E 00	5157.21	71875.00
STRAIN RATE =				1.660E-02	
B1I79	80.	110937.50	0.450E 00	0.00	0.00
B1I79	80.	110937.50	0.450E 00	977.49	9375.00
B1I79	80.	110937.50	0.450E 00	1954.97	21875.00
B1I79	80.	110937.50	0.450E 00	2541.47	33593.75
B1I79	80.	110937.50	0.450E 00	3421.20	46875.00
B1I79	80.	110937.50	0.450E 00	4300.94	58593.75
B1I79	80.	110937.50	0.450E 00	5239.33	75000.00
B1I79	80.	110937.50	0.450E 00	6255.92	89062.56
B1I79	80.	110937.50	0.450E 00	6940.16	103125.00
STRAIN RATE =				1.630E-02	
B1I56	80.	124783.00	0.155E-01	0.00	0.00
B1I56	80.	124783.00	0.155E-01	796.54	10487.00
B1I56	80.	124783.00	0.155E-01	2041.13	28935.19
STRAIN RATE =				8.160E-01	
B1I58	80.	122974.50	0.168E-01	0.00	0.00
B1I58	80.	122974.50	0.168E-01	1493.51	23509.84
B1I58	80.	122974.50	0.168E-01	1991.34	32552.08
B1I58	80.	122974.50	0.168E-01	2738.10	43402.78

BORON EPOXY STRAIN RATE DATA

SPEC.NO	TEMP	FSTRES	FTIME	STRAIN	STRESS
				STRAIN RATE =	6.850E-01
B1159	80.	126591.30	0.174E-01	0.00	0.00
B1159	80.	126591.30	0.174E-01	733.93	10489.00
B1159	80.	126591.30	0.174E-01	1223.22	18084.49
				STRAIN RATE =	6.120E-01
B1138	200.	110937.50	0.475E 04	0.00	0.00
B1138	200.	110937.50	0.475E 04	1054.05	12500.00
B1138	200.	110937.50	0.475E 04	1528.38	18750.00
B1138	200.	110937.50	0.475E 04	1791.89	23750.00
B1138	200.	110937.50	0.475E 04	2108.11	28906.25
B1138	200.	110937.50	0.475E 04	2371.62	34687.50
B1138	200.	110937.50	0.475E 04	2635.14	40625.00
B1138	200.	110937.50	0.475E 04	2951.35	46562.50
B1138	200.	110937.50	0.475E 04	3162.16	53125.00
				STRAIN RATE =	1.320E-06
B1139	200.	112640.80	0.514E 04	0.00	0.00
B1139	200.	112640.80	0.514E 04	791.03	11733.42
B1139	200.	112640.80	0.514E 04	1318.38	17209.01
B1139	200.	112640.80	0.514E 04	1582.05	21902.38
B1139	200.	112640.80	0.514E 04	1845.73	26595.74
B1139	200.	112640.80	0.514E 04	2241.24	31289.11
B1139	200.	112640.80	0.514E 04	2636.76	37234.04
B1139	200.	112640.80	0.514E 04	2979.54	43022.53
B1139	200.	112640.80	0.514E 04	3427.78	48498.12
				STRAIN RATE =	1.430E-06
B1142	200.	98437.50	0.840E 01	0.00	0.00
B1142	200.	98437.50	0.840E 01	1328.64	17986.75
B1142	200.	98437.50	0.840E 01	2097.86	29687.50

BORCN EPOXY STRAIN RATE DATA

SPEC.NO	TEMP	FSTRES	FTIME		STRAIN	STRESS
B1142	200.	98437.50	0.840E 01		2727.21	39062.50
B1142	200.	98437.50	0.840E 01		3426.50	48437.50
B1142	200.	98437.50	0.840E 01		4265.64	59375.00
B1142	200.	98437.50	0.840E 01		5244.64	71875.00
B1142	200.	98437.50	0.840E 01		6265.59	85156.25

STRAIN RATE = 7.460E-04

B1141	200.	107031.10	0.900E 01		0.00	0.00
B1141	200.	107031.10	0.900E 01		1413.53	12500.00
B1141	200.	107031.10	0.900E 01		2182.66	21875.00
B1141	200.	107031.10	0.900E 01		3076.51	34375.00
B1141	200.	107031.10	0.900E 01		3533.83	45312.50
B1141	200.	107031.10	0.900E 01		4365.31	56250.00

STRAIN RATE = 8.730E-04

B1193	200.	100781.10	0.425E 00		0.00	0.00
B1193	200.	100781.10	0.425E 00		808.60	7812.50
B1193	200.	100781.10	0.425E 00		1617.20	20312.50
B1193	200.	100781.10	0.425E 00		2425.80	32812.50
B1193	200.	100781.10	0.425E 00		3234.40	45312.50
B1193	200.	100781.10	0.425E 00		4043.00	56562.50
B1193	200.	100781.10	0.425E 00		5053.75	70312.50
B1193	200.	100781.10	0.425E 00		6064.50	85937.50

STRAIN RATE = 1.620E-02

B1196	200.	89531.25	0.360E 00		0.00	0.00
B1196	200.	89531.25	0.360E 00		539.41	6250.00
B1196	200.	89531.25	0.360E 00		1294.59	15625.00
B1196	200.	89531.25	0.360E 00		1941.88	31250.00
B1196	200.	89531.25	0.360E 00		2589.18	42187.50
B1196	200.	89531.25	0.360E 00		3236.47	54687.50
B1196	200.	89531.25	0.360E 00		4099.53	68750.00
B1196	200.	89531.25	0.360E 00		5070.47	82812.50

STRAIN RATE = 1.450E-02

BORCN EPOXY STRAIN RATE DATA

SPEC.NO	TEMP	FSTRES	FTIME	STRAIN	STRESS
B11104	200.	86805.56	0.180E-01	0.00	0.00
B11104	200.	86805.56	0.180E-01	1528.94	18084.49
B11104	200.	86805.56	0.180E-01	2293.40	32552.08
B11104	200.	86805.56	0.180E-01	3057.87	45211.23
B11104	200.	86805.56	0.180E-01	4204.57	57870.37
B11104	200.	86805.56	0.180E-01	4969.04	72337.94
B11104	200.	86805.56	0.180E-01	5733.51	83188.69
B11104	200.	86805.56	0.180E-01	6345.08	86805.56

STRAIN RATE = 2.280E-01

B11144	200.	113208.80	0.245E-01	0.00	0.00
B11144	200.	113208.80	0.245E-01	495.87	9042.25
B11144	200.	113208.80	0.245E-01	1062.57	21701.39
B11144	200.	113208.80	0.245E-01	1671.78	32552.08
B11144	200.	113208.80	0.245E-01	2266.82	43402.78
B11144	200.	113208.80	0.245E-01	2833.53	54253.47
B11144	200.	113208.80	0.245E-01	3357.73	65104.17
B11144	200.	113208.80	0.245E-01	3966.94	77763.31
B11144	200.	113208.80	0.245E-01	4533.64	87890.63
B11144	200.	113208.80	0.245E-01	5157.02	101273.10
B11144	200.	113208.80	0.245E-01	5596.22	113208.80

STRAIN RATE = 3.530E-01

B1175	300.	106250.00	0.459E 04	0.00	0.00
B1175	300.	106250.00	0.459E 04	731.25	10937.50
B1175	300.	106250.00	0.459E 04	1112.77	17187.50
B1175	300.	106250.00	0.459E 04	1398.91	21875.00
B1175	300.	106250.00	0.459E 04	1780.43	29687.50
B1175	300.	106250.00	0.459E 04	2161.96	35937.50
B1175	300.	106250.00	0.459E 04	2543.48	42187.50
B1175	300.	106250.00	0.459E 04	3020.38	48437.50
B1175	300.	106250.00	0.459E 04	3465.49	54687.50
B1175	300.	106250.00	0.459E 04	3942.39	61328.13

STRAIN RATE = 1.460E-06

BORON EPOXY STRAIN RATE DATA

SPEC.NO	TEMP	FSTRES	FTIME	STRAIN	STRESS
B1174	300.	102343.60	0.416E 04	0.00	0.00
B1174	300.	102343.60	0.416E 04	882.04	11562.50
B1174	300.	102343.60	0.416E 04	1356.99	18437.50
B1174	300.	102343.60	0.416E 04	1831.94	24687.50
B1174	300.	102343.60	0.416E 04	2239.03	31250.00
B1174	300.	102343.60	0.416E 04	2713.98	37500.00
B1174	300.	102343.60	0.416E 04	3229.64	43750.00
B1174	300.	102343.60	0.416E 04	3772.43	50781.25
B1174	300.	102343.60	0.416E 04	4315.23	57812.50

STRAIN RATE = 1.800E-06

B1176	300.	110937.50	0.430E 01	0.00	0.00
B1176	300.	110937.50	0.430E 01	1244.05	20312.50
B1176	300.	110937.50	0.430E 01	1836.46	28125.00
B1176	300.	110937.50	0.430E 01	2488.10	39062.50
B1176	300.	110937.50	0.430E 01	3258.23	49218.75
B1176	300.	110937.50	0.430E 01	4087.59	62500.00
B1176	300.	110937.50	0.430E 01	5035.44	75000.00
B1176	300.	110937.50	0.430E 01	6042.53	90625.00
B1176	300.	110937.50	0.430E 01	7168.10	103125.00

STRAIN RATE = 1.790E-03

B1177	300.	109375.00	0.430E 01	0.00	0.00
B1177	300.	109375.00	0.430E 01	1307.65	18750.00
B1177	300.	109375.00	0.430E 01	1954.59	29687.50
B1177	300.	109375.00	0.430E 01	2642.82	37187.50
B1177	300.	109375.00	0.430E 01	3441.18	48437.50
B1177	300.	109375.00	0.430E 01	4267.06	60937.50
B1177	300.	109375.00	0.430E 01	5230.56	73437.50
B1177	300.	109375.00	0.430E 01	6056.47	85937.50
B1177	300.	109375.00	0.430E 01	7157.64	100000.00

STRAIN RATE = 1.790E-03

B1194	300.	96875.00	0.400E 00	0.00	0.00
-------	------	----------	-----------	------	------

BORON EPOXY STRAIN RATE DATA

SPEC.NO	TEMP	FSTRES	FTIME	STRAIN	STRESS
B1I94	300.	96875.00	0.400E 00	1017.75	10156.25
B1I94	300.	96875.00	0.400E 00	1984.61	23437.50
B1I94	300.	96875.00	0.400E 00	2671.59	34375.00
B1I94	300.	96875.00	0.400E 00	3562.12	46875.00
B1I94	300.	96875.00	0.400E 00	4452.65	59375.00
B1I94	300.	96875.00	0.400E 00	5597.62	73437.50
B1I94	300.	96875.00	0.400E 00	6615.37	88281.25
STRAIN RATE =				1.740E-02	
B1I95	300.	109375.00	0.460E 00	0.00	0.00
B1I95	300.	109375.00	0.460E 00	513.06	5000.00
B1I95	300.	109375.00	0.460E 00	1282.65	17500.00
B1I95	300.	109375.00	0.460E 00	2052.23	26875.00
B1I95	300.	109375.00	0.460E 00	2821.82	37500.00
B1I95	300.	109375.00	0.460E 00	3847.94	50781.25
B1I95	300.	109375.00	0.460E 00	4874.05	67187.50
B1I95	300.	109375.00	0.460E 00	5900.17	81250.00
B1I95	300.	109375.00	0.460E 00	7182.81	96875.00
STRAIN RATE =				1.750E-02	
B1I110	300.	94039.38	0.205E-01	0.00	0.00
B1I110	300.	94039.38	0.205E-01	659.00	10850.69
B1I110	300.	94039.38	0.205E-01	1318.00	21701.39
B1I110	300.	94039.38	0.205E-01	1647.50	34360.53
B1I110	300.	94039.38	0.205E-01	2471.25	43402.78
B1I110	300.	94039.38	0.205E-01	3295.00	57870.37
B1I110	300.	94039.38	0.205E-01	3954.00	70529.50
B1I110	300.	94039.38	0.205E-01	4613.00	81380.19
B1I110	300.	94039.38	0.205E-01	5272.00	94039.38
STRAIN RATE =				2.570E-01	
B1I97	300.	104890.00	0.233E-01	0.00	0.00
B1I97	300.	104890.00	0.233E-01	570.16	10127.31
B1I97	300.	104890.00	0.233E-01	1140.32	21701.39

BORON EPOXY STRAIN RATE DATA

SPEC.NO	TEMP	FSTRES	FTIME	STRAIN	STRESS
B1197	300.	104890.00	0.233E-01	1781.75	32552.08
B1197	300.	104890.00	0.233E-01	2351.91	43402.78
B1197	300.	104890.00	0.233E-01	3064.61	54253.47
B1197	300.	104890.00	0.233E-01	3634.77	66912.63
B1197	300.	104890.00	0.233E-01	4204.93	77763.31
B1197	300.	104890.00	0.233E-01	4703.82	90422.44
B1197	300.	104890.00	0.233E-01	5416.52	99464.69
B1197	300.	104890.00	0.233E-01	5701.60	104890.00

STRAIN RATE = 2.450E-01

B11105	-50.	106250.00	0.441E 04	0.00	0.00
B11105	-50.	106250.00	0.441E 04	525.25	6250.00
B11105	-50.	106250.00	0.441E 04	931.13	12500.00
B11105	-50.	106250.00	0.441E 04	1337.00	20312.50
B11105	-50.	106250.00	0.441E 04	1719.00	26562.50
B11105	-50.	106250.00	0.441E 04	2148.75	32812.50
B11105	-50.	106250.00	0.441E 04	2578.50	39843.75
B11105	-50.	106250.00	0.441E 04	3056.00	47265.63

STRAIN RATE = 1.270E-06

B11109	-50.	119531.10	0.467E 04	0.00	0.00
B11109	-50.	119531.10	0.467E 04	668.50	9375.00
B11109	-50.	119531.10	0.467E 04	1337.00	21875.00
B11109	-50.	119531.10	0.467E 04	1766.75	28906.25
B11109	-50.	119531.10	0.467E 04	2148.75	35937.50
B11109	-50.	119531.10	0.467E 04	2578.50	42968.75
B11109	-50.	119531.10	0.467E 04	3056.00	50781.25

STRAIN RATE = 1.270E-06

B11107	-50.	118281.10	0.100E 02	0.00	0.00
B11107	-50.	118281.10	0.100E 02	48.72	0.00
B11107	-50.	118281.10	0.100E 02	97.45	390.03
B11107	-50.	118281.10	0.100E 02	438.52	4687.50
B11107	-50.	118281.10	0.100E 02	1802.81	26562.50

BORCN EPOXY STRAIN RATE DATA

SPEC.NO	TEMP	FSTRES	FTIME	STRAIN	STRESS
B11107	-50.	118281.10	0.100E 02	2606.76	39843.75
B11107	-50.	118281.10	0.100E 02	3410.72	53125.00
B11107	-50.	118281.10	0.100E 02	4336.48	68750.00
STRAIN RATE =				6.190E-04	
B1167	-50.	121093.60	0.840E 01	0.00	0.00
B1167	-50.	121093.60	0.840E 01	1266.84	14062.50
STRAIN RATE =				8.900E-04	
B11112	-50.	117968.60	0.380E 00	0.00	0.00
B11112	-50.	117968.60	0.380E 00	889.85	3125.00
B11112	-50.	117968.60	0.380E 00	2076.32	15625.00
B11112	-50.	117968.60	0.380E 00	2966.18	32812.50
B11112	-50.	117968.60	0.380E 00	3856.03	46875.00
B11112	-50.	117968.60	0.380E 00	5042.50	64062.50
B11112	-50.	117968.60	0.380E 00	6228.97	82812.50
B11112	-50.	117968.60	0.380E 00	7563.75	101562.50
STRAIN RATE =				2.160E-02	
B11120	-50.	110937.50	0.360E 00	0.00	0.00
B11120	-50.	110937.50	0.360E 00	238.78	2343.75
B11120	-50.	110937.50	0.360E 00	1193.89	14062.50
B11120	-50.	110937.50	0.360E 00	2089.30	31250.00
B11120	-50.	110937.50	0.360E 00	2984.72	46875.00
B11120	-50.	110937.50	0.360E 00	4178.60	64062.50
B11120	-50.	110937.50	0.360E 00	5372.49	82812.50
B11120	-50.	110937.50	0.360E 00	6566.37	101562.50
STRAIN RATE =				1.930E-02	
B11113	-50.	104890.00	0.205E-01	0.00	0.00
B11113	-50.	104890.00	0.205E-01	698.10	14467.59
B11113	-50.	104890.00	0.205E-01	1116.96	23509.84

BORGN EPOXY STRAIN RATE DATA

SPEC.NO	TEMP	FSTRES	FTIME	STRAIN	STRESS
B1I113	-50.	104890.00	0.205E-01	2024.49	39785.88
B1I113	-50.	104890.00	0.205E-01	2513.16	50636.57
B1I113	-50.	104890.00	0.205E-01	3071.64	65104.17
B1I113	-50.	104890.00	0.205E-01	3769.74	75954.88
B1I113	-50.	104890.00	0.205E-01	4188.60	86805.56
B1I113	-50.	104890.00	0.205E-01	5026.32	95847.81
B1I113	-50.	104890.00	0.205E-01	5165.94	104890.00

STRAIN RATE = 2.520E-01

B1I111	-50.	112123.80	0.228E-01	0.00	0.00
B1I111	-50.	112123.80	0.228E-01	1100.99	19892.94
B1I111	-50.	112123.80	0.228E-01	1857.92	32552.08
B1I111	-50.	112123.80	0.228E-01	2339.61	39785.87
B1I111	-50.	112123.80	0.228E-01	3027.73	57870.37
B1I111	-50.	112123.80	0.228E-01	3715.85	68721.06
B1I111	-50.	112123.80	0.228E-01	4403.97	84997.13
B1I111	-50.	112123.80	0.228E-01	4954.46	94039.38
B1I111	-50.	112123.80	0.228E-01	5504.96	104890.00

STRAIN RATE = 2.570E-01

GRAPHITE EPOXY STRAIN RATE DATA

SPEC.NO	TEMP	FSTRES	FTIME	STRAIN	STRESS
G3I1	80.	62162.16	0.357E 04	0.00	0.00
G3I1	80.	62162.16	0.357E 04	949.93	7432.43
G3I1	80.	62162.16	0.357E 04	1461.42	11891.89
G3I1	80.	62162.16	0.357E 04	1943.69	15540.54
G3I1	80.	62162.16	0.357E 04	2425.97	20270.27
G3I1	80.	62162.16	0.357E 04	3013.54	24324.32
G3I1	80.	62162.16	0.357E 04	3653.56	29594.59
G3I1	80.	62162.16	0.357E 04	4238.13	34459.46
G3I1	80.	62162.16	0.357E 04	4968.84	39864.86
G3I1	80.	62162.16	0.357E 04	5451.11	45270.27
G3I1	80.	62162.16	0.357E 04	6181.83	50675.68
G3I1	80.	62162.16	0.357E 04	6941.77	56756.76

STRAIN RATE = 2.100E-06

G3I2	80.	67945.19	0.386E 04	0.00	0.00
G3I2	80.	67945.19	0.386E 04	1200.21	8219.18
G3I2	80.	67945.19	0.386E 04	1821.01	12328.77
G3I2	80.	67945.19	0.386E 04	2441.81	17123.29
G3I2	80.	67945.19	0.386E 04	2993.63	21232.88
G3I2	80.	67945.19	0.386E 04	3545.45	26027.40
G3I2	80.	67945.19	0.386E 04	4130.04	30821.92
G3I2	80.	67945.19	0.386E 04	4856.02	35616.44
G3I2	80.	67945.19	0.386E 04	5476.82	40410.96
G3I2	80.	67945.19	0.386E 04	6125.21	45890.41
G3I2	80.	67945.19	0.386E 04	6856.37	50684.93
G3I2	80.	67945.19	0.386E 04	7546.15	56849.32

STRAIN RATE = 2.290E-06

G3I3	80.	71428.56	0.384E 04	0.00	0.00
G3I3	80.	71428.56	0.384E 04	1132.91	8051.95
G3I3	80.	71428.56	0.384E 04	1683.63	13636.36
G3I3	80.	71428.56	0.384E 04	2234.34	18441.56
G3I3	80.	71428.56	0.384E 04	2706.39	23376.62
G3I3	80.	71428.56	0.384E 04	3257.11	27922.08
G3I3	80.	71428.56	0.384E 04	3807.83	32857.14
G3I3	80.	71428.56	0.384E 04	4437.22	38051.95

GRAPHITE EPOXY STRAIN RATE DATA

SPEC.NO	TEMP	FSTRES	FTIME		STRAIN	STRESS
G313	80.	71428.56	0.384E 04		5066.61	42857.14
G313	80.	71428.56	0.384E 04		5696.00	48701.30
G313	80.	71428.56	0.384E 04		6404.07	54545.45
STRAIN RATE =					2.130E-06	
G314	80.	48455.06	0.530E 01		0.00	0.00
G314	80.	48455.06	0.530E 01		941.08	7022.47
G314	80.	48455.06	0.530E 01		1788.06	14044.94
G314	80.	48455.06	0.530E 01		2258.60	17556.18
G314	80.	48455.06	0.530E 01		2666.40	21067.42
G314	80.	48455.06	0.530E 01		3011.46	24578.65
G314	80.	48455.06	0.530E 01		3482.01	28792.13
G314	80.	48455.06	0.530E 01		3952.55	32303.37
G314	80.	48455.06	0.530E 01		4501.51	37219.10
G314	80.	48455.06	0.530E 01		4893.63	40730.34
G314	80.	48455.06	0.530E 01		5521.02	45646.07
STRAIN RATE =					1.100E-03	
G315	80.	57162.53	0.670E 01		0.00	0.00
G315	80.	57162.53	0.670E 01		718.23	7575.75
G315	80.	57162.53	0.670E 01		1265.45	10330.58
G315	80.	57162.53	0.670E 01		1710.07	15840.22
G315	80.	57162.53	0.670E 01		2000.78	18595.04
G315	80.	57162.53	0.670E 01		2428.30	22727.27
G315	80.	57162.53	0.670E 01		2770.31	26033.06
G315	80.	57162.53	0.670E 01		3197.83	28512.40
G315	80.	57162.53	0.670E 01		3710.85	33608.82
G315	80.	57162.53	0.670E 01		4138.37	37465.56
STRAIN RATE =					9.200E-04	
G317	80.	68614.13	0.730E 01		0.00	0.00
G317	80.	68614.13	0.730E 01		901.76	7744.57
G317	80.	68614.13	0.730E 01		1595.42	14673.91
G317	80.	68614.13	0.730E 01		2115.67	17663.04

GRAPHITE EPOXY STRAIN RATE DATA

SPEC.NO	TEMP	FSTRES	FTIME		STRAIN	STRESS
G3I7	80.	68614.13	0.730E 01		2549.21	21059.78
G3I7	80.	68614.13	0.730E 01		2896.04	25815.22
G3I7	80.	68614.13	0.730E 01		3329.58	29211.96
G3I7	80.	68614.13	0.730E 01		3763.12	33967.39
G3I7	80.	68614.13	0.730E 01		4283.36	38043.48
G3I7	80.	68614.13	0.730E 01		4716.90	42119.57
G3I7	80.	68614.13	0.730E 01		5237.15	46195.65
G3I7	80.	68614.13	0.730E 01		5757.39	50951.09

STRAIN RATE = 1.050E-03

G3I22	80.	62500.00	0.300E 00		0.00	0.00
G3I22	80.	62500.00	0.300E 00		1073.03	7638.89
G3I22	80.	62500.00	0.300E 00		2341.16	18750.00
G3I22	80.	62500.00	0.300E 00		3511.74	30555.56
G3I22	80.	62500.00	0.300E 00		4779.86	42361.11
G3I22	80.	62500.00	0.300E 00		6145.54	54166.67

STRAIN RATE = 2.230E-02

G3I19	80.	43333.33	0.210E 00		0.00	0.00
G3I19	80.	43333.33	0.210E 00		391.80	2777.78
G3I19	80.	43333.33	0.210E 00		1567.20	11111.11
G3I19	80.	43333.33	0.210E 00		2938.50	23611.11
G3I19	80.	43333.33	0.210E 00		4309.80	35416.67

STRAIN RATE = 2.330E-02

G3I25	80.	67515.44	0.140E-01		0.00	0.00
G3I25	80.	67515.44	0.140E-01		649.09	8037.55
G3I25	80.	67515.44	0.140E-01		1135.91	12860.08
G3I25	80.	67515.44	0.140E-01		1866.14	20897.63
G3I25	80.	67515.44	0.140E-01		2434.09	27327.67
G3I25	80.	67515.44	0.140E-01		2920.91	32150.21
G3I25	80.	67515.44	0.140E-01		3245.46	36972.74
G3I25	80.	67515.44	0.140E-01		3651.14	40187.76
G3I25	80.	67515.44	0.140E-01		3894.55	45010.29

GRAPHITE EPOXY STRAIN RATE DATA

SPEC.NO	TEMP	FSTRES	FTIME	STRAIN	STRESS
G3I25	80.	67515.44	0.140E-01	4219.10	48225.31
G3I25	80.	67515.44	0.140E-01	4543.64	51440.33
G3I25	80.	67515.44	0.140E-01	4868.19	56262.86
G3I25	80.	67515.44	0.140E-01	5273.87	57870.37

STRAIN RATE = 4.390E-01

G3I24	80.	53047.81	0.112E-01	0.00	0.00
G3I24	80.	53047.81	0.112E-01	571.01	6430.04
G3I24	80.	53047.81	0.112E-01	1356.15	12860.08
G3I24	80.	53047.81	0.112E-01	1855.79	19290.11
G3I24	80.	53047.81	0.112E-01	2498.18	25720.15
G3I24	80.	53047.81	0.112E-01	3069.19	30542.68
G3I24	80.	53047.81	0.112E-01	3568.82	35365.21
G3I24	80.	53047.81	0.112E-01	3854.33	38580.23
G3I24	80.	53047.81	0.112E-01	4282.59	41795.25
G3I24	80.	53047.81	0.112E-01	4568.10	46617.78
G3I24	80.	53047.81	0.112E-01	4924.98	51440.30

STRAIN RATE = 4.920E-01

G3I27	80.	57870.37	0.112E-01	0.00	0.00
G3I27	80.	57870.37	0.112E-01	876.54	12860.08
G3I27	80.	57870.37	0.112E-01	1773.95	19611.62
G3I27	80.	57870.37	0.112E-01	2295.70	25720.16
G3I27	80.	57870.37	0.112E-01	2921.80	32150.20
G3I27	80.	57870.37	0.112E-01	3547.90	38580.24
G3I27	80.	57870.37	0.112E-01	3965.30	41795.27
G3I27	80.	57870.37	0.112E-01	4382.70	45010.29
G3I27	80.	57870.37	0.112E-01	4800.10	49832.82
G3I27	80.	57870.37	0.112E-01	5008.80	54655.35
G3I27	80.	57870.37	0.112E-01	5426.20	57870.37

STRAIN RATE = 4.840E-01

G3I10	200.	70833.31	0.417E 04	0.00	0.00
G3I10	200.	70833.31	0.417E 04	1151.92	6944.44

GRAPHITE EPOXY STRAIN RATE DATA

SPEC.NO	TEMP	FSTRES	FTIME		STRAIN	STRESS
G3I10	200.	70833.31	0.417E 04		2218.52	14166.67
G3I10	200.	70833.31	0.417E 04		2798.74	18055.56
G3I10	200.	70833.31	0.417E 04		3327.77	22222.22

STRAIN RATE = 2.770E-06

G3I11	200.	62500.00	0.387E 04		0.00	0.00
G3I11	200.	62500.00	0.387E 04		1119.03	6944.44
G3I11	200.	62500.00	0.387E 04		2065.90	13888.89
G3I11	200.	62500.00	0.387E 04		2668.46	17777.78
G3I11	200.	62500.00	0.387E 04		3184.93	21527.78
G3I11	200.	62500.00	0.387E 04		3787.49	25000.00
G3I11	200.	62500.00	0.387E 04		4390.04	29166.67
G3I11	200.	62500.00	0.387E 04		4992.60	33750.00
G3I11	200.	62500.00	0.387E 04		5681.23	38194.44
G3I11	200.	62500.00	0.387E 04		6369.87	43055.56
G3I11	200.	62500.00	0.387E 04		7058.50	47222.22
G3I11	200.	62500.00	0.387E 04		7747.14	52777.78
G3I11	200.	62500.00	0.387E 04		8435.77	57638.89

STRAIN RATE = 2.340E-06

G3I8	200.	84615.38	0.900E 01		0.00	0.00
G3I8	200.	84615.38	0.900E 01		1794.05	13076.92
G3I8	200.	84615.38	0.900E 01		2918.03	23846.15
G3I8	200.	84615.38	0.900E 01		3739.40	30769.23

STRAIN RATE = 1.250E-03

G3I9	200.	88888.88	0.940E 01		0.00	0.00
G3I9	200.	88888.88	0.940E 01		1983.86	13333.33
G3I9	200.	88888.88	0.940E 01		3114.45	23611.11
G3I9	200.	88888.88	0.940E 01		3946.40	30277.78

STRAIN RATE = 1.320E-03

GRAPHITE EPOXY STRAIN RATE DATA

SPEC.NO	TEMP	FSTRES	FTIME	STRAIN	STRESS
G3I21	200.	57638.88	0.290E 00	0.00	0.00
G3I21	200.	57638.88	0.290E 00	731.14	5555.56
G3I21	200.	57638.88	0.290E 00	2193.42	13888.89
G3I21	200.	57638.88	0.290E 00	3411.98	25000.00
G3I21	200.	57638.88	0.290E 00	4630.55	34722.22
G3I21	200.	57638.88	0.290E 00	6092.83	47222.22
STRAIN RATE =				2.340E-02	
G3I20	200.	42361.11	0.225E 00	0.00	0.00
G3I20	200.	42361.11	0.225E 00	928.51	4861.11
G3I20	200.	42361.11	0.225E 00	2247.98	13888.89
G3I20	200.	42361.11	0.225E 00	3665.19	25000.00
G3I20	200.	42361.11	0.225E 00	5131.27	36111.11
STRAIN RATE =				2.570E-02	
G3I103	200.	70730.44	0.217E-01	0.00	0.00
G3I103	200.	70730.44	0.217E-01	1071.00	6430.04
G3I103	200.	70730.44	0.217E-01	1785.00	19290.11
G3I103	200.	70730.44	0.217E-01	2677.50	27327.66
G3I103	200.	70730.44	0.217E-01	3570.00	35365.21
G3I103	200.	70730.44	0.217E-01	4105.50	40187.74
G3I103	200.	70730.44	0.217E-01	4819.50	48225.28
STRAIN RATE =				3.390E-01	
G3I80	200.	81983.00	0.233E-01	0.00	0.00
G3I80	200.	81983.00	0.233E-01	904.50	6430.04
G3I80	200.	81983.00	0.233E-01	1809.00	16075.10
G3I80	200.	81983.00	0.233E-01	2894.40	28935.18
G3I80	200.	81983.00	0.233E-01	3346.65	36972.73
G3I80	200.	81983.00	0.233E-01	4160.70	45010.29
STRAIN RATE =				3.620E-01	

GRAPHITE EPOXY STRAIN RATE DATA

SPEC.NO	TEMP	FSTRES	FTIME	STRAIN	STRESS
G3I12	300.	81944.44	0.492E 04	0.00	0.00
G3I12	300.	81944.44	0.492E 04	936.32	6944.44
G3I12	300.	81944.44	0.492E 04	1605.12	12500.00
G3I12	300.	81944.44	0.492E 04	2173.60	16319.44
G3I12	300.	81944.44	0.492E 04	2675.20	20138.89
G3I12	300.	81944.44	0.492E 04	3210.24	23958.33
G3I12	300.	81944.44	0.492E 04	3745.28	28472.22
G3I12	300.	81944.44	0.492E 04	4347.20	32986.11
G3I12	300.	81944.44	0.492E 04	4915.68	37500.00
G3I12	300.	81944.44	0.492E 04	5517.60	42361.11
G3I12	300.	81944.44	0.492E 04	6119.52	47222.22
G3I12	300.	81944.44	0.492E 04	6688.00	52083.33
G3I12	300.	81944.44	0.492E 04	7356.80	56944.44
G3I12	300.	81944.44	0.492E 04	7958.72	62500.00
G3I12	300.	81944.44	0.492E 04	8560.64	68055.56
G3I12	300.	81944.44	0.492E 04	9095.68	73888.88

STRAIN RATE = 2.020E-06

G3I14	300.	71875.00	0.432E 04	0.00	0.00
G3I14	300.	71875.00	0.432E 04	895.21	6250.00
G3I14	300.	71875.00	0.432E 04	1724.11	13194.44
G3I14	300.	71875.00	0.432E 04	2320.92	17361.11
G3I14	300.	71875.00	0.432E 04	2785.10	20833.33
G3I14	300.	71875.00	0.432E 04	3315.60	25000.00
G3I14	300.	71875.00	0.432E 04	3912.41	29861.11
G3I14	300.	71875.00	0.432E 04	4509.22	34375.00
G3I14	300.	71875.00	0.432E 04	5106.02	38888.89
G3I14	300.	71875.00	0.432E 04	5702.83	43750.00
G3I14	300.	71875.00	0.432E 04	6332.80	48611.11
G3I14	300.	71875.00	0.432E 04	6929.60	53819.44
G3I14	300.	71875.00	0.432E 04	7559.57	59027.78
G3I14	300.	71875.00	0.432E 04	8222.69	64305.56
G3I14	300.	71875.00	0.432E 04	8832.76	69722.25

STRAIN RATE = 2.100E-06

G3I16	300.	72919.69	0.852E 01	0.00	0.00
-------	------	----------	-----------	------	------

GRAPHITE EPOXY STRAIN RATE DATA

SPEC.NO	TEMP	FSTRES	FTIME		STRAIN	STRESS
G3I16	300.	72919.69	0.852E 01		1784.79	9722.22
G3I16	300.	72919.69	0.852E 01		2608.54	18055.56
G3I16	300.	72919.69	0.852E 01		3569.58	25000.00
G3I16	300.	72919.69	0.852E 01		4530.63	32638.89
G3I16	300.	72919.69	0.852E 01		5491.67	40972.22
G3I16	300.	72919.69	0.852E 01		6452.71	49305.56
G3I16	300.	72919.69	0.852E 01		7688.34	58333.33
G3I16	300.	72919.69	0.852E 01		8786.67	68402.75
STRAIN RATE =					1.100E-03	
G3I17	300.	65833.31	0.730E 01		0.00	0.00
G3I17	300.	65833.31	0.730E 01		1385.01	10416.67
G3I17	300.	65833.31	0.730E 01		2150.47	17361.11
G3I17	300.	65833.31	0.730E 01		3025.24	24652.78
G3I17	300.	65833.31	0.730E 01		4009.35	32291.67
G3I17	300.	65833.31	0.730E 01		4957.02	41666.67
G3I17	300.	65833.31	0.730E 01		6014.03	50347.22
G3I17	300.	65833.31	0.730E 01		7107.49	60069.44
STRAIN RATE =					1.020E-03	
G3I23	300.	69722.25	0.340E 00		0.00	0.00
G3I23	300.	69722.25	0.340E 00		941.70	4166.67
G3I23	300.	69722.25	0.340E 00		2421.51	11805.56
G3I23	300.	69722.25	0.340E 00		3766.80	23611.11
G3I23	300.	69722.25	0.340E 00		5246.61	34722.22
G3I23	300.	69722.25	0.340E 00		6726.43	45833.33
G3I23	300.	69722.25	0.340E 00		8340.77	58333.33
STRAIN RATE =					2.780E-02	
G3I26	300.	81944.44	0.400E 00		0.00	0.00
G3I26	300.	81944.44	0.400E 00		387.98	3472.22
G3I26	300.	81944.44	0.400E 00		1551.91	11111.11
G3I26	300.	81944.44	0.400E 00		2586.51	22222.22
G3I26	300.	81944.44	0.400E 00		3879.77	33333.33

GRAPHITE EPOXY STRAIN RATE DATA

SPEC.NO	TEMP	FSTRES	FTIME	STRAIN	STRESS
G3I26	300.	81944.44	0.400E 00	5173.02	43055.56
G3I26	300.	81944.44	0.400E 00	6466.28	55555.56
G3I26	300.	81944.44	0.400E 00	7759.53	69444.44
STRAIN RATE =				2.220E-02	
G3I43	300.	86805.56	0.255E-01	0.00	0.00
G3I43	300.	86805.56	0.255E-01	1439.29	12860.08
G3I43	300.	86805.56	0.255E-01	2201.27	22505.14
G3I43	300.	86805.56	0.255E-01	3132.58	28935.18
G3I43	300.	86805.56	0.255E-01	3725.25	35365.22
STRAIN RATE =				2.980E-01	
G3I98	300.	80375.50	0.239E-01	0.00	0.00
G3I98	300.	80375.50	0.239E-01	833.62	9645.06
G3I98	300.	80375.50	0.239E-01	1917.33	20897.63
G3I98	300.	80375.50	0.239E-01	2834.31	25720.16
G3I98	300.	80375.50	0.239E-01	3334.49	32150.20
G3I98	300.	80375.50	0.239E-01	4251.47	41795.27
G3I98	300.	80375.50	0.239E-01	4835.01	49832.82
G3I98	300.	80375.50	0.239E-01	5418.54	54655.35
G3I98	300.	80375.50	0.239E-01	6002.08	61085.39
G3I98	300.	80375.50	0.239E-01	6502.25	70730.44
G3I98	300.	80375.50	0.239E-01	7169.15	80375.50
STRAIN RATE =				3.000E-01	
G3I33	-50.	71527.75	0.374E 04	0.00	0.00
G3I33	-50.	71527.75	0.374E 04	477.50	2083.33
G3I33	-50.	71527.75	0.374E 04	1575.75	10416.67
G3I33	-50.	71527.75	0.374E 04	2244.25	15972.22
G3I33	-50.	71527.75	0.374E 04	2912.75	21527.78
G3I33	-50.	71527.75	0.374E 04	3533.50	26388.89
G3I33	-50.	71527.75	0.374E 04	4106.50	31944.44
G3I33	-50.	71527.75	0.374E 04	4727.25	37500.00
G3I33	-50.	71527.75	0.374E 04	5348.00	43750.00

GRAPHITE EPOXY STRAIN RATE DATA

SPEC.NO	TEMP	FSTRES	FTIME	STRAIN	STRESS
G3I33	-50.	71527.75	0.374E 04	6016.50	49305.55
G3I33	-50.	71527.75	0.374E 04	6637.25	55555.56
STRAIN RATE =				2.210E-06	
G3I37	-50.	63474.22	0.334E 04	0.00	0.00
G3I37	-50.	63474.22	0.334E 04	286.50	1388.89
G3I37	-50.	63474.22	0.334E 04	1432.50	10416.67
G3I37	-50.	63474.22	0.334E 04	2196.50	18055.56
G3I37	-50.	63474.22	0.334E 04	2817.25	22222.22
G3I37	-50.	63474.22	0.334E 04	3390.25	27777.78
G3I37	-50.	63474.22	0.334E 04	4011.00	32638.89
G3I37	-50.	63474.22	0.334E 04	4631.75	38888.89
G3I37	-50.	63474.22	0.334E 04	5204.75	44444.44
G3I37	-50.	63474.22	0.334E 04	5968.75	50000.00
G3I37	-50.	63474.22	0.334E 04	6589.50	56250.00
STRAIN RATE =				2.200E-06	
G3I36	-50.	81805.56	0.720E 01	0.00	0.00
G3I36	-50.	81805.56	0.720E 01	1699.90	13888.89
G3I36	-50.	81805.56	0.720E 01	2559.40	23611.11
STRAIN RATE =				1.420E-03	
G3I38	-50.	84861.13	0.690E 01	0.00	0.00
G3I38	-50.	84861.13	0.690E 01	1539.87	13888.89
G3I38	-50.	84861.13	0.690E 01	2699.64	29166.67
G3I38	-50.	84861.13	0.690E 01	3800.94	38194.44
G3I38	-50.	84861.13	0.690E 01	4785.29	47916.67
G3I38	-50.	84861.13	0.690E 01	5750.14	62500.00
STRAIN RATE =				1.150E-03	
G3I35	-50.	73611.13	0.290E 00	0.00	0.00
G3I35	-50.	73611.13	0.290E 00	1229.00	2777.78

GRAPHITE EPOXY STRAIN RATE DATA

SPEC.NO	TEMP	FSTRES	FTIME	STRAIN	STRESS
G3I35	-50.	73611.13	0.290E 00	2458.00	12500.00
G3I35	-50.	73611.13	0.290E 00	4038.14	27777.78
G3I35	-50.	73611.13	0.290E 00	5618.29	41666.67
G3I35	-50.	73611.13	0.290E 00	7022.86	56250.00
STRAIN RATE =				3.050E-02	
G3I16	-50.	53055.56	0.230E 00	0.00	0.00
G3I16	-50.	53055.56	0.230E 00	591.40	3055.56
G3I16	-50.	53055.56	0.230E 00	2129.04	15833.33
G3I16	-50.	53055.56	0.230E 00	3755.39	30555.56
G3I16	-50.	53055.56	0.230E 00	5440.88	44444.44
STRAIN RATE =				2.720E-02	
G3I53	-50.	61085.39	0.172E-01	0.00	0.00
G3I53	-50.	61085.39	0.172E-01	1089.88	9645.06
G3I53	-50.	61085.39	0.172E-01	2024.06	16075.10
G3I53	-50.	61085.39	0.172E-01	3113.93	32150.20
G3I53	-50.	61085.39	0.172E-01	3736.72	35365.22
G3I53	-50.	61085.39	0.172E-01	4281.66	41795.27
G3I53	-50.	61085.39	0.172E-01	4826.59	48225.31
G3I53	-50.	61085.39	0.172E-01	5293.68	51440.33
G3I53	-50.	61085.39	0.172E-01	6072.17	61085.39
STRAIN RATE =				3.530E-01	
G3I85	-50.	70730.44	0.222E-01	0.00	0.00
G3I85	-50.	70730.44	0.222E-01	798.74	6430.04
G3I85	-50.	70730.44	0.222E-01	1437.73	12860.08
G3I85	-50.	70730.44	0.222E-01	2076.72	19290.12
G3I85	-50.	70730.44	0.222E-01	2715.71	28935.18
G3I85	-50.	70730.44	0.222E-01	3594.32	33757.71
G3I85	-50.	70730.44	0.222E-01	4233.31	41795.27
G3I85	-50.	70730.44	0.222E-01	4952.18	48225.31
G3I85	-50.	70730.44	0.222E-01	5591.17	57870.37
G3I85	-50.	70730.44	0.222E-01	6230.16	62692.90

GRAPHITE EPOXY STRAIN RATE DATA

SPEC.NO	TEMP	FSTRES	FTIME	STRAIN	STRESS
G3I85	-50.	70730.44	0.222E-01	7028.89	70730.44
		STRAIN RATE =		3.170E-01	

VITA

The author was born in Bombay, India on August 9, 1947. He graduated from New Era High School in Bombay in June 1964. He then entered S.I.E.S. College, Bombay and completed the requirements of the Intermediate of Science degree in 1966. In 1970, he received the Bachelor of Engineering degree with honors in Civil Engineering from Victoria Jubilee Technical Institute of Bombay University.

In 1970, he came to the United States to pursue graduate studies. He obtained a Master of Science in Civil Engineering from South Dakota School of Mines and Technology, Rapid City, South Dakota, in 1971. He then joined Virginia Polytechnic Institute and State University to do graduate work in Engineering Science and Mechanics, where he was appointed Teaching and Research Assistant. He received Professional Engineer's Certification in Virginia in 1974. Upon obtaining a Ph.D. in Engineering Mechanics at Virginia Polytechnic Institute he will be employed by Alcoa Research Laboratory in Alcoa Technical Center, Pennsylvania.

A handwritten signature in black ink that reads "Ashok B. Thakker". The signature is written in a cursive, flowing style with a long horizontal stroke extending to the left from the first letter.

Ashok B. Thakker

VISCOELASTIC CHARACTERIZATION
OF ANGLE PLY ADVANCED COMPOSITES

by

Ashok B. Thakker

(ABSTRACT)

Time dependent properties of angle ply laminated Boron/Epoxy and Graphite/Epoxy fiber controlled composites were investigated. The main objective of this study was to develop a technique to establish interconversion of different test results using appropriate viscoelastic theory to formulate an accelerated testing procedure.

To achieve this aim, forced vibration, constant strain rate and creep tests were performed at different temperature levels. Due to its practical importance, behavior below the glass transition temperature was studied. Multiple regression techniques were used to generate response surfaces for significant variables. Master curves using the time-temperature superposition principle were established for individual tests. Mechanical model representation, integral equation formulation and numerical integration methods based on linear viscoelasticity were used to predict constant strain rate and long time creep behavior of composites from nondestructive short time dynamic tests.

It has been shown that a regression equation and its constants can be conveniently used to obtain horizontal and vertical shift and also to perform viscoelastic analysis. While time-temperature

superposition can be applied to each test its validity in general needs further study. Simple mechanical models fail to predict constant strain rate tests. Constant strain rate and creep tests were predicted using measured damping ratios and storage moduli from dynamic tests. Also, relaxation moduli were obtained over eleven decades of time scale from different tests. Thus, applicability of linear viscoelastic theory to predict the gross behavior of these composites is established.